RATE-BASED MODELING OF STEAM ETHANE CRACKER

A THESIS SUBMITTED TO
THE GRADUATE SCHOOL OF NATURAL AND APPLIED SCIENCES
OF
MIDDLE EAST TECHNICAL UNIVERSITY

BY

SELİN GÜNDÜR

IN PARTIAL FULFILLMENT OF THE REQUIREMENTS
FOR
THE DEGREE OF MASTER OF SCIENCE
IN
CHEMICAL ENGINEERING

JANUARY 2015

Approval of the thesis:

RATE-BASED MODELING OF STEAM ETHANE CRACKER

submitted by **SELİN GÜNDÜR** in partial fulfillment of the requirements for the degree of **Master of Science in Chemical Engineering Department, Middle East Technical University** by,

Prof. Dr. Gülbin Dural Ünver
Dean, Graduate School of **Natural and Applied Sciences** _____

Prof. Dr. Halil Kalıpçılar
Head of Department, **Chemical Engineering** _____

Prof. Dr. Canan Özgen
Supervisor, **Chemical Engineering Dept., METU** _____

Prof. Dr. Erdoğan Alper
Co-Supervisor, **Chemical Eng. Dept., Hacettepe University** _____

Examining Committee Members:

Prof. Dr. Hayrettin Yücel
Chemical Engineering Dept., METU _____

Prof. Dr. Canan Özgen
Chemical Engineering Dept., METU _____

Prof. Dr. Erdoğan Alper
Chemical Engineering Dept., Hacettepe University _____

Prof. Dr. Ahmet Rifat Özdural
Chemical Engineering Dept., Hacettepe University _____

Assoc. Prof. Dr. Naime Aslı Sezgi
Chemical Engineering Dept., METU _____

Date: January 30, 2015

I hereby declare that all information in this document has been obtained and presented in accordance with academic rules and ethical conduct. I also declare that, as required by these rules and conduct, I have fully cited ad referenced all material and results that are not original to this work.

Name, Last Name: SELİN GÜNDÜR

Signature

ABSTRACT

RATE-BASED MODELING OF STEAM ETHANE CRACKER

Gündür, Selin
M.S., Department of Chemical Engineering
Supervisor: Prof. Dr. Canan Özgen
Co-supervisor: Prof. Dr. Erdoğan Alper

January 2015, 110 pages

Ethylene production is the main building block of petrochemical industry and it is produced via thermal cracking process which does not require a catalyst and takes one of the refinery white products, that is straight run naphtha, as a feedstock. In some processes, ethane which is produced as a result of naphtha cracking is fed into a separate ethane cracker which also yields same products as ethylene and propylene etc. The main reason to process produced ethane in a separate cracker is that, ethane which is harder to crack when compared with naphtha requires higher residence times within the cracker tubes to achieve the desired conversion.

When crackers or furnaces used in refineries and petrochemical plants are considered, process gas temperature within the tubes is very crucial to be able to monitor the cracking process. In general temperature measurements are done at the inlet and outlet of the furnaces, as well as at some points on tube surface. However, temperature profile of process gas within the tubes cannot be monitored. Since ethane cracking process has a run length of approximately three months followed by a decoking period, in order to maintain operational safety, accurate modeling of the

process has to be done to find gas temperature profiles. At high temperatures coking rate increases and coke formed deposits on the tube internal walls and prevents efficient transfer of heat. Because of this inefficient heat transfer, cracker duty is increased at a level of maximum allowable tube surface temperature in order to obtain desired ethane conversion. When that maximum surface temperature is obtained, process is shut down and decoking period is started. Thus, modeling of ethane cracker is crucial to find the temperature profile of the process gas within the coil as well as coke formation profile within the tubes.

In this study, three different reaction network models were constructed and separate mass, energy and momentum balance equations were solved simultaneously using an algorithm developed in MATLAB software for each case. Model validation is achieved using two studies found from literature. In the three models that are considered in this study, in Model-I basic reaction mechanism are included in which neither coke formation nor removal reactions are involved , whereas in Model-II only coke formation and in Model-III additionally coke removal reactions are included. In each model different number of components and reactions are considered. The input data from PETKİM and reactor specifications are used and outputs, such as conversion, temperature, pressure are compared. Program outputs are compared with the industrial data that is provided by PETKİM Co. Since Model-III considers more number of reactions and coke formation and removal, it yielded similar results with the real plant data and therefore selected as the appropriate model. Using this model, process gas temperature profile can easily be evaluated by the input plant data and control of operation can be done in a better way.

Keywords: coking, ethylene production, rate-based modeling, thermal/steam cracking,

ÖZ

REAKSİYON HIZI TEMELLİ BUHARLA ETAN PARÇALAMA ÜNİTESİNİN MODELLEME ÇALIŞMASI

Gündür, Selin
Yüksek Lisans, Kimya Mühendisliği Bölümü
Tez Yöneticisi: Prof. Dr. Canan Özgen
Ortak Tez Yöneticisi: Prof. Dr. Erdoğan Alper

Ocak 2015, 110 sayfa

Etilen üretimi petrokimya endüstrisinin temel üretim süreçlerinden birisidir. Etilen rafineri beyaz ürünlerinden birisi olan naftanın, buharla katalizör gerektirmeyen bir süreçte parçalanması sonucu üretilir. Ancak, bu çalışmada da ele alındığı üzere naftanın parçalanması sonucu oluşan etan ayrı bir fırında kullanılarak istenilen hafif ürünler etilen, propilen vb. elde edilebilir. Nafta parçalanması sonucu oluşan etanın ayrı bir fırında işlenmesinin temel sebeplerin birisi besleme/şarjın istenilen dönüşüm oranına ulaşması için gerekli olan proseste kalma zamanının farklılık göstermesidir.

Hali hazırda rafineri ve birçok petrokimya tesisinde bulunan fırınlarda; fırına beslenen akım işlenirken tüp içerisindeki proses gazının sıcaklığı takip edilememektedir. Sıcaklık ölçümleri fırın giriş, çıkışlarında ve bazı noktalarda da tüp dış yüzeyinde yapılmaktadır. Ancak tüp içerisindeki akımın sıcaklık profili hakkında öngörüde bulunulamamaktadır. Özellikle, etan parçalama ünitesinde proses edilen akımın sıcaklığının takibi ünitenin güvenli işletilebilmesi için çok büyük önem arz etmektedir. Yüksek sıcaklıklarda koklaşmanın artması ve tüp cidarında birikmesi

sonucu ısı transferinde verim düşmekte ve bu da istenilen etan dönüşüm miktarının elde edilmesini zorlaştırıcı bir durum oluşturmaktadır. Maksimum dizayn tüp sıcaklığına yaklaşıldığı noktada proses durdurulmakta ve kok giderme işlemi ile tüp iç yüzeyi temizlenmektedir.

Yapılan çalışmada üç farklı reaksiyon ağı modeli oluşturularak her bir durum için kütle, enerji ve momentum denklikleri ayrı ayrı çözülmüş ve MATLAB programlama ortamında yazılmış olan algoritma ile hesaplanmıştır. Model-II ve Model-III için model doğrulama çalışmaları literatürde bulunan iki çalışma ile yapılmıştır. Oluşturulan üç farklı modelden Model-I'de en temel reaksiyonlar hesaba katılmış, Model-II de birinci modele ek olarak kok oluşum reaksiyonları eklenmiştir. Her modelde farklı komponentler ve reaksiyonlar ele alınmıştır. PETKİM'den alınan giriş verileri ve reaktör özellikleri kullanılarak dönüşüm, sıcaklık ve basınç gibi çıktılar incelenmiştir. Program çıktıları PETKİM'den temin edilen endüstriyel çıktılar ile karşılaştırılmıştır. Model-III daha fazla reaksiyon içerdiği, kok oluşumu ve kok giderimi modele dahil edildiği için hakiki saha sonuçlarına yakın çıktılar vermiştir. Bu nedenle, en uygun model olarak Model-III seçilmiştir. Böylece bu model kullanılarak süreç gaz sıcaklık profili girdi verileri kullanılarak elde edilebilecek ve operasyonun kontrolü daha iyi yapılabilecektir.

Anahtar Sözcükler: etilen üretimi, hız temelli modelleme, koklaşma, termal/buharla parçalama

To my family,

ACKNOWLEDGEMENTS

I wish to express my gratitude to my supervisor Prof. Dr. Canan Özgen for her great encouragement and patience throughout this study. I also wish express my deepest gratitude to my co-supervisor Prof. Dr. Erdoğan Alper for his guidance, advise, patience and standing beside me all the way.

I am grateful to Manager of PETKİM Ethylene Unit Hasan Ali Karavacıoğlu and Ethylene Unit Process Superintendent Haydar Şahin for supplying all necessary plant data and their support.

I am also grateful to Mehmet Caner Demiryürek for listening me at every step I take throughout the study as well as his encouragement and great patience. I would like to thank to Merve Çetinkol for her intimate friendship and optimistic manner. And I also would like to thank to Tuba Kahya, Eda Çelik for their friendship and support.

Finally, I would like to thank to my parents and my little brother Mehmet Egemen Gündür for their belief on me throughout this long and exhausting period, without their support this thesis would not be possible.

TABLE OF CONTENTS

LIST OF TABLES

TABLES

LIST OF FIGURES

FIGURES

LIST OF SYMBOLS

Symbol	Definition	Unit
AC	Cross-sectional area of the tube	m^2
A_{cp}	Cold plane surface area	ft^2
A_{rad}	Total area exposed to radiant heat	ft^2
A_s	Inside surface area	ft^2
A_w	The refractory area	ft^2
BMM	Molecular weight of the gas (*MATLAB)*	kg/kmol
BM(i)	Molecular weight of the component i=1-12 *(MATLAB)*	kg/kmol
ctc	Center-to-center distance	m
C_j	Concentration of component j	$kmol/m^3$
C(i)	Concentration of component i=1-12 *(MATLAB)*	$kmol/m^3$
c_pj	Specific heat capacity of component j	j.mol/K
CP(i)	Specific heat capacity of component i=1-12 *(MATLAB)*	j.mol/K
CPT	Specific heat capacity of the gas *(MATLAB)*	j.mol/K
d_t	Diameter of the tube	m
DH(i)	Heat of reaction I *(MATLAB)*	j/mol
DHF(i)	Enthalpy of formation of component I=1-12 through the tube *(MATLAB)*	j/mol
DHFO(i)	Standart enthalpy of formation of component I=1-12 *(MATLAB)*	j/mol
EE	Nekrasov factor *(MATLAB)*	
F	The exchange factor	
f	Fanning friction factor	
F(i)	Molar flow rate of component i=1-12 *(MATLAB)*	mol/s

FF	Friction factor *(MATLAB)*	
F_j	Molar flow rate of component j	mol/s
Ft	Total molar flow rate of process gas	mol/s
G	Mass flux	$kg/m^2.s$
G_f	Flue gas mass flow rate	Ib/h
H	Height of the furnace	ft
L	Length of the furnace	ft
L_{tube}	Total length of the tubes	ft
M_m	Molecular weight of the gas	kg/kmol
P_c	Critical pressure	bar
P_t	Total Pressure	atm
Q(z)	Heat flux along the length z	$j/m^2.s$
Q_g	The enthalpy of flue gas	Btu/Ib
Q_n	The net heat release	Btu/Ib
q_{rad}	The average radiant heat flux	$Btu/ Ib.ft^2$
Q_{total}	The total radiant heat amount	Btu/Ib
R	Ideal Gas Constant	J/mol.K
R_b	Radius of the bend	m
RB	Radius of the bend *(MATLAB)*	m
Re	Reynolds Number	
R(i)	Rate of reaction i	$kmol/m^3.s$
RX	Ideal gas constant *(MATLAB)*	m^3.atm/kmol.K
RZ	Ideal gas constant *(MATLAB)*	L.atm/kmol.K
SUMDHR	Sum of the enthalpy change of the reactions *(MATLAB)*	$j/m^3.s$
SUMYDO	Sum of the rate of reaction *(MATLAB)*	$kmol/m^3.s$
T	Temperature	K
T_c	Critical temperature	K
T_t	Mean tube wall temperature	^oF
u	Velocity of the gas	m/s
V_c	Critical volume	$m^3/kmol$
VISC	Viscosity in *(MATLAB)*	Pa.s

yy(i)	Molar composition of component i=1-12 *(MATLAB)*	
z	Length	m
Zc	Compressibility factor	
z_{ent}	The fraction of excess air	
x_{excess_air}	Excess air to burners	

GREEK SYMBOLS

ΔH_i	Heat of reaction i	j/mol
ΔH_f	Heat of formation of component j	j/mol
ϕ	Emissivity of the furnace	
η	Furnace Efficiency	
α	The absorptivity of the tubes	
α_{ij}	Stoichiometric coefficient component j in reaction i	
ζ	Nekrasov factor	
μmixture	Viscosity of mixture	Pa.s
ξ	Angle described by the bend	
ρ_g	Density of the gas	kg/m^3

CHAPTER 1

INTRODUCTION

Petroleum/Oil is drilled from wells, transported and goes through some processes such as cracking, reforming etc. and then fractionated to derive valuable products. Oil is processed in refineries and their product slate mainly comprised by fuels ranging from LPG, light and heavy naphtha, kerosene, light and heavy diesel and fuel oil cuts. Petrochemical company products are comprised of products derived from naphtha such as low and high density polyethylene (LDPE, HDPE), polyvinyl chloride (PVC) mainly.

Ethane is one of the downstream products of petroleum fraction and also main feedstock of LDPE, HDPEs. It is produced as a result of naphtha cracking process which is carried out in high-duty crackers. In this study, kinetic modeling studies are carried out for thermal/steam ethane cracker. In process, steam is used as a dilution medium to reduce hydrocarbon partial pressure and is injected into feed stream (ethane) at the inlet of radiant section of the cracker. Process requires vast amount of heat and as temperature within the coil increases, coke formation rate also increases. Since during operation temperature and coke formation profile within the coils/tubular reactors cannot be measured because of high temperatures, accurate kinetic modeling is necessary to provide these profiles. Determination of the accurate reaction model for the ethane cracking forms the main issue of the thesis. As the number of reactions increases, simulation results fit the plant data better. In the thesis three kinetic models are studied. In Model-I basic reactions are included whereas Model-II involves additional coke formation reactions. Model-III involves both coke formation and removal reactions.

It is seen from the literature that, most of studies about steam ethane cracking process do not involve coke formation and coke removal reactions. As the number of reactions is increased the complexity of the problem and its solution algorithm also increases. Molecular reaction scheme instead of free radical mechanism is taken for the three kinetic models. MATLAB software is used for simulation and profiles for process variables such as process gas temperature within coils, operating pressure, ethane conversion, ethylene/ propylene yield can be obtained. In the written code, mass, energy and momentum balance equations are solved simultaneously for the selected compounds. The simulation is carried out by using real plant input data and geometrical information related to cracker such as fired heater/ furnace dimensions, coil length and internal diameter. As stated before, this work is done to determine the most appropriate reaction network model which can predict process gas temperature profile within cracker tubes as well as overall ethane conversion, precisely.

In Chapter 4 detailed information about cracking processes and crucial points during the ethane cracking reaction network development is described. In Chapter 5 modeling approach and case studies performed are given. In Chapter 6 developed algorithm is presented. And finally in Chapter 7 results and discussion section comparison of three models is given and effects of operational parameters are given. Additional information about the code generated in MATLAB is given in Appendices.

CHAPTER 2

LITERATURE SURVEY

Thermal cracking of hydrocarbon mixtures are studied by many researchers both experimentally and theoretically by simulation studies. Steam/thermal cracking of hydrocarbon cut selected has great importance on the operation characteristics. Naphtha, Light Cycle oil, FCC Gas, n-butane, propane, ethane and their mixtures might be taken as feedstock for the cracking operation. As stated before, cracking kinetics of ethane and naphtha differs from each other. Since ethane is a lower molecular weight hydrocarbon, it is harder to crack when compared with naphtha. And ethane cracking requires higher residence time through coils and higher heat duty (higher operation temperature) within the furnace.

2.1 Steam Ethane Cracking Process

G. F. Froment and K.M. Sundaram (Froment et al., 1981) are the frontier researchers who studied hydrocarbon thermal cracking for many years. Modeling or experimental studies might consider molecular or free-radical mechanism for the selected hydrocarbon fractions. In 1981 G. Froment has adopted free radical mechanism and conducted experimental studies to determine kinetic parameters such as pre-exponential factor k_o, activation energies for the selected reaction network. Experiments were conducted in a pilot plant reactor under conditions as close as possible those used in the industry. The majority of the data obtained at atmospheric pressures, low temperature and low conversion values. Some assumptions were done such as steady-state conditions were maintained and free-radical species concentration was constant within reactor. In this study ethane, propane, n-butane, iso-butane, olefin and mixture of these components are considered for thermal

cracking operation in a pilot plant, respectively. Earlier studies before Froment have proposed, several number of reactions ranging from six to twelve for ethane cracking. But Froment has increased the number of reactions for thermal ethane cracking up to forty nine involving twenty species. The reaction scheme involved eleven molecular and nine radical components. Only continuity equations were solved according to the experimentally determined kinetic parameters. Solution of these continuity equations provided concentration profiles of both free radicals and the product distribution through pilot plant reactor used.

The cracker was operated at temperatures of about 850-900^{o}C and as a result of this high severity operation of the steam cracker, the rate of coke formation through the coils increase. Accurate kinetic modeling of cracking and coking reactions directly affected the run length of the cracker that also affected profitability of the whole plant. G.F. Froment and his co-workers (Froment et al., 1981) carried out another study for ethane pyrolysis by considering coke formation reactions and coke deposition within the coil internals. These carbonaceous material deposited on the inner wall of cracking coils, thus, this phenomenon limited the tube skin temperature, increased the pressure drop through coil and reduced the transfer of heat required for the cracking reactions to occur. In general, steam crackers operating run length is about ninety days. In fact coke formation determines the run length if the cracker is operated at highly severe conditions (high heat duty) and ninety days of operation may not be an achievable target. In the study ethane, ethylene and C4+ components were taken to be coke precursors. Kinetic parameters related to considered reactions were determined in pilot plant experiments. Total amount of coke formed within the wall internals and coke formation profile through reactor were obtained.

Decoking operation time of the cracker was highly depended on tube skin temperature. And when external tube skin temperature within the furnace exceeded maximum allowable tube skin temperature which was about 1030^{o}C, cracker was shut down and steam/air decoking operation was started. The study involved three main coke formation reactions as well as molecular cracking reactions for ethane cracking. The study also considered simultaneous solution of mass, energy and momentum balance equations for the selected components. In addition required heat flux per tube was calculated from the correlations proposed by Froment et. al.

(Froment et al., 1981) and derived from the two dimensional simulation of cracker using industrial geometric data of an industrial steam cracker. According to the study, performed profiles related to ethane conversion and yield through reactor length, % reduction of internal tube diameter and profile of maximum allowable tube skin temperatures were obtained.

Another study which considers thermal cracking of pure ethane was conducted by Ranjan, P. (Ranjan et al., 2012). Sensitivity analysis on process parameters such as coil outlet temperature, residence time, steam-to-ethane ratio on ethylene yield were all studied by them. Reaction network was based on Froment's earlier studies (Froment et al., 1981) and it was improved by additional cracking reactions. But network neglected coke formation reactions. And there was an assumption related to under estimation of coke formation reactions; since coke was not considered the reactor core temperature was assumed to be the same as the reactor wall temperature. Only molecular species were considered in the network. No reactions occur at the entry of the radiant section. Hydrodynamic parameters were neglected due bending of the coils. All these assumptions were the possible reasons for the deviation from plant data. The main difference of study from other studies on same topic is improved reaction network and simulation part which was conducted using Aspen's built-in PFR module.

One of the recent studies on ethane thermal cracking belongs to Yancheshmeh (Yancheshmesh and Haghighi, 2013). Study was carried out only considering ethane as a feedstock. Cracking process was named as thermal or steam cracking. Steam was injected into feed stream but it did not go into reaction. It was used as a diluting medium. This study answers the question. Modeling studies were carried out for both steam and CO_2 used cases as a diluting medium and the results are compared. Reaction network consisted of eight cracking reactions, three coke formation reactions and two partial removals of coke reactions in general. Component based mass balances as well as energy and momentum balances were solved simultaneously. Since coke formation and removal reactions were considered, results were expected to be closer to industrial plant data. But number of reactions considered was very limited. In fact thousands of reactions both including molecular and free radical mechanisms should be considered. Assumptions made in this study

are given as follows; plug flow conditions are valid through the reactor length, gas mixture is as an ideal gas, one dimensional variations of all independent parameters flow (or concentration), process temperature and pressure are accepted. The case was studied by assuming steady-state conditions for simulation of coke deposition rate.

CHAPTER 3

ETHYLENE PRODUCTION AND ITS USES

Ethylene which has a simple structure is the simplest olefin with carbon-carbon double bonds. It has the formula of C_2H_4 and the simplest unsaturated hydrocarbon after acetylene (C_2H_2), (Zhang and Evans, 2012). It can be produced in high yields easily from any straight run paraffin source by steam thermal cracking. Since the compound itself is highly reactive and relatively inexpensive, ethylene is used widely as a base product for many syntheses in the petrochemical industry. As a result of the reaction of ethylene with inexpensive compounds such as water, chlorine, hydrogen chloride and oxygen, it is possible to produce valuable chemicals (Matar and Hatch, 1981).

3.1 Products derived from ethylene

The main industrial uses of ethylene include polymerization, oxidation, alkylation halogenation, hydration, oligomerization and hydroformylation. Figure 3.1-3.4 represents various compounds which can be derived from ethylene, C_2H_4.

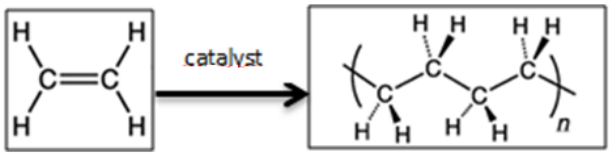

Figure 3.1 Polyethylene Derivation from ethylene

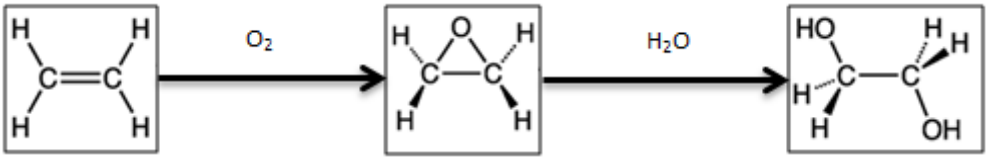

Figure 3.2 Ethylene Glycol Derivation from Ethylene oxide and Ethylene oxide Derivation from ethylene

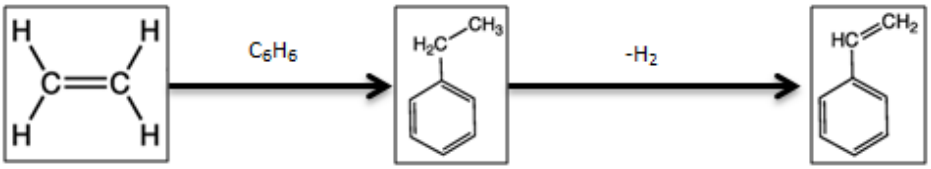

Figure 3.3 Styrene Derivation from Ethyl Benzene and Ethyl Benzene Derivation from Ethylene

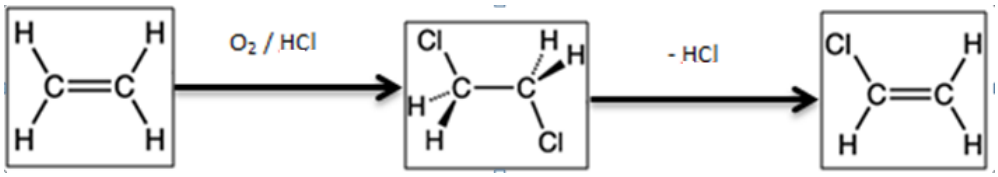

Figure 3.4Vinyl Chloride from Ethylene Dichloride and Ethylene Dichloride Derivation from Ethylene

The primary use of ethylene is the polyethylene production which consumes approximately 50% of total ethylene supply. Polyethylene is mainly used in film applications for packaging, carrier bags and trash liners (Geem, 2006).

The other use of ethylene is the ethylene oxide production which is an important raw material for the intermediate raw materials in the chemical industry. Ethylene oxide is able to react with almost all compounds which have available hydrogen such as water, alcohols, organic acids and amines. Ethylene glycol which is the derivative of ethylene is used for the production of soft drinks, food packaging and textiles. In addition, ethanolamines are used for the production of surfactants (Matar and Hatch, 1981), (Geem, 2006). Styrene monomer is the alkylation product of ethylene and the polystyrene form is used for packaging and insulation. In addition, the styrene butadiene form is used in tire and footwear production (Geem, 2006). Olefin production is the third largest petrochemical sector after ammonia production and

petroleum refining around the world (Tham, 2014). The demand for ethylene, which is simplest olefin has been increasing with a growth rate of 3.5% per year around the world. The demand had a significant growth in the late century and reached over 140 million tons per year at the end of 21st century (Zhang and Evans, 2012). In general, in petrochemical plants, two types of the furnaces are used. The biggest ethane gas cracking furnace in operation has the capacity of around 210kta ethylene production capacity whereas the biggest liquid I.e. naphtha cracking furnace has the capacity of 170 kta. Nowadays, mega plants which have the capacity of greater than 2000kta are in construction. The largest ethylene production complex, Formosa Petrochemical Corporation, has the capacity of 3000kta ethylene production (Zhang and Evans, 2012). The main licensors for olefin production are Kellogg Brown & Root, CBI Lummus, Stone & Webster, Linde and KTI-Technip, etc. (Tham, 2014). PETKIM, which is located in Izmir, is the single manufacturer of ethylene in Turkey. The plant has the production capacity of 520kta and it has been in operation since 1985. The main raw material is the naphtha which is coming from Aromatics Plants of PETKIM complex and TUPRAS refineries. Moreover, some imported light naphtha can be processed in PETKIM Ethylene Plant. The raw material is cracked by steam and separated to the components such as ethylene, propylene, pyrolysis gasoline, C_4 and hydrogen.

3.2 Ethylene Production

The olefin plants are generally the centerpiece of an entire petrochemical complex. The feed for olefin production is provided from the refineries; on the other hand, the effluent streams of the olefin plants are used in other petrochemical plants such as polyethylene and polypropylene units (Hernandez, 2012). Figure 3.5 represents the block diagram of ethylene plant and downstream units in PETKIM. As it can be seen on the Figure 3.5, the ethylene plant in PETKIM Complex is capable of using light and heavy naphtha as a feedstock some of is imported and some comes from TUPRAS Refinery.

In general, typical feed stocks for the ethylene plants vary from light hydrocarbons; ethane and propane up to heavier hydrocarbons naphtha and even gas oils. The Ethylene Plant related downstream units at PETKIM are the plants that are shown in

the Figure 3.5. Polyvinyl Chloride (PVC), Low Density Polyethylene (LDPE), High Density Polyethylene (HDPE) and Ethylene Glycol Plants process the ethylene produced at the Ethylene Plant. On the other hand, Polypropylene and Acrylonitrile Plants process the propylene. The other products of the Ethylene Plant are the aromatic oil, C_4, fuel gas, H_2 and the unconverted feedstock which is fed to the Aromatic Plant.

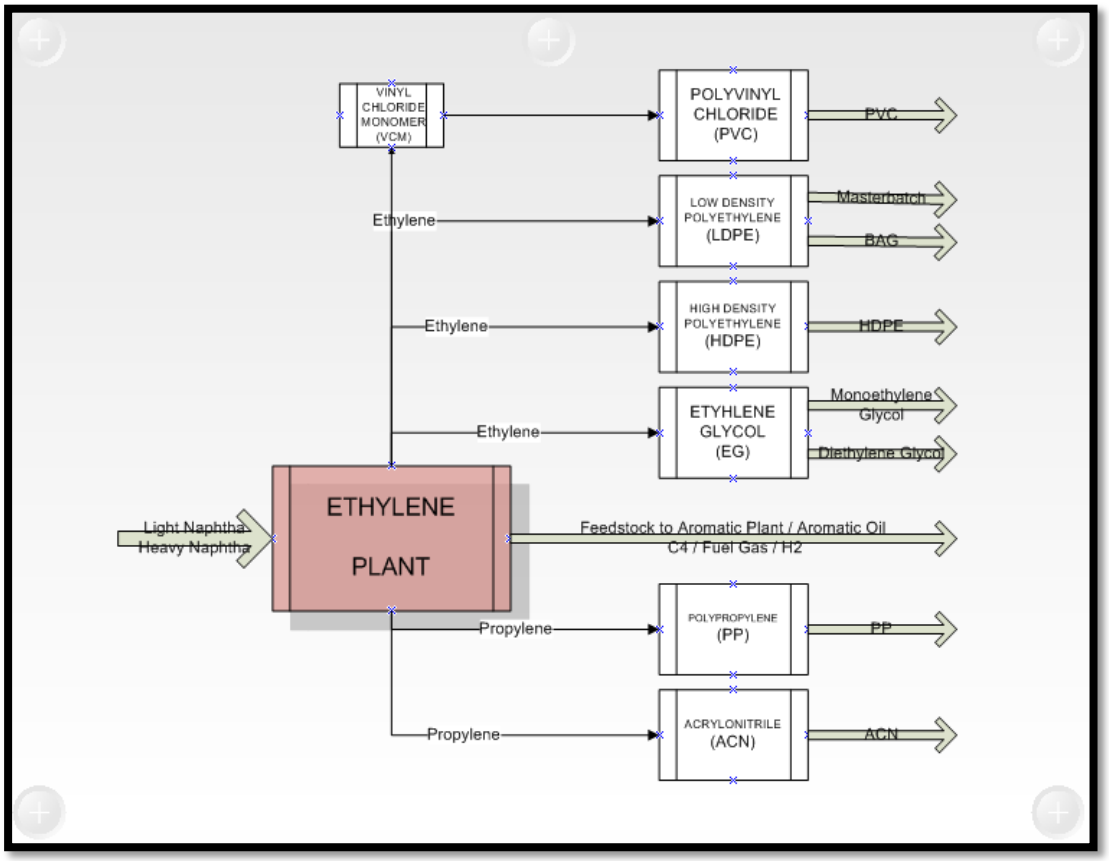

Figure 3.5 Ethylene Plant in the Petrochemical Complex (PETKIM Case)

The Ethylene Plants can be divided into two main sections named hot section and cold section. The hot section comprises the furnace at which the feedstock is cracked to olefins. On the other hand, the cold section comprises sequential distillation columns to separate and purify the effluent of the furnace (Geem, 2006).

The cracker of the ethylene plant can be divided further into three sections named radiation section, transition section and convection section as can be seen on Figure 3.6. The radiation section comprises the long adjacent tubes which serve as a reactor. Theses tubes are suspended in a gas fired furnace and the endothermic steam

cracking reactions take place inside these tubes by the heat provided from the gas burners. The heat of flue gas which is generated in the furnace is recovered in the convection section by preheating the feed, dilution steam. In addition, some amount of high pressure steam can be produced in the convection section and this produced steam might be used in steam-driven equipment like turbines. The next zone is the quench/transition section at which the effluent of the furnace is quenched by heavy oil and water. The purpose of this section is to cool the effluent to terminate the reactions. As the water cools the reactor effluent, the heat is recovered as steam to be used in the petrochemical complex (Geem, 2006).

The other section of the ethylene plant is the cold section where the purpose is to separate and purify the products. First of all, the gaseous product of the hot section should be liquefied by compressing. Later on, the liquefied products are fed to various distillation columns to be separated as ethylene, propylene, a crude C_4 fraction, pyrolysis gasoline and fuel gas. Moreover, additional distillation columns may take place to improve the purity further such as propylene splitter unit, butadiene extraction unit to separate 1,3 butadiene and aromatics extraction unit to recover benzene, xylene and toluene (Geem, 2006).

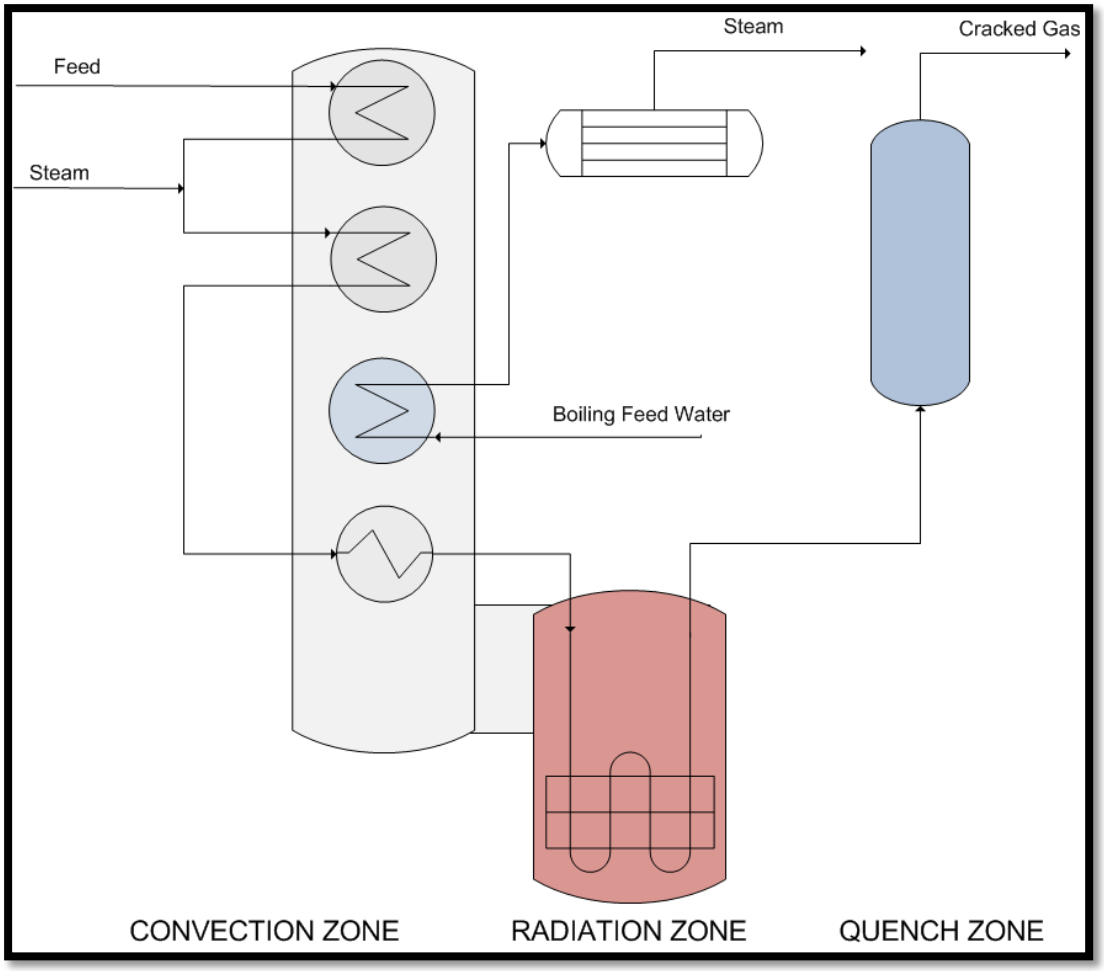

Figure 3.6 Typical Steam Cracker

3.3 Furnace Types

The main purpose of the furnace (instead of simple heat exchangers) is to supply the vast amount of heat for the process fluid so that temperature can be increased to high values. The furnace can also be named as process heater and fired heater depending on the involved industry. The furnaces can be classified according to the service, tube arrangement, combustion air supply and burner location. The furnaces may serve as a reboiler of the distillation column, fractionator column preheater, reactor feed preheater and fired reactors. The tubes can be arranged as horizontal or vertical inside the combustion chamber. Combustion air can be supplied by induced fan at the stack or compressor at the inlet of the combustion chamber. Moreover, the burners can be located at the bottom, side and top of the combustion chamber or namely radiation zone. The Figure 3.7 represents the furnace classifications.

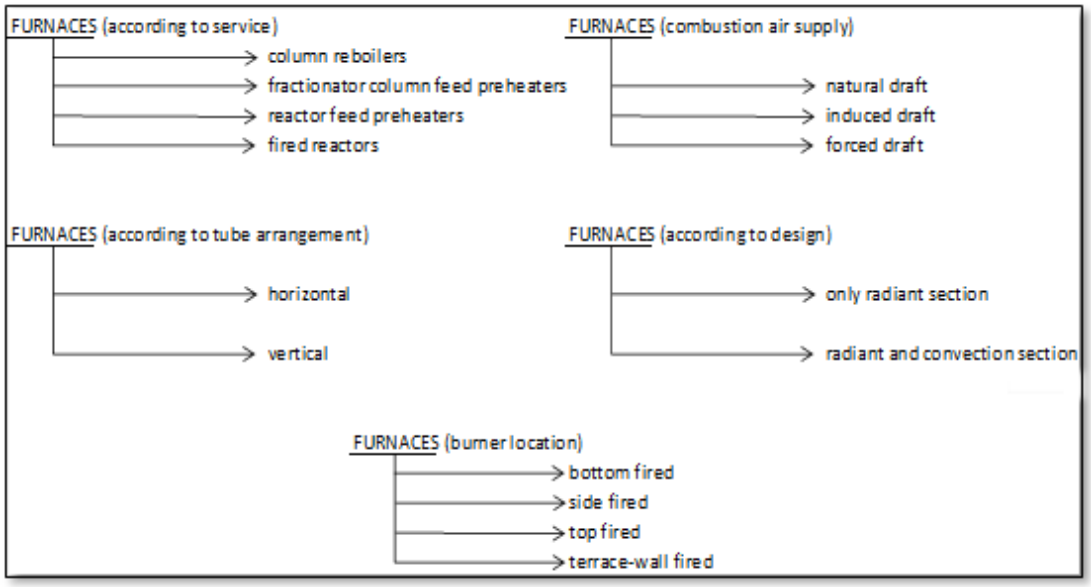

Figure 3.7 Classification of the furnaces

Column reboilers, are the mildest and the least critical application of the furnace types. The bottom product of the distillation column is heated up by the furnace to partially vaporize the stream. Later on, the heated and partially vaporized stream is recirculated to the distillation column in order to heat up the distillation column bottom. In these types of furnaces there is relatively small differential between the temperature of inlet and outlet streams and partial vaporization can take place.

Fractionating column feed preheaters, area widely used in the refinery and petrochemical industry. These types of the furnaces are used for increasing the temperature of the fractionator feed. The outlet temperature of the furnace should be high enough to achieve the partial vaporization before feeding the stream to the fractionator column. Reactor feed preheaters, are mainly used for increasing the temperature of reactants to the level which is required for the control of the reactions taking place at the reactor which is adjacent to the furnace. The feed for this type of the furnaces can be single phase/single component, single phase/multicomponent and mixed phase/multicomponent. Fired reactors, are the most sophisticated furnace types at which the reaction takes place through the coils of the furnace. The coils in the furnace may be filled with the catalyst. Steam reformers and pyrolysis (thermal cracking) heaters are the major applications of this type of the furnaces in the petrochemical industry. Reforming reactions take place over nickel based catalyst through the coils inside the furnace to yield hydrogen rich gas in the steam reformers.

On the other hand, olefins are produced from gaseous or liquid feedstock by thermal cracking through the coils inside the furnace in the pyrolysis heaters. Rather than the classification according to service, there are also different applications of the furnaces according to the layout, design, detailed mechanical construction and tube arrangements. The choice of the design depends on the investment capital, required furnace efficiency and the service to be used for. Typically, the simplest type of the furnaces is the "all radiant" design wherein the coils are all located inside the combustion chamber and the flue gas is directly flows through the stack as can be seen in Figure 3.8. The capital investment and normally the thermal efficiency are low for this kind of design. The heat in the flue gas is lost through the stack. On the other hand, most modern furnaces include convection section also as can be seen in Figure 3.9. Convection section includes some coils which are located on the way to stack after the radiant section. The residual heat which is flowing through the stack is used for heating the coils which generally includes the feedstock for preheating or some other fluids to be heated up or several grade (such as MP and HP) steam production. The additional convection section increases the thermal efficiency of the furnace although the capital investment increases, too.

The other classification of the furnaces is related with the orientation of the coils in the radiant section. The furnaces can be classified as vertical or horizontal according to the coil orientation in the radiation box. The vertical coil arrangement of the coils can be accomplished either with only radiant section or with the radiant and convection section. The majority of the new projects in the petrochemical industry prefer to construct vertical furnaces with the convection section above the radiation zone as can be seen on Figure 3.10. These types of furnaces provide an economical, high efficiency design with the minimum plot area. Typical duty of these furnaces varies between 0.01 MJ/h and 200000 MJ/h. In addition, the tubes of the vertical furnaces can be designed as straight tube or U-tube according to the process fluid.

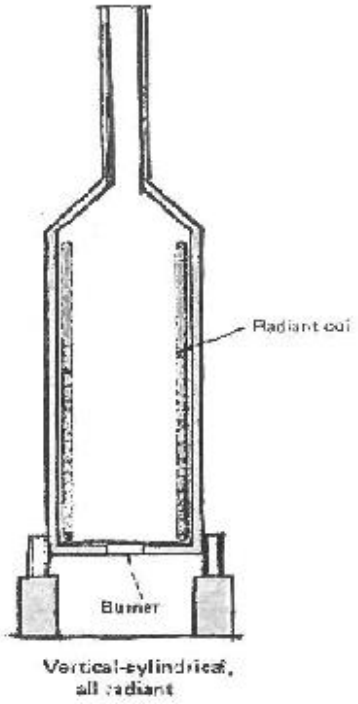

Figure 3.8 All radiant/vertical design

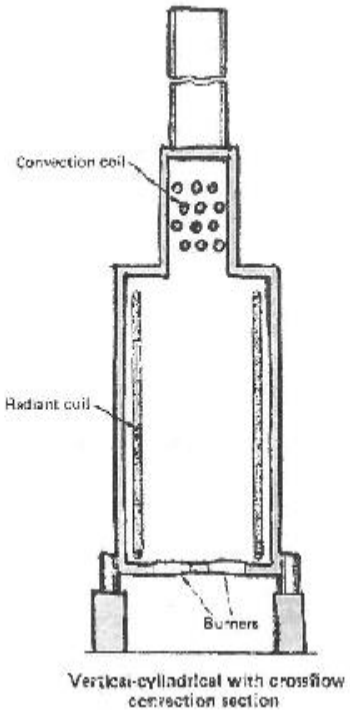

Figure 3.9 Vertical design with convection

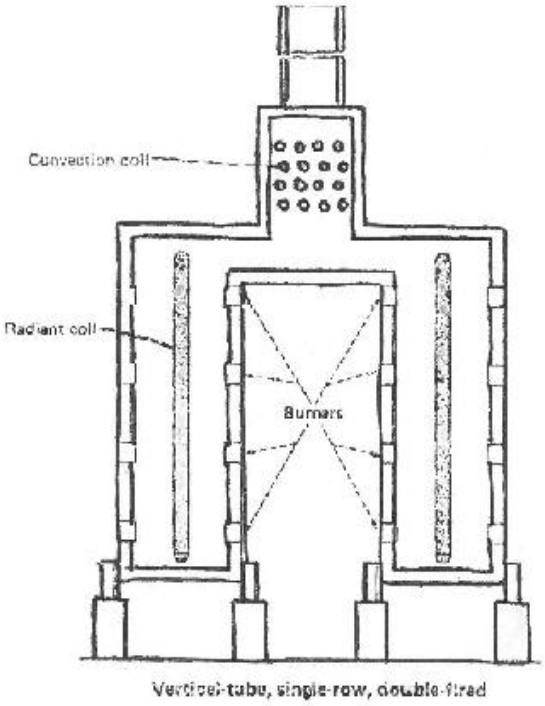

Figure 3.10 Vertical/double-fired design

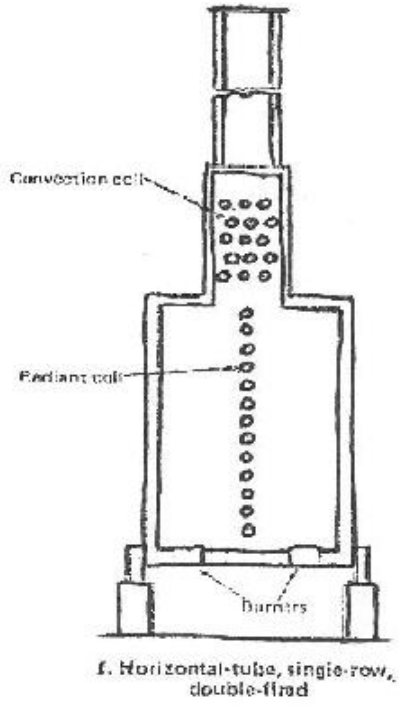

Figure 3.11 Horizontal design

All these tube arrangements directly affect the pressure drop along the reactor length. U-tube arrangement is generally suitable for heating large flow of gas with low pressure drop. Moreover, the furnaces with horizontal coil arrangement (Berman,

1978) as in Figure 3.11 can also be used for special purposes. The furnaces can also be categorized according to combustion air supply, flue-gas removal and burner arrangement. The natural draft furnaces introduce the combustion air and remove the flue gas by the stack effect. The hot flue gas inside the combustion box creates a draft pressure which is less than the atmospheric pressure. As a result, the combustion air is induced naturally through the combustion box/radiation section and flue gas is removed naturally through the stack. If there exist any obstruction to the flow of the flue gas, pressure greater than the atmospheric pressure can result in the radiation section. For these cases, an induced draft fan can be used to maintain the negative pressure inside the radiation section with the stack. Forced draft furnace includes a compressor which supplies the combustion air under positive pressure. However, it should be noted that although the compressor outlet has a positive pressure, the inside of radiant section remains with negative pressure during the operation.

The PETKIM Ethylene Cracker Furnace which is studied in this study is a vertical, side fired, natural draft fired reactor with a convection section above the radiant section. Ethane crackers have similar design that is shown in Figure 3.9 whereas naphtha cracker furnace in PETKİM has similar design that is shown in Figure 3.10. The modern conventional cracking furnaces can be operated with the residence time between 0.8-0.25 seconds, which is provided by the reduced tube diameters. Since ethane is harder to crack when compared with naphtha, ethane cracking requires higher residence time.The reduced tube diameters which vary between 25.4-101.6 mm (1-4in.) provides higher surface to volume ratio. Thus, the required heat for cracking can be provided in a shorter distance which will also reduce the residence time. As the residence time decreases, the formation of the byproducts decrease and the ethylene yield increases. The ratio of the length of the tube to the inside diameter is an important design parameter. The optimum value for this parameter is determined as 500 (Tham, 2014).

CHAPTER 4

REACTIONS AND VARIABLES IN ETHYLENE PRODUCTION

Petrochemical intermediates constitute a great portion of the petrochemical industry. The main processes which are involved in intermediate manufacture are steam reforming, catalytic reforming and steam cracking. As can be seen on the Figure 4.1, various kinds of intermediates can be produced by the related conversion technology from many feed stocks which range from methane and ethane to naphtha and gasoil.

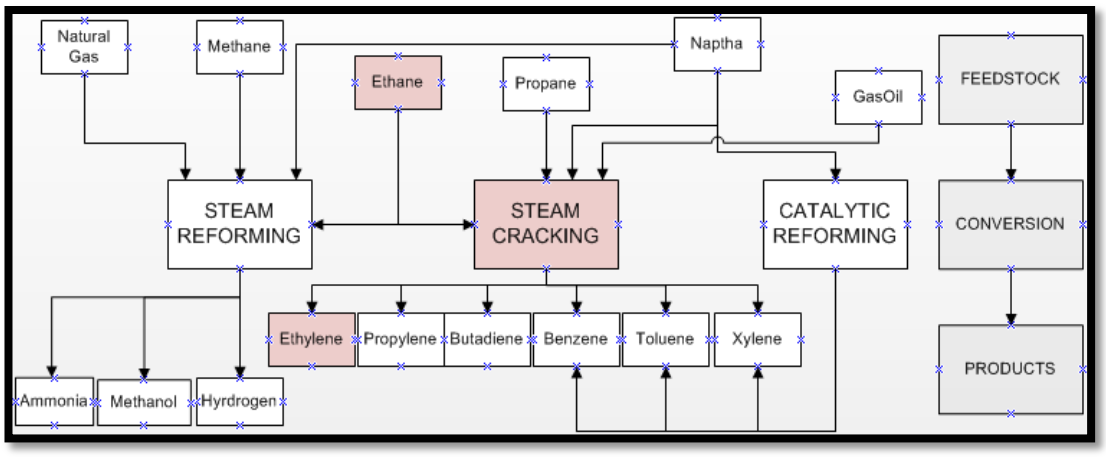

Figure 4.1 Overall intermediate productions in petrochemical industry (Matar and Hatch, 1981)

4.1 Steam Reforming, (Wiseman, 1986)

Steam reforming process produces a mixture of carbon monoxide and hydrogen from natural gas and methane if they are available. Otherwise, naphtha can also be used as a feedstock. The main applications of the steam reforming are the ammonia and methanol production. In addition to ammonia and methanol production, it is also widely used in refineries to produce hydrogen gas, which is required for many hydrogenation and cracking reactions.

4.2 Catalytic Reforming, (Wiseman, 1986)

Catalytic reforming process is used for manufacturing petrochemicals such as benzene, toluene and xylene. The main feedstock for catalytic reforming is naphtha. If naphtha is also used as a major feedstock for ethylene plant in petrochemical complex, then ethylene plants produce the important amounts of aromatic hydrocarbons. Catalytic reforming reactions also take place in the refineries to improve the octane number of the hydrocarbon, especially, if naphtha is used in the gasoline pool.

4.3 Steam (Thermal) Cracking, (Wiseman, 1986)

Steam cracking is also known as a thermal cracking which processes different kinds of hydrocarbons to produce ethylene. The feed stocks for steam cracking may vary from ethane, propane to naphtha and gas oil depending on the price and availability.
If ethane is used as a feedstock for ethylene production, ethylene is the major product. In addition, propane, as a feedstock, produces significant amount of propylene as by-product. On the other hand, processing of naphtha/gasoil produces propylene, butene, butadiene and aromatic hydrocarbon in addition to ethylene. Because of these valuable intermediate petrochemicals in the ethylene plants, steam crackers are crucial equipments of the petrochemical complexes.

Processing ethane as feedstock for ethylene production minimizes the production of methane, propylene and C_4 hydrocarbon as by-products. However, selection of ethane as feedstock requires high coil outlet temperatures for cracking reactions.

Besides that, strong refractories are required. On the other hand, heavier hydrocarbons than ethane require higher investment costs due to more complex design of cold separation unit (Geem, 2006). The common feedstock for olefin production in Europe is naphtha, to supply the high demand for LPG and gas oil. PETKIM, the domestic company for olefin production, also utilizes naphtha as a feedstock (Geem, 2006).

4.4 Reactions involved in Steam (Thermal) Cracking

The reactions which are involved in steam cracking can be divided as; primary thermal cracking, secondary thermal cracking, and dehydrogenations, cycloaddition of butadiene and ethylene, dehydrogenation of resulting aromatics and condensation reactions which lead to coke formation (Wiseman, 1986). The thermal cracking, dehydrogenation and coke formation reactions become significant if the process gas temperature is above 700^{o}C, 800-850^{o}C and 900-1000^{o}C, respectively (Wiseman, 1986).

The thermal cracking reactions of ethane can be analyzed by series of free radical reactions which are given in Equations 4.1 to 4.4. Assumed reactions are divided into four steps: initiation, hydrogen abstraction, radical decomposition and termination. In case of high operating temperature and long residence time, the olefins and the other hydrocarbons which form in the termination step decompose further (Tham, 2014).

The cracking reactions initiate with the formation of two alkyl radicals as a result of breaking C-C bonds Equation 4.1. C-C bonds are less stable than C-H bonds. Therefore, C-C bond breakage takes place at first in the reaction mechanism. Later on, propagation step starts and it involves three main steps: hydrogen abstraction and addition, radical decomposition and radical isomerization. Hydrogen transfer reactions takes place in order to form a new molecule by the abstraction of hydrogen atom. Radical decomposition provides the hydrogen atom and hydrogen addition reaction forms the new radical as given by Equation 4.4 these can be seen on the following scheme provided below.

The final step of the reaction mechanism is the termination step at which the radicals disappear and the products form. The termination reactions occur after the collision of two radical molecules or the collision of the radical with the tube wall. Collisions of two radicals are more frequent while the redox properties of the metallic structure of the tube involve in the termination reactions (Angeria, 2008).

Initiation	$C_2H_6 \rightarrow CH_3* + CH_3*$	(4.1)
Hydrogen Abstraction	$CH_3* + C_2H_6 \rightarrow CH_4 + C_2H_5*$	(4.2)
Radical Decomposition	$C_2H_5* \rightarrow C_2H_4 + H*$	(4.3)
	$H* + C_2H_6 \rightarrow H_2 + C_2H_5*$	
Termination	$H* + H* \rightarrow H_2$	(4.4)
	$H* + CH_3* \rightarrow CH_4$	
	$H* + C_2H_5* \rightarrow C_2H_6$	
	$C_2H_5* + CH_3* \rightarrow C_3H_8$	
	$C_2H_5* + C_2H_5* \rightarrow C_2H_5*$	

4.5 Coke Formation

The condensation reactions which lead to coke formation become more significant if the process gas temperature is above 900-1000^{o}C. Thus, high temperature and long residence time should be avoided to prevent the coke formation. In addition, DMDS injection sulfurizes the steel which reduces the catalytic activity of iron and nickel which in turn reduces the first mechanism coke formation (Hernandez, 2012).

Coke formation is related with the operating conditions such as operating temperature, residence time and steam to hydrocarbon ratio. As the coke layer covers the tube, the pressure drop along the tube increases and the tubes have to be heated to high temperatures to overcome the reduced heat transfer because of coke formation. As a result, coke formation not only increases the energy consumption but also reduces the tube life (Froment et al., 1994).

Coke formation during thermal cracking occurs with three different mechanisms. Firstly, catalytic phase takes place during which the tube material catalyzes the coke precursors to form coke deposits on the tube wall. Generally, steam cracking units

are constructed with heat resistant alloys of Fe-Ni-Cr. These metals also promote the deposition of coke precursors. Some coatings on the reactor surface and some additives can be used to prevent this first mechanism. This mechanism has the highest rate at the starting period of the operation, and for the low operating temperatures between 500-600^{o}C (Cai et al., 2002).

After the inner surface of the tube is covered with coke, second heterogeneous and non-catalytic mechanism starts. The gas phase coke precursors react with the cokes which cover the inside of the wall of the furnace. The contribution of this mechanism to overall coke formation is much less for light feedstock such as ethane and for the operating temperatures lower than 900^{o}C (Cai et al., 2002).

The third mechanism for coke formation is the homogenous non-catalytic mechanism during which condensation products remain on the coke layer inside the tube wall. In the condensation reaction two or more small molecules react with each other to form heavier and more stable compound such as cyclo-diolefins and aromatics. The gas phase composition is important for the contribution of this mechanism. In addition, the coke formation with this mechanism also depends on some characteristics such as surface area, porosity, C/H ratio of the coke layer which is formed by the first mechanism (Cai et al., 2002).

4.6 Process Variables for Steam Cracking

Steam cracker acts both as a reactor and a fired heater. Thermal cracking of feed (ethane) occurs through tubular coils. These coils are placed vertically within the furnace and require vast amount of heat in order to maintain necessary reaction conditions. Steam cracking operation is affected by many variables such as operation temperature, pressure, residence time. The cracking temperature depends on the feedstock used. The hydrocarbons with high molecular weight crack at low temperatures, whereas the hydrocarbons with lower molecular weight are difficult to crack and necessitates higher process temperatures are required. For example, the outlet temperature of ethane cracker is around 800-850^{O}C, while the outlet temperature is around 675-700^{o}C for naphtha or gasoil. The steam cracking reactions are highly endothermic reactions; therefore high temperature increases the rate of

formation of olefins and aromatics. However, high temperature also increases the rate of coke formation. Therefore, optimum temperatures are selected to maximize the olefin production and minimize coke formation (Froment et al., 1994).

The downside of the tube is exposed to a higher temperature which increases the coking rate and coke formation which reduces the life of the tube. This bottleneck encourages the engineers to develop the technology to suppress coke formation and better materials for the tubes to resist higher temperatures (Matar and Hatch, 1981). The overall cracking reactions increase the total molar flow rate of the gaseous species. Therefore, lower operating pressure favors the cracking reaction. Modern steam crackers operate under low pressures such as 175-240 kPa (Matar and Hatch, 1981).

Residence time affects the formation of aromatics and higher molecular weight hydrocarbons as a result of secondary reactions of formed olefins. Therefore, short residence time is required for higher olefin yield. However, residence time is also affected by the reaction temperature and other process variables (Matar and Hatch, 1981). As a result of cracking reactions, the number of moles increases. Therefore, the production of olefins as a result of cracking is favored at low pressure. Steam reduces the partial pressure of the hydrocarbon mixture which favors the olefin production. Therefore, olefin yield increases as a result of the increase in steam/hydrocarbon ratio. In addition, steam is required to reduce the coke deposition. For example, steam to hydrocarbon ratio varies between 0.3-0.4 for ethane feedstock and 1.0-1.2 for heavier feedstock such as gas oil and petroleum residues (Matar and Hatch, 1981).

The rates of feedstock for steam cracking depend on the structure and molecular weight of the hydrocarbon. Paraffinic hydrocarbons can be cracked more easily than the cyclo-paraffin and aromatics. In addition, the iso-paraffins such as iso-butane and iso-pentane give higher yields of propylene. The heavier feedstock with lower H/C ratio reduces the ethylene yield and increases the required amount of feedstock to produce the unit of ethylene production. In addition, liquid by-product and aromatic production increase dramatically with heavier feedstock (Matar and Hatch, 1981).

Ethane provides a high ethylene yield with minimum production of by-products of methane, propylene and C_4 hydrocarbon. The required furnace outlet temperature for the cracking is higher for ethane than the other heavier feedstock such as propane and liquid feedstock. On the other hand, propane provides lower ethylene yield, higher propylene and butadiene yields with more aromatic pyrolysis gasoline. The residual gas which consists of methane and H_2 is about two and half times greater for propane cracking. In addition, the separation section is more complex since the by-product formation is greater (Matar and Hatch, 1981).

There are many feed stocks which can be utilized for steam cracking such as light naphtha, full range naphtha, reformer raffinate, atmospheric gas oil residues and crude oils. The steam to carbon ratio is greater and the residence time is lower for the liquid feedstock than the gas feedstock. Depending on the source of the feedstock, the aromatic and sulfur content may increase. The presence of aromatic content reduces the ethylene yield and increases the heavy fuel oil production. In addition, the presence of sulfur in the feedstock may require additional desulfurization unit for feedstock to avoid further treatment sections (Matar and Hatch, 1981).

CHAPTER 5

PETKIM STEAM ETHANE CRACKER

Steam crackers are the main building blocks of petrochemical industry. ABB Lumnus Global is the first company that build steam cracker for an ethylene plant in 1942. They are also the first company that built vertical coil cracking furnaces with a capacity of 200,000 metric tons per annum (MTA) in 1960. They improved their designs to process ethane propane mixture and also they reduced the residence time of feed which is an important parameter for the operation below one second. Kellog, Brown and Root (KBR) which is another Engineering Procurement and Construction EPC Contractor also signed a license agreement with Exxon Mobile for novel coil configuration technology in steam crackers, Selective Cracking, Optimum Recovery Technology (SCORE) in 1998.

Finally Stone & Webster (S&W) which is another EPC Contractor is known with their major ethylene plant revamps. This contractor built PETKİM Ethylene Plant in 1985 with a initial capacity of 300,000 ton/ year ethylene production. But according to investments done, capacity of the plant is increased to produce 520,000 ton/ year ethylene in 2005 at maximum capacity usage. This capacity is expected to increase to 588,000 ton ethylene per year by November, 2014. Main feedstock to ethylene plant namely thermal crackers is naphtha this could be either light naphtha, LPG or FCC Gas from petroleum refinery. At current conditions there are nine naphtha and one ethane cracker operated in the ethylene plant. First of all light naphtha imported or transported from petroleum refinery is fed to naphtha crackers. Produced ethane as a result of naphtha cracking is recycled back to separate ethane cracker which enables the engineers to increase ethylene selectivity or to increase ethane conversion. All effluent streams from both naphtha and ethane crackers are collected at the cracked gas header and sent to fractionation section of the ethylene plant. Hot section of the

plant includes only the naphtha and ethane crackers whereas fractionation section which includes many distillation columns which are named as demethanizer, deethanizer, depropanizer and debutanizer, respectively. These hot and cold sections of the plant can roughly be seen in the following Figure 5.1. Steam crackers which are located at the back scene are shown in Figure 5.1. Before giving more details of ethane cracker at PETKİM Co. some points should be emphasized among naphtha and ethane crackers in general. Since naphtha which is roughly C_5-C_6 fraction, it is easier to crack when compared with C_2, ethane cut.

Figure 5.1 Steam Cracker and Fractionator (Hot& Cold) sections of the ethylene plant (Alper, 2012)

These naphtha crackers require less residence time about 0.2-0.3 sec. that is 0.2-1.2 sec. for ethane crackers through coils. And also heat duty of naphtha crackers is lower than that of ethane cracker. Cracking reactions take place at the radiant section of the furnaces. And required temperature value at the radiant section is about 850-900^{o}C for ethane crackers and lower for naphtha crackers. At the outlet of the cracker there is a quench boiler/ tower in which collected effluent streams are suddenly cooled to prevent further cracking and polymerization reactions especially. One of the advantages of these high duty crackers are their steam production/generation capabilities. Each extra tons of steam produced affect directly plant profit. Figure 5.2

shows the process steam generators. In this study, PETKİM steam ethane cracker is modeled, where naphtha cracker effluent ethane is recycled back to ethane cracker for ethylene production. Ethane feed is divided into two main streams and they are fed to convection section of the furnace. These streams are heated up to 450^{o}C at the inlet of radiant section. Dilution steam is injected and mixed with heated ethane feed afterwards combined stream goes through radiant section where reactions take place at about 850^{o}C. The point of using steam as a diluting medium is to reduce hydrocarbon partial pressures. Since cracking reactions are reversible, reducing the partial pressures will drive the reactions towards product side which in turn increases ethane conversion and the ethylene production, respectively.

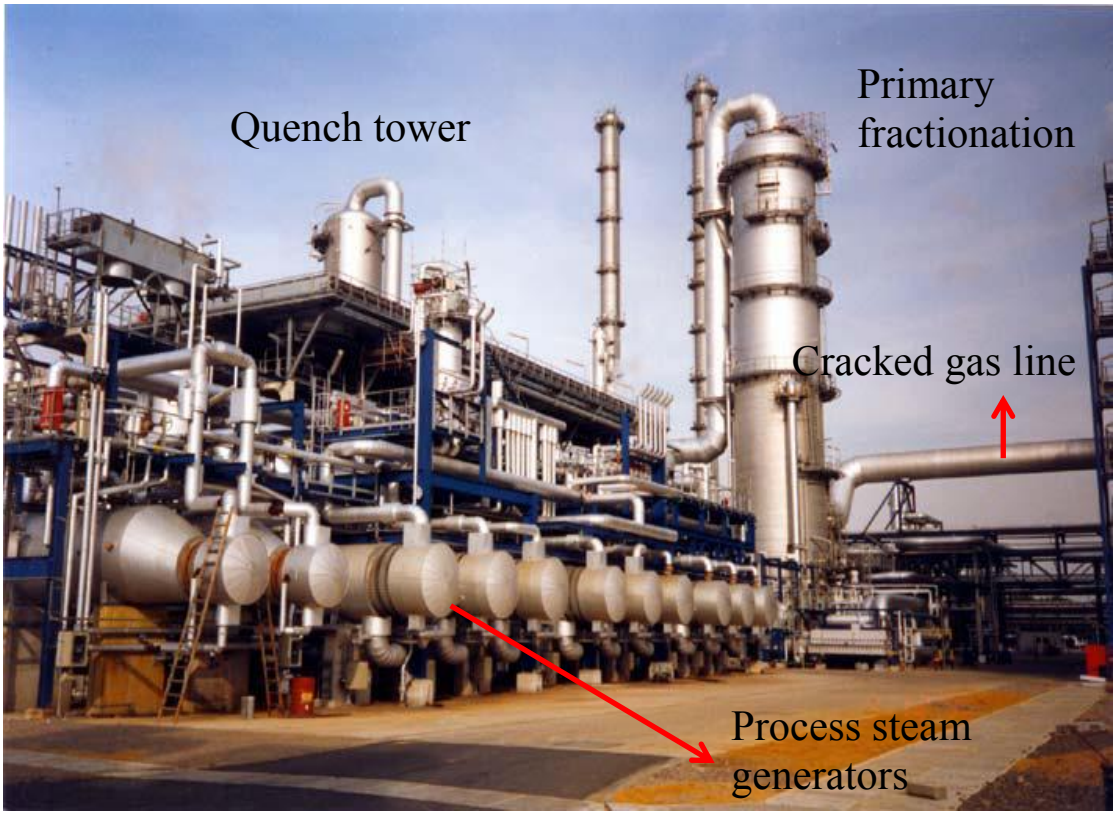

Figure 5.2 Ethylene Plant view including quench boiler, primary fractionator and process steam generators (Alper, 2012)

In Figure 5.3 the steam cracker furnace configuration is shown. They are known as vertical-tube, single row, double fired type furnace. At the top of the furnaces separate stacks and one quench boiler for collected effluent streams are placed. Below the stack, convection section which combines two radiant sections is also placed. The point at which convection ends and radiant section begins is the mixing

point of diluting steam and ethane feed. That point might be seen clearly on the isometric view of the cracker provided in Figure 5.4. Details of the furnace types are given in Chapter 2.

Figure 5.3 Steam Crackers in Ethylene Plant (Alper, 2012)

It is seen in Figure 5.4 that heat is supplied to furnace through wall burners. In PETKİM, as it is stated feed stream that is ethane produced from naphtha cracker is divided into two separate streams. Coils are placed vertically, but at the bottom of the furnace they have U or S shaped configuration which reduces pressure drop along the reactor length. Then on the effluent stream there is a quench boiler which suddenly cools down the streams from nearly 850^{o}C to 450^{o}C to prevent further reactions such as polymerization reactions. After quench boiler collected cracked streams are sent to fractionation section as a result final products such as propylene and ethylene are produced.

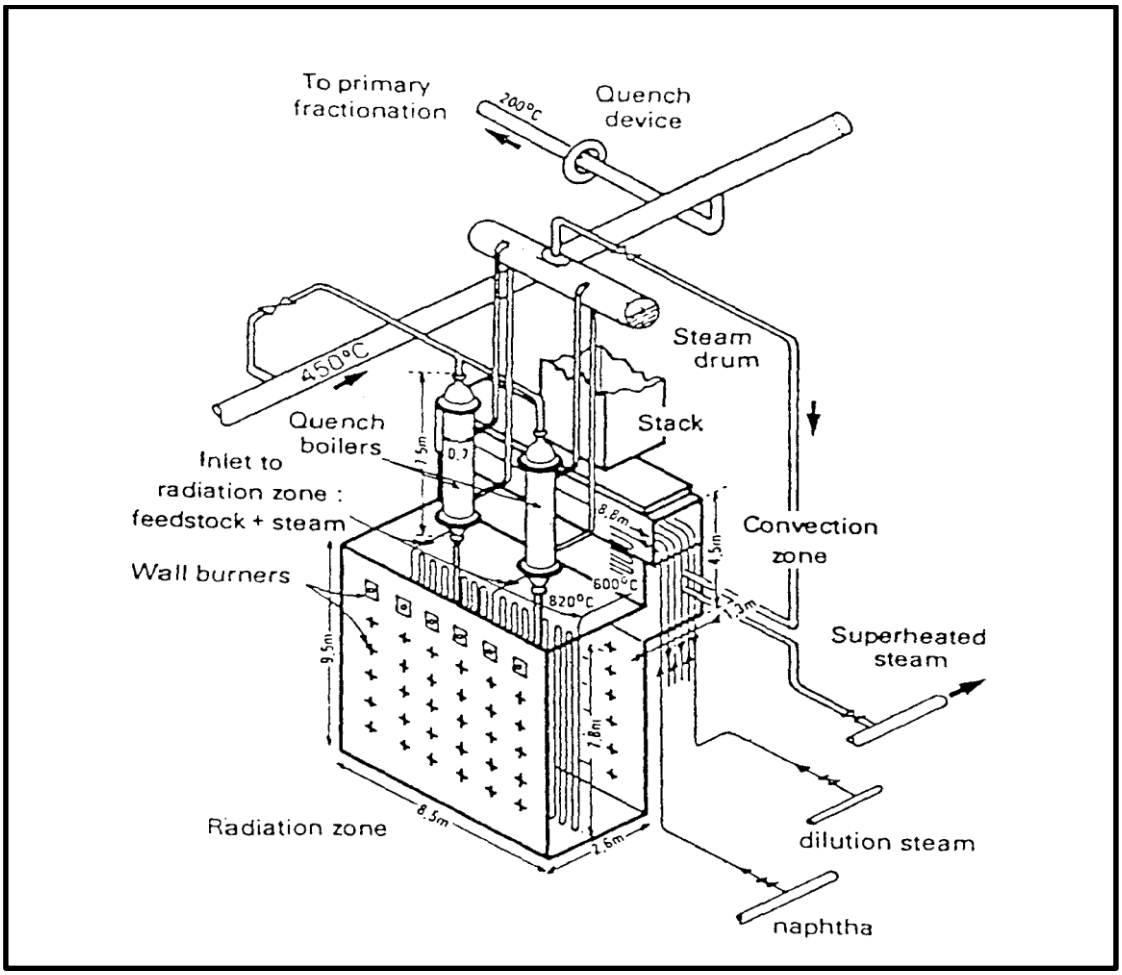

Figure 5.4 Isometric view industrial Steam ethane cracker (Alper, 2012)

The geometric specifications of PETKİM steam cracker is given in Table 5.1.

Table 5.1 Geometric details of the ethane cracker at PETKİM

Internal tube diameter, m	0.121
Tube wall thickness, m	0.011
Outer Tube diameter, m	0.132
Center-to-center distance, m	0.254
Tube length, m	10.4
Number of tubes per coil	15

5.1 Modeling Studies for Ethylene Production

Ethylene production process might be divided into two main sections which are basically hot section where thermal cracking of hydrocarbon feedstock occurs into lighter components and the cold section where fractionation of the product streams takes place. This chapter focuses on the reaction network modeling of the tubular flow reactors which are placed vertically in fired heater/furnace (hot side). According to literature survey there are two approaches for modeling (Rase, 1977);

- Molecular reaction scheme
- Free-radical mechanism based reaction scheme

Free-radical mechanism includes thousands of compounds; both molecular and free-radical state components. Both approaches conduct quasi same assumptions such as taking heat flux per tube as constant. When free-radical mechanism is considered as a basis for network modeling complexity increases and the solution rate in the use of MATLAB software slows down. Therefore, molecular reaction network which is widely accepted and used in many researches [references] is also used in this study. In the following sections, molecular reaction scheme will be presented.

5.2 Molecular Reaction Scheme

Thermal cracking operation has wide range of feed stocks from heavier to lighter; Heavy vacuum gas oil (HVGO), naphtha, ethane / propane mixture and only ethane like in this study. Some crackers also differ from each other according to their feedstock condition liquid or vapor. In this study ethane at quasi pure state (99 %mol C_2H_6) is to be processed, all the feed and product components will be in gas state. The assumptions done for mathematical modeling in molecular reaction scheme are given below (Yancheshmesh and Haghighi, 2013).

1. The gas mixture is assumed as an ideal gas due to relatively high temperature and low pressure.
2. The length of the tube is very long, and the tube diameter is much smaller than the length of the tube. Thus, the radial gradients such as mass, heat and concentration are neglected.
3. Quasi-steady state is assumed to simulate the coke deposition rate.
4. Plug flow pattern is employed.
5. The velocity through the coils is nearly constant.
6. The second mechanism of coke formation which is the heterogeneous non-catalytic mechanism is the most dominant mechanism for the operating conditions of the industrial cracking units.

5.2.1 Mass Balance Equation

In the molecular reaction scheme the continuity equation of mass for each component in the steady state is given in Equation (5.1).

$$\frac{dF_j}{dz} = R_j * \frac{\pi {d_t}^2}{4} = \left(\sum_i \alpha_{ij} * r_i\right) * \frac{\pi {d_t}^2}{4} \quad (5.1)$$

Where above F_j and R_j are the molar flow rate and rate of reaction of component j, respectively. Also (i) denote the number of reactions; (j) denotes the number of components and α_{ij} is i^{th} component stoichiometric coefficient in the j^{th} reaction.
General rate expressions are given and as stated in Equation (5.2) and concentration of components are calculated in the Equation (5.3) by assuming ideal gas law.

$$r_i = k_i \prod {C_j}^{\alpha_j} \quad (5.2)$$

$$C_j = \frac{F_j}{\sum_{j=1}^{n} F_j} \frac{P_t}{RT} \quad (5.3)$$

5.2.2 Energy Balance Equation

Energy balance Equations (5.4) and (5.5) give the temperature profile, T (z), of the process gas within the tubes as a function of reactor length. In the energy balance equation, c_{pj} corresponds to the specific heat capacity of each component which varies with respect to the temperature along the tube. On the other hand, ΔH_i represents the heat of each reaction which is a function of both temperature and the concentration of the components along the tube. Thus, heat of reactions as well as heat capacity of components must be calculated in order to determine the temperature profile along the tubes.

$$\sum_{j=1}^{9} F_j c_{pj} * \frac{dT}{dz} + \frac{\pi {d_t}^2}{4} \sum_i \Delta H_i * r_i = q(z) * \pi d_t \tag{5.4}$$

$$\frac{dT}{dz} = \frac{1}{\sum_{j=1}^{9} F_j c_{pj}} \left[q(z) * \pi d_t + \frac{\pi {d_t}^2}{4} \sum_i (-\Delta H_i) * r_i \right] \tag{5.5}$$

For the calculation of the heat capacity values of components, an appropriate expression from literature is used (Perry, 1997) but the crucial point to be determined is whether the selected expression is valid for the operation temperature range or not. Applicability of the selected hyperbolic expression shown in Equation (5.6) for the heat capacity is valid for temperature range of 800-1300 K. Numerical values of the coefficients used in the expression will be tabulated in the Development of MATLAB Model Section.

$$c_p = C1 + C2 * \left[\frac{({}^{C3}/_{T})}{\sinh({}^{C3}/_{T})} \right]^2 + C4 * \left[\frac{{}^{C5}/_{T}}{\cosh({}^{C5}/_{T})} \right] \tag{5.6}$$

Specific heat of mixture can be calculated by multiplying each component by its heat capacity molar fractions. Heats of formation of reactants which are denoted by (j) at standard state are found using (Perry, 1997). The required heat amount to increase the compound temperature from reference state temperature T_{ref} to process gas temperature, T is evaluated by the use of heat capacities calculated using Equation (5.6).

The heats of reactions can be calculated for the reactions considered by the expressions given in Equation (5.7) and (5.8).

$$\Delta H_{fj} = \Delta H_{fj}{}^{o} + \int_{T_{ref}}^{T} c_{pj} dT \tag{5.7}$$

$$-\Delta H_i = -\sum_j \alpha_{ij} \Delta H_{fj} \tag{5.8}$$

5.2.3 Momentum Balance Equation

The momentum balance equation around the tubular reactor can be expressed by Equation (5.10). In the expression, f represents the Fanning Friction Factor, whereas ζ represents the Nekrasov factor for the bends, r_b represents for the radius of the bends and the u represents for the velocity of the gas inside the tube.

$$-\frac{dP_t}{dz} = \left[\frac{2f}{d_t} + \frac{\zeta}{\pi r_b}\right] * \rho_g u^2 + \rho_g u \frac{du}{dz} \tag{5.9}$$

Equation (5.10) must be rearranged and the total pressure P_t must be expressed only in terms of changes in process temperature and flow rates of components as a function of reactor length (z). G; the mass flux, M_m ; the molecular weight of the process gas.

$$u = \frac{M_m F_t}{\rho_g \frac{\pi {d_t}^2}{4}} = \frac{G}{M_m} \frac{RT}{P_t} \tag{5.10}$$

When derivative of Equation (5.11) is taken with respect to reactor length (z), Equation (5.12) is obtained

$$\frac{du}{dz} = \frac{GR}{P_t} \left[T \frac{d\left(\frac{1}{M_m}\right)}{dz} + \frac{1}{M_m} \frac{dT}{dz}\right] - \frac{G}{M_m} \frac{RT}{{P_t}^2} \frac{dP_t}{dz} \tag{5.11}$$

Equation (5.9), (5.10) and (5.11) can be solved for pressure variation along the tube as given in Equation (5.12).

$$\frac{dP_t}{dz} = \frac{\frac{d}{dz}\left(\frac{1}{M_m}\right)+\frac{1}{M_m}\left[\frac{1}{T}\frac{dT}{dz}+\left(\frac{2f}{d_t}+\frac{\zeta}{\pi r_b}\right)\right]}{\frac{1}{M_m P_t}-\frac{P_t}{G^2 RT}} \tag{5.12}$$

And molecular weight variation along the tube is given below Equation (5.13)

$$\frac{d}{dz}\left(\frac{1}{M_m}\right) = \frac{d}{dz}\left(\frac{\sum_j F_j}{G}\right) = \frac{\sum_j \frac{dF_j}{dz}}{G} \tag{5.13}$$

The Fanning Friction Factor f, for straight tubes can be correlated to Reynolds number assuming turbulent flow in the tubes with highly roughness as (Yancheshmesh and Haghighi, 2013).

$$f = 0.046 Re^{-0.2} \tag{5.14}$$

where;

$$Re = \frac{d_t\, G}{\mu_{mixture}} \tag{5.15}$$

The pressure losses through the bends can be evaluated using Nekrasov factor (Yancheshmesh and Haghighi, 2013) that is given in Equations (5.16) and (5.17).

$$\xi = \left(0.7 + \frac{\Lambda}{90^o}\, 0.35\right) \xi' \tag{5.16}$$

where;

$$\xi' = (0.051 + 0.19\, \frac{d_t}{r_b}) \tag{5.17}$$

These ordinary differential equations are written in a MATLAB code, parameters related to mixture values evaluated separately. In order to get the outputs one of the built in functions of MATLAB ode23 is used among the other built-in ODE solvers. As initial values, flow rates, process gas temperature and pressure at the inlet of the radiant section of an industrial steam ethane cracker of PETKİM Co. are used.

5.3 Models used in Simulations

Three different models are used for simulations. The first model is used in order to validate the model with the literature data and then the validated model is run with PETKIM operation values in the Model II and Model III. Model II includes the coke formation reactions additional to the model of Model I. Whereas, Model III includes additional coke removal reactions. The detailed information about the Models is specified in the following sections.

5.3.1 Model-I: Modeling without Coke Formation

Feedstock to be processed affects the types of the cracking reactions. The following network (Model-I) considers steam cracking of ethane (98.2%mol) and includes seven reactions, in which two of them are equilibrium reactions with eight hydrocarbon components and steam as a ninth component. Steam does not take place within the reactions only serves as a dilution medium. It's used for the reduction of the partial pressures of hydrocarbons If the one considers the partial removal of coke formed than steam should be included within the reaction network like the Model-III. Dilution medium steam or CO_2, (Yancheshmesh and Haghighi, 2013) directly affects the equilibrium reactions and shifts the reactions to product side. According to provided kinetic parameters two equilibrium reactions are evaluated separately. Table 5.2 shows the reactions considered for the thermal (steam) cracking of ethane and their Arrhenius constants, activation energies which are used in Equation (5.18).

$$k = A_O * e^{-\frac{E}{RT}} \tag{5.18}$$

Table 5.2 Reactions and kinetic parameters for the thermal cracking of ethane (Froment and Bischoff, 1979)

Reactions	A_o (s-1) or (m^3/ kmol.s)*	E (kcal/kmol)	E (j/mol)
1. $C_2H_6 \rightarrow C_2H_4 + H_2$	4.65E13	65,210	273,020
2. $C_2H_4 + H_2 \rightarrow C_2H_6$	*8.75E8	32,690	136,870
3. $2C_2H_6 \rightarrow C_3H_8 + CH_4$	3.85E11	65,250	273,190
4. $C_3H_6 \rightarrow C_2H_2 + CH_4$	9.81E8	36,920	154,580
5. $C_2H_2 + CH_4 \rightarrow C_3H_6$	*5.87E4	7,040	29,480
6. $C_2H_2 + C_2H_4 \rightarrow C_4H_6$	*1.03E12	41,260	172,750
7. $C_2H_4 + C_2H_6 \rightarrow C_3H_6 + CH_4$	*7.08E13	60,430	253,010

The continuity equations will be solved for the selected reaction network. The approach and procedure details for the other models are given as follows.

5.3.2 Model-II: Modeling with Coke Formation

In the Model-II, thermal (steam) cracking of ethane instead of naphtha or ethane/ propane mixture is considered. Reaction network includes eleven reactions and ten species which include coke formation reactions additionally.

Rate expressions (Yancheshmesh and Haghighi, 2013) for the Model-II reaction network are tabulated in Table 5.3. According to these expressions and kinetic parameters in Table 5.4, mass balance equations are solved.

Table 5.3 Reaction rate expressions for Model-II (Yanchesmeh and Haghighi, 2013)

Rate Expression	**Reaction**
$r_1 = k_1\left[\frac{F_{C_2H_6}}{F_t}\left(\frac{P_t}{RT}\right) - \frac{F_{C_2H_6}F_{H_2}}{{F_t}^2 Kc_1}\left(\frac{P_t}{RT}\right)^2\right]$	$C_2H_6 \leftrightarrow C_2H_4 + H_2$
$r_2 = k_2\left[\frac{F_{C_2H_6}}{F_t}\left(\frac{P_t}{RT}\right)\right]$	$2C_2H_6 \rightarrow C_3H_8 + CH_4$
$r_3 = k_3\left[\frac{F_{C_3H_8}}{F_t}\left(\frac{P_t}{RT}\right)\right]$	$C_3H_8 \rightarrow C_3H_6 + H_2$
$r_4 = k_4\left[\frac{F_{C_3H_8}}{F_t}\left(\frac{P_t}{RT}\right)\right]$	$C_3H_8 \rightarrow C_2H_4 + CH_4$
$r_5 = k_5\left[\frac{F_{C_3H_6}}{F_t}\left(\frac{P_t}{RT}\right) - \frac{F_{C_2H_2}F_{C4}}{{F_t}^2 Kc_5}\left(\frac{P_t}{RT}\right)^2\right]$	$C_3H_6 \leftrightarrow C_2H_2 + CH_4$
$r_6 = k_6\left[\frac{F_{C_2H_2}F_{C_2H_4}}{{F_t}^2}\left(\frac{P_t}{RT}\right)^2\right]$	$C_2H_2 + C_2H_4 \rightarrow C_4H_6$
$r_7 = k_7\left[\frac{F_{C_2H_6}}{F_t}\left(\frac{P_t}{RT}\right)\right]$	$2C_2H_6 \rightarrow C_2H_4 + 2CH_4$
$r_8 = k_8\left[\frac{F_{C_2H_6}F_{C_2H_4}}{{F_t}^2}\left(\frac{P_t}{RT}\right)^2\right]$	$C_2H_6 + C_2H_4 \rightarrow C_3H_6 + CH_4$
$r_9 = k_9\left[\left(\frac{F_{C_2H_4}}{F_t}\frac{P_t}{RT}\right)^{1.34}\right]$	$C_2H_4 \rightarrow Coke$
$r_{10} = k_{10}\left[\left(\frac{F_{C_3H_6}}{F_t}\frac{P_t}{RT}\right)^{1.34}\right]$	$C_3H_6 \rightarrow Coke$
$r_{11} = k_{11}\left[\left(\frac{F_{C_4H_6}}{F_t}\frac{P_t}{RT}\right)^{1.37}\right]$	$C_4H_6 \rightarrow Coke$

Table 5.4 Kinetic Parameters for Model-II (Yancheshmesh and Haghighi, 2013)

Rate Coefficient	**A** (s^{-1}) **or** $(l.mole^{-1}s^{-1})$	**E** **(j/ mole)**
k_1	4.65*E13	2.73*E5
k_2	3.85*E11	2.73*E5
k_3	5.89*E10	2.15*E5
k_4	4.69*E10	2.12*E5
k_5	9.81*E8	1.54*E5
k_6	1.03*E12	1.73*E5
k_7	6.37*E23	5.30*E5
k_8	7.08*E13	2.53*E5
k_9	5.00*E10	2.24*E5
k_{10}	2.77*E8	1.16*E5
k_{11}	5.61*E12	2.74*E5

For the formed coke, heat capacity expression will differ and their values must be added in the mixture heat capacity in Table 5.5.

Table 5.5 Coke Heat Capacity Expressions (Perry, 1997)

Name	**Form**	**Heat Capacity at constant P** **(cal/ mol.K)**	**Temperature range** ^{o}**K**
Carbon	Graphite	$2.673+0.002617xT-116900/T^2$	273- 1373
Carbon	Diamond	$2.162+0.003059xT-130300/T^2$	273- 1373

5.3.3 Model-III: Modeling with Removal of Coke

There are two reactions as well as two components to be added to Model-II network. For the first two reaction networks, steam is only used as a dilution medium. But in Model-III steam reacts with formed coke and must be taken into account in the mass balance equation as well as energy and momentum balance equations. In Tables 5.6-5.9, certain data and parameters are added for CO and CO_2. Same solution algorithm is applied and results will be compared in Chapter 7.

Table 5.6 Added Component Properties for Model-III (Yanchesmeh, 2013)

Name	**Chemical Formula**	**Molecular Weight, kg/ kmol**	**Heat of Formation, kj/ mole**
Carbon Monoxide	CO	28	-110.60
Carbon Dioxide	CO_2	44	-393.80
Carbon	C	12	0

Table 5.7 Added rate expressions for Model-III (Yanchesmeh, 2013)

Rate Expression	**Reaction**
$r_{12} = k_{12}\left[\frac{F_{H_2O}}{F_t}P_t\right]$	$C + H_2O \rightarrow C + H_2$
$r_{13} = k_{13}\left[\left(\frac{F_{CO_2}}{F_t}P_t\right)^{0.31}\right]$	$C + CO_2 \rightarrow 2CO$

Table 5.8 Kinetic Parameters added reaction for Model-III (Froment et al., 1981)

Rate Coefficient	**A (s^{-1} or $l.mole^{-1}s^{-1}$)**	**E (j/ mole)**
k_{12}	5.09xE4	2.38xE5
k_{13}	1.12xE8	2.45xE5

Table 5.9 Industrial PETKİM Co. Steam Ethane Cracker SPYRO Data

Process Variables	**Units**	**Values**
Absorbed radiant heat duty	j/ m^2.s	4.775E8
Maximum coking rate	mol/ s	1.3168
Inlet pressure at the radiant zone	atm	3.37
Pressure Drop	atm	1.37
Ethane Conversion	----	0.60
Run length	day	90

As stated before, three different models are considered in order to reach the similar results with the plant data. Model-I includes the basic reaction mechanism in which neither coke formation nor coke removal reactions are involved. Model-II includes only coke formation reactions and finally Model-III includes coke removal reactions, additionally. Basic characterizations of these cases are summarized in Table 5.11. In Model-II and Model-III equilibrium reactions are not evaluated separately as it is done in Model-I.

Table 5.10 Properties of the Evaluated Models

	Model –I	Model – II	Model - III
Number of components	9	10	12
Number of reactions	7	11	13
Coke formation	--	✓	✓
Coke Removal	--	--	✓

Model-I includes two equilibrium reactions but according to data available, they are evaluated separately as can be seen in Figure 5.5. So total number of reaction in Model-I is seven. The same reactions also take place in Model-II but first and fourth reactions are taken as equilibrium reactions. In addition to these reactions coke formation reactions are included in the Model-II. And finally Model-III is formed by adding coke removal reactions into reaction network.

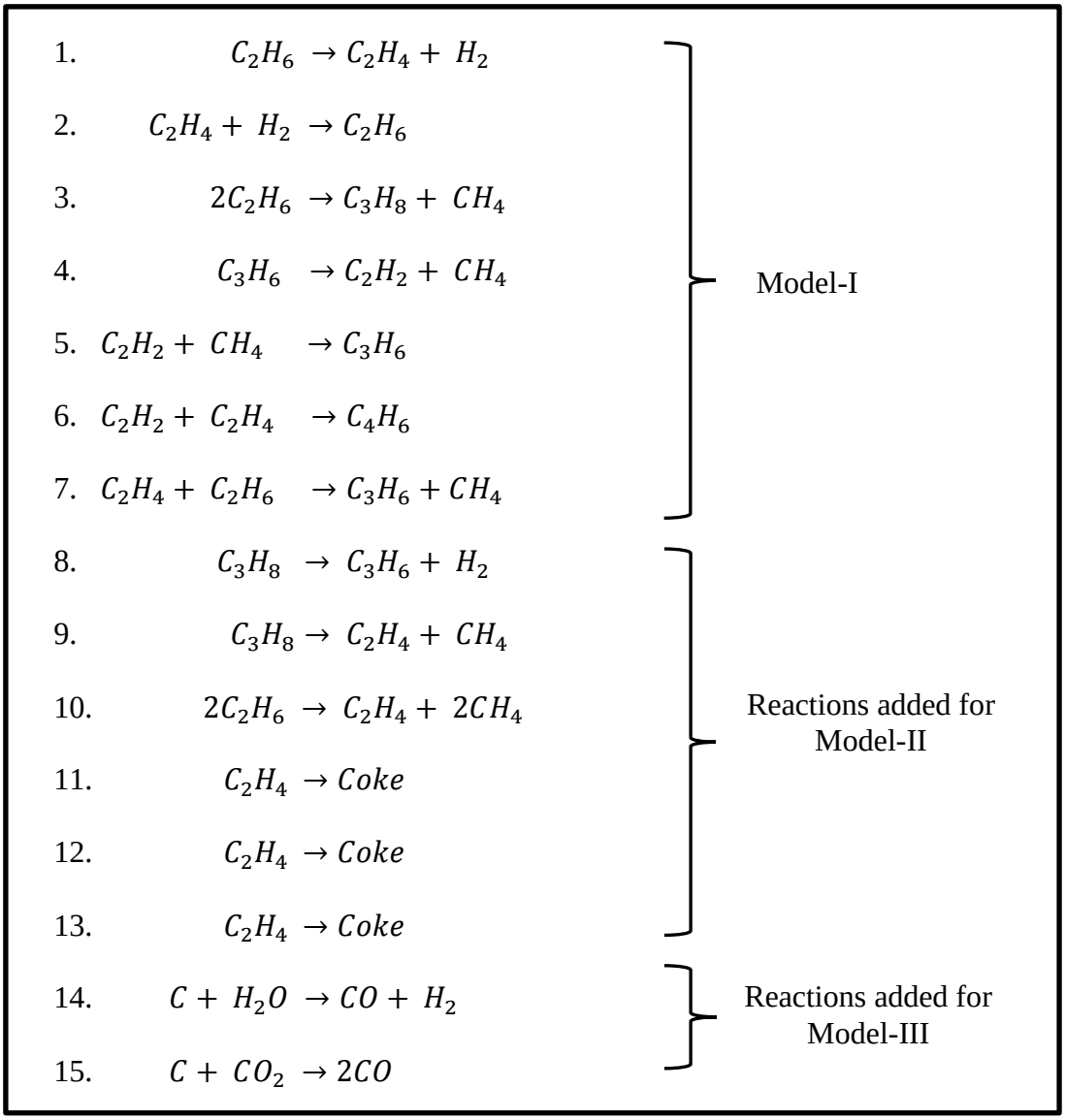

Figure 5.5 Reactions used in modeling studies

CHAPTER 6

MATLAB CODE FOR MATHEMATICAL MODELING OF STEAM CRACKER

In order to carry out mass, energy and momentum balance for the selected ethane cracking reaction scheme, firstly all property values should be calculated for the reaction mixture, such as molecular weight mixture (BMM), heat capacity (CP) etc. After defining the molar fraction of so-called components mixture properties can be calculated such as mixture molecular weight (BMM). Table 6.1 shows the properties of components used in the MATLAB code. The terms which are expressed with (i) or (z) notation are varying along the tube in the steam cracker furnace.

$$F(i) = y(i), \ {}^{mol}/_{s} \tag{6.1}$$

$$FT = FT + F(i), \frac{mol}{s} \tag{6.2}$$

$$yy(i) = \frac{F(i)}{FT} \tag{6.3}$$

$$BMM = BMM + \ yy(i) * BM(i) \tag{6.4}$$

Table 6.1 Reaction Network Component Properties (Perry, 1997)

Name	**Chemical Formula**	**Molecular Weight, kg/kmol**	**Heat of Formation, kj/mole**
Ethane	C_2H_6	30,07	-84.74
Ethylene	C_2H_4	28,05	+52.34
Propane	C_3H_8	44,1	-103.9
Propylene	C_3H_6	42,08	+20.43
Acethylene	C_2H_2	26,04	+226.90
Methane	CH_4	16,04	-74.90
1-3 Butadiene	C_4H_6	54	+110.2
Hydrogen	H_2	2	0
Steam	H_2O	18,02	-242.00
Carbon	C	12	0

The concentration of each component to be used in the rate expressions are calculated using Equation (6.5). The reaction rate expressions are stated in the Chapter 5 for each case.

$$C(i) = \frac{F(i)*T(z)}{FT*RX*P(z)} \tag{6.5}$$

According to heat capacity expression given the Equation (6.6), the tabulated coefficients which are given in Appendix section are used and then the heat capacity of the mixture values can be calculated.

$$CP(i) = C1 + C2 * \left[\frac{\left(C3/T(z)\right)}{\sinh\left(C3/T(z)\right)}\right]^2 + C4 * \left[\frac{C5/T(z)}{\cosh\left(C5/T(z)\right)}\right] \tag{6.6}$$

$$CPT = CPT + yy(i) * CP(i) \tag{6.7}$$

As previously stated enthalpy of formation of components (DHFOi) at standard states are found from literature and indicated in the Table 6.1 (Perry, 1997). And in order to calculate the component enthalpy (DHFi) at process gas temperature Equation (6.8) can be used.

$$DHF(i) = DHFO(i) + \int CP(i)dT \tag{6.8}$$

Then, the heat of reaction is calculated for each reaction by using the Equation (6.9).

$$DH(i) = DHF(i)products - DHF(i)reactants \tag{6.9}$$

To calculate pressure drop through the coil mixture viscosity must be determined before. Mixture viscosity can be found using Equation (6.10).

The critical temperature, pressure, volume and compressibility factors of the mixture are calculated along the furnace by using the parameters tabulated in the Table A.2.

The viscosity of the mixture can be calculated by using the Yoon-Thodos Model as given by the Equation (6.10).

$$VISC = \frac{46{,}1\ TRM^{0.618} - 20.4\exp(-0.449\ Tr) + 19.4\exp(-4.058Tr) + 1}{2.173424 * 10^{11}\left(Tc^{\frac{1}{6}}\right)(BMM^{-1})(Pc^{-\frac{2}{3}})} \tag{6.10}$$

where T_c, P_c are critical values for temperature and pressure.

The heat flux for radiant section of the furnace is assumed and set as variable and optimized as a result of the modeling. Finally, the continuity equations (Equations 6.11-6.12) are established and solved by MATLAB ODE to calculate the temperature, pressure, concentrations and conversion variation along the tube.

$$\frac{dF_j}{dz} = \left(\sum_i R(i)_j * AC\right) \tag{6.11}$$

$$\frac{dT(z)}{dz} = \frac{Qz*PI*DT+SUMDHR*AC}{CPT*FT} \tag{6.12}$$

$$\frac{dP(z)}{dz} = \frac{\left(\frac{SUMYDOT}{G}\right)+\frac{\frac{dT(z)}{dz}}{G}+\left(\frac{FF}{DT}+\frac{EE}{PI.RB}\right)}{\frac{BMM}{\left(\frac{1}{(BMM*P(z)-\frac{P(z)}{RX*G^2*T(z)})}\right)}} \tag{6.13}$$

6.1 Heat Flux Algorithm Development

Heat flux per tube is taken as constant in the all performed analysis for the selected cases. It is adjusted in order to reach desired ethane conversion value. Thus, the total amount of heat required for the reaction as well as its distribution along the tube length are the main aim of this written algorithm. In the kinetic modeling approach, heat flux values scaled up and used to achieve / approach the conversion as well as temperature profile along the reactor length. Procedure is started with the heat amount taken from the kinetic modeling code. In Table 5.1, geometric details of industrial steam ethane cracker are given.

$$q_z\left(\frac{1}{\pi d_t}\right)\left[\sum_{j=1}^{9} F_j cp_j \frac{dT}{dz} + \frac{\pi {d_t}^2}{4}\sum_i \Delta H_i r_i\right], [j/m^2 s] \tag{6.14}$$

First, heat flux values per tube are assigned and then both the output of ode solver and the result of Equation 6.14 are compared whether these two values are same. Then that total radiant heat flux value is defined as global which means value is used among separate m.files.

Furnace efficiency η (eitha) and the excess air to burners (x_{excess_air}) are taken 0.75 and 0.25, respectively. Center-to-center (ctc) distance among the tubes is taken as 0.254 m (Tham, 2014). Net heat released, Q_n in [Btu/ Ib] by the furnace is expressed in Equation 6.15.

$$Q_n = \frac{Q_{total}}{\eta} \tag{6.15}$$

The fraction of net heat release that is absorbed by the radiant section is assumed to be 0.75, x_{rad}. So the total radiant heat amount is given in Equation 6.16.

$$Q_{rad} = x_{rad} * Q_{total} \tag{6.16}$$

The average radiant heat flux, q_{rad} is assumed and then since total radiant heat amount is determined previously, A_{rad} which is the total area exposed to radiant heat is calculated.

$$A_{rad} = \frac{Q_{rad}}{q_{rad}} \tag{6.17}$$

$$L_{tube\_total} = \frac{A_{rad}}{(PI * d_{outer})} \tag{6.18}$$

The flue gas mass flow rate G_f in [lb/ MBtu] is found according to expressions below.

$$\frac{10^6 G_f}{Q_n} = 840 + 8 * x_{excess\_air} \quad with\ fuel\ oil \tag{6.19}$$

$$\frac{10^6 G_f}{Q_n} = 822 + 7.78 * x_{excess\_air} \quad with\ fuel\ gas \tag{6.20}$$

The cold plane area (A_{cp}) is defined in Equation 6.21

$$A_{cp} = \text{exposed tube length} * \text{ctc spacing} * \#\ \text{of tubes excl. of the sh. tubes} \tag{6.21}$$

The inside surface area of the shell (A_s) and the refractory area (A_w) are defined in Equation 6.22-6.23

$$A_s = 2 * [W * (H + L) + H * L] \tag{6.22}$$

$$A_w = 2 * [W * (H + L) + H * L] - A_{cp} \tag{6.23}$$

The absorptivity α of the tube surface with a single row of tubes is defined in Equation 6.24 and Equation 6.25, for the shield tubes $= 1$.

$$\alpha = 1 - [0.0277 + 0.0927(x - 1)](x - 1) \tag{6.24}$$

where

$$\text{x} = (\text{center} - \text{to} - \text{center spacing})/(\text{outside tube diameter}) \tag{6.25}$$

Thus absorptivity for the shell, refractory and absorptivity expressions the sum of products in the radiant zone is determined. αA_R is denoted as (M) and A_w/M is denoted as (N) in the code.

$$\alpha A_R = A_{shield} + \alpha A_{cp} \tag{6.26}$$

Shield tubes are placed between convection and the radiant zones. The number of shield tubes in the cracker is four.

$$M = (4) * L_{tube} * (ctc) + \alpha * A_{cp} \tag{6.27}$$

$$N = A_w/M \tag{6.28}$$

Since ethane cracker furnace has a box-shaped shell, then calculation of the mean beam length is expressed by the shell dimensions in Equation 6.29.

$$L = \left(\frac{2}{3}\right) * (W * H * L)^{\frac{1}{3}} \tag{6.29}$$

The partial pressures p of CO_2 and H_2O is given in terms of excess air fraction is given in Equation 6.30.

$$\text{p}= 0.288 - 0.229x_{excess\_air} + 0.090{x_{excess\_air}}^2 \tag{6.30}$$

Mean tube wall temperature is estimated according to inlet and outlet temperatures of radiant zone as given in Equation (6.31). T1 denotes inlet and T2 denotes the f(11) outlet temperature values, all in ^{o}F.

$$T_t = 100 + 0.5 * (T_1 + T_2) \tag{6.31}$$

Taking flue gas temperature as T_g, procedure initiates in order to find total radiant heat amount. In the following expressions emissivities of combustion gases (ϕ) are lumped and estimated.

$$\phi = a + b * (PL) + c * (PL)^2 \tag{6.32}$$

where

$$\text{PL} = \text{Equation (5.20)} * \text{Equation (5.19)} \tag{6.33}$$

$$z_{emis} = \frac{T_g + 460}{1000} \tag{6.34}$$

$$a = 0.47916 - 0.19847 * z_{emis} + 0.022569 * {z_{emis}}^2 \tag{6.35}$$

$$b = 0.047029 + 0.0699 * z_{emis} - 0.01528 * {z_{emis}}^2 \tag{6.36}$$

$$c = 0.000803 - 0.00726 * z_{emis} + 0.001597 * {z_{emis}}^2 \tag{6.37}$$

Then the exchange factor, F is calculated using the following equations

$$F = a\_exch + b\_exch * \phi + c\_exch * \phi^2 \tag{6.38}$$

$$z_{exch} = \frac{A_w}{M} \tag{6.39}$$

$$a_{exch} = 0.00064 + 0.0591 * z_{exch} + 0.00101 * {z_{exch}}^2 \tag{6.40}$$

$$b_{exch} = 1.0256 + 0.4908 * z_{exch} - 0.058 * {z_{exch}}^2 \tag{6.41}$$

$$c_{exch} = -0.144 - 0.552 * z_{exch} + 0.040 * {z_{exch}}^2 \tag{6.42}$$

The enthalpy of the flue gas Q_g as a function of temperature is estimated and Q_g/Q_n is denoted as K in the code.

$$\frac{Q_g}{Q_n} = \left[a + b\left(\frac{T}{1000} - 0.1\right)\right]\left(\frac{T}{1000} - 0.1\right) \tag{6.43}$$

$$a = 0.22048 - 0.35027 * z_{ent} + 0.92344 * {z_{ent}}^2 \tag{6.44}$$

$$b = 0.016086 + 0.29393 * z_{ent} - 0.48139 * {z_{ent}}^2 \tag{6.45}$$

where

$$z_{ent} = \text{fraction of excess air} \tag{6.46}$$

Radiant Zone heat transfer is calculated as

$$\frac{Q_R}{\alpha A_R F} = 1730\left[\left(\frac{T_g+460}{1000}\right)^4 - \left(\frac{T_t+460}{1000}\right)^4\right] + 7\left(T_g - T_t\right) \quad (6.47)$$

Radiant zone heat balance can further be formed as

$$\frac{Q_R}{\alpha A_R F} = \frac{Q_n}{\alpha A_R F}\left(1 + \frac{Q_a}{Q_n} + \frac{Q_f}{Q_n} - \frac{Q_L}{Q_n} - \frac{Q_g}{Q_n}\right) \quad (6.48)$$

Q_R = the enthalpy absorbed in the radiant zone

Q_a = enthalpy of entering air

Q_f = that of entering fuel

Q_L = enthalpy loss to the surroundings

Q_g = enthalpy of the gas leaving the radiant zome

Q_n = net enthalpy released in the furnace

CHAPTER 7

RESULTS AND DISCUSSION

In Chapter 5; mass, energy and momentum balance equations are solved simultaneously for three different models. As a result of these solution algorithms, process gas temperature profile, pressure drop along the tubes and component flow rates are determined. These algorithms were run with the same initial conditions taking 26.27mol/s ethane, 0.025mol/s propylene, steam-to-ethane ratio of 0.35, radiant zone inlet temperature of 889 K and 4atm inlet pressures for comparison.

PETKİM, the domestic ethylene producer, uses licensed SPYRO (steam pyrolysis) software for the evaluation of the operating parameters as well as yield and product distribution of the steam ethane cracker. Program has an embedded large reaction network both considering molecular and free-radical mechanisms. In addition to the comparison of three models, the output of the most accurate and realistic model is compared with the industrial plant outputs which are provided by SPYRO.

7.1 Model Validation

Model I is the simplest model which does not include coke formation and coke removal reactions. It was found by simulations in Model I that the required conversion value cannot be obtained for a reactor length of 160 m. As can be seen in Figure 7.1 the results can only be obtained at 100 m of reactor tube length. Therefore model validation will be done only for Model II and Model III. The proposed model in this study is validated with the models which are proposed by Froment and Sundaram in 1981 and Yancheshmeh in 2013. The Froment's model includes coke formation reactions in the reaction network. On the other hand, Yancheshmeh's

reaction network includes coke removal reactions in addition to coke formation reactions. Therefore, the proposed model in this study, which is named as Model II, is validated with the Froment's model results. Later on, the proposed model, which is named as Model III, is validated with the results of Yancheshmeh's model results.

In the first validation, the reference model is the one which is proposed by Froment and Sundaram in 1981. They have modeled the ethane cracker of which the input parameters are tabulated in Table 7.1. These input variables are used in the proposed model in order to validate the Model II. The comparison of the results is shown in Figures 7.1 – 7.4 and Table 7.2.

Table 7.1 Inlet Parameters which are used in Froment's model (Froment et al., 1981)

Inlet Parameters	
Length (m)	88.252
Diameter (m)	0.108
Radius of the Bend (m)	0.153
Inlet Temperature (K)	925.000
Inlet Pressure (bar)	2.900
Ethane Flow Rate (kmol/h)	66.474
Dilution Factor (kg)	0.510

Figure 7.1 and 7.2 show the results of the proposed model. The red dots on the graph indicate the results of Froment's model. According to Figures 7.1 and 7.2 the temperature and pressure variation along the tube can be calculated very closely with the Froment's results.

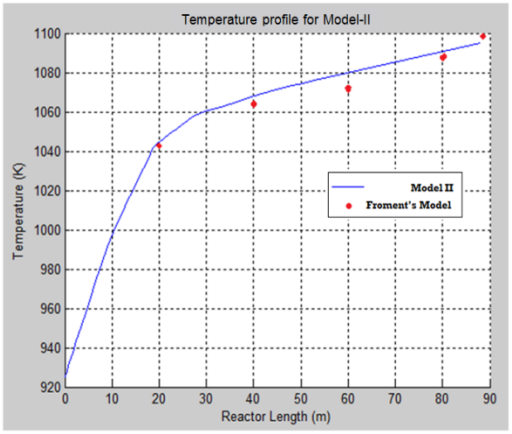

Figure 7.1 Temperature Profile

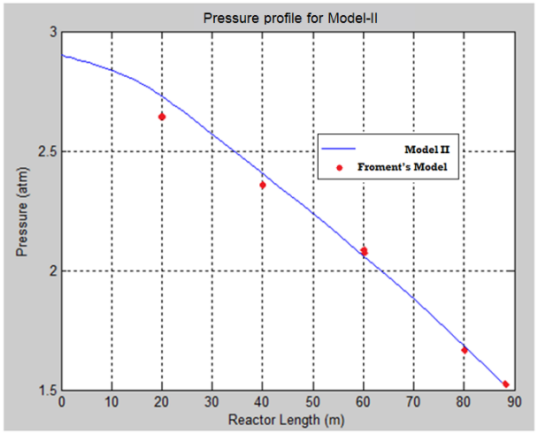

Figure 7.2 Pressure Profile

Furthermore, the product yields are also compared in the model validation as can be seen from Figure 7.3. Rather than temperature and pressure variation along the tube, there is a slight difference in the conversion of ethane between the proposed model and Froment's model. The difference in the conversions after 20m reactor length decreases by reactor length where finally difference reduces to 11%. The main reason of the difference may be due to the selected reaction network. The reaction network of Froment's model includes five reactions only, whereas the proposed model includes eight reactions in the reaction network. Froment's study uses as initial data which were obtained in a pilot plant scale set-up.

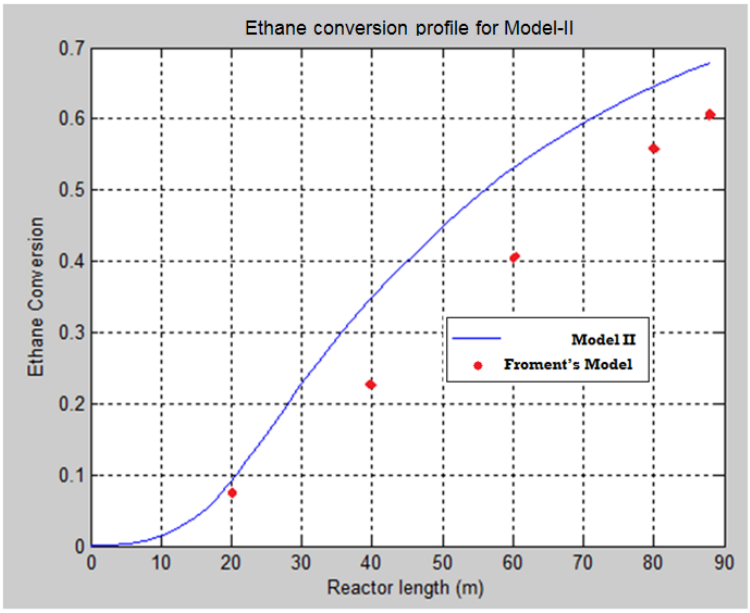

Figure 7.3 Ethane Conversion Profile

Moreover, Table 7.2 and Figure 7.4 represent the product yield of Froment's model and ethylene production result of the proposed model, respectively. According to the proposed study, ethylene production is calculated as 9.3mol/s at a reactor length of 90 m. That is also equal to 710.1 ton/cycle where the cycle length is assumed as 760h like in the Froment's study. On the other hand, ethylene production is calculated as 695.1 ton/cycle in Froment's study. Although this difference can be acceptable, the main reason is due to the number of reactions in the networks between this study and Froment's studies.

Table 7.2 Comparison of Froment and Model-II Outputs

Product Yields	**Froment's Study**	**Model II**
Conversion	59.2 %	68 %
Ethane Feed	1520.0 ton/ cycle	1520 ton/ cycle
Ethylene Production	695.1 ton/cycle	710.1 ton/ cycle
Cycle Length	760 h	760 h

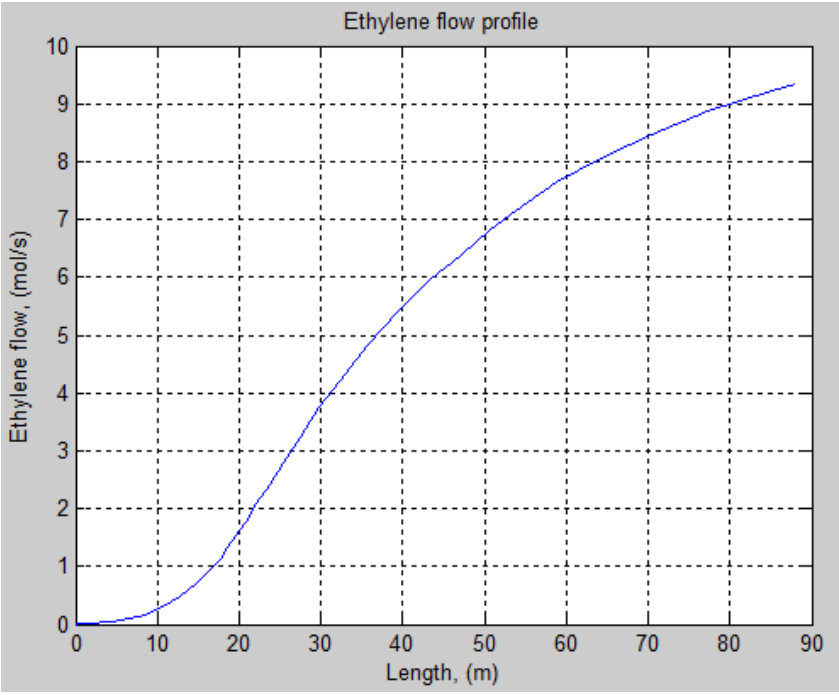

Figure 7.4 Ethylene Flow Profile

In the second validation, Yancheshmeh model is used to validate the eight-reactions network after validating model with respect to temperature and pressure variation. Yancheshmeh's Model includes not only eight-reactions but also coke removal reactions in the reaction network. Therefore, the model which is named as Model-III is used for comparison with the Yancheshmeh's Model. Table 7.3 tabulates the input variables for the proposed model which are taken from the Yancheshmeh's study. The required heat is provided in the model in such a way that, the coil outlet temperature is set to approximately 1150 K.

Table 7.3 Inlet Parameters which are used in Yancheshmeh's model

Inlet Parameters	
Length (m)	78.000
Diameter (m)	0.100
Radius of the Bend (m)	0.153
Inlet Temperature (K)	968.000
Inlet Pressure (bar)	3.090
Ethane Flow Rate (mol/s)	62.000
Dilution Factor (kg)	0.300

First of all, the heat balance is validated as can be seen in Figure 7.5 by comparing the temperature profile of the proposed model with the output of Yancheshmeh's Model. The temperature variation which is obtained from Yancheshmeh's Model is indicated as single red dots on Figure 7.5. The temperature is found to be approximately 40^{o}C lower which is the highest at the inlet. On the other hand, the difference decreases with length through the coil. The difference is found to be acceptable since it is due to the assumed heat flux which can be different in the Yancheshmeh's Model. As previously mentioned, the ethylene production reactions are highly endothermic. Therefore, the ethylene production is also found to be slightly less than Yancheshmeh's Model in the proposed model as can be seen on Figure 7.6 in accordance with the temperature profile.

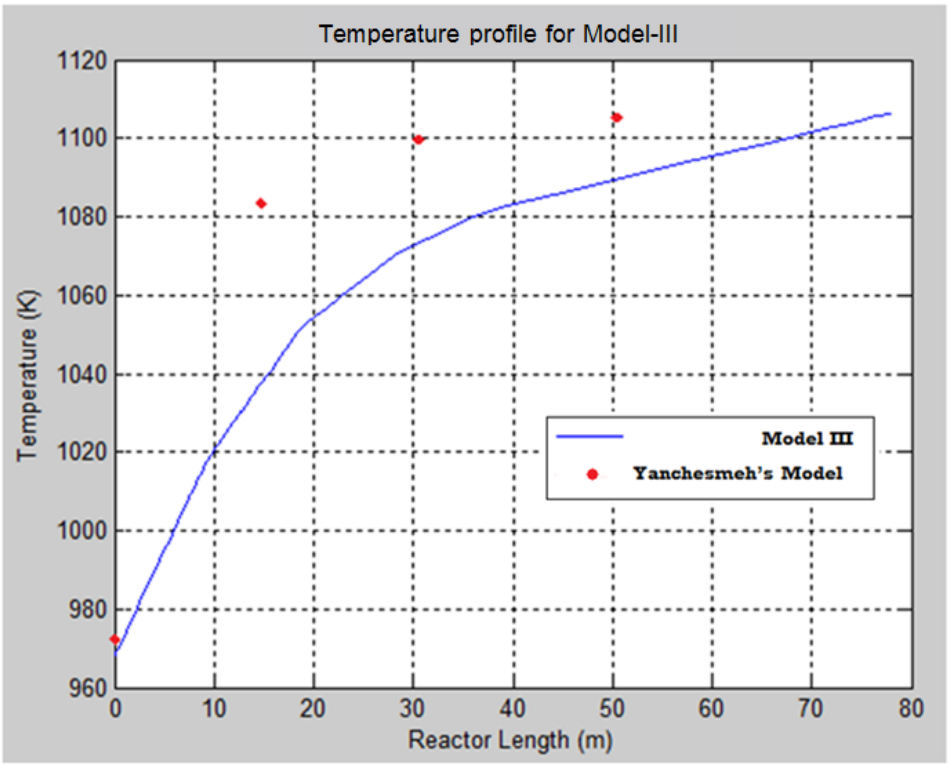

Figure 7.5 Temperature Profile

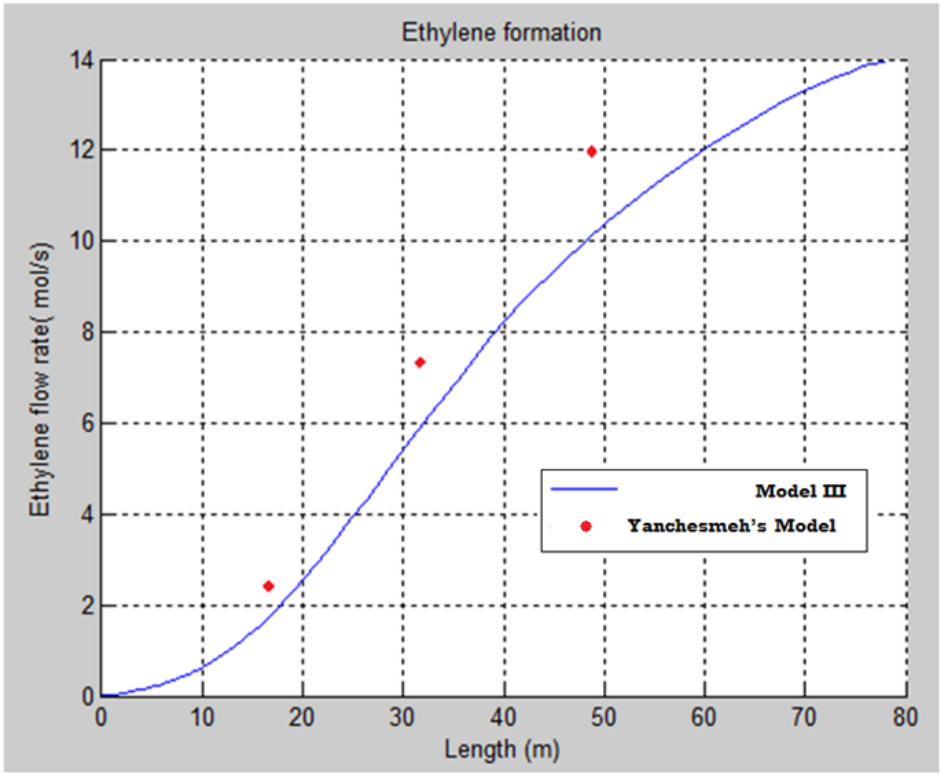

Figure 7.6 Ethylene Production

In addition, the ethane consumption which is calculated by the proposed model is represented on the Figure 7.7. It shows that the ethane consumption is also found to be very close with the Yancheshmeh's Model.

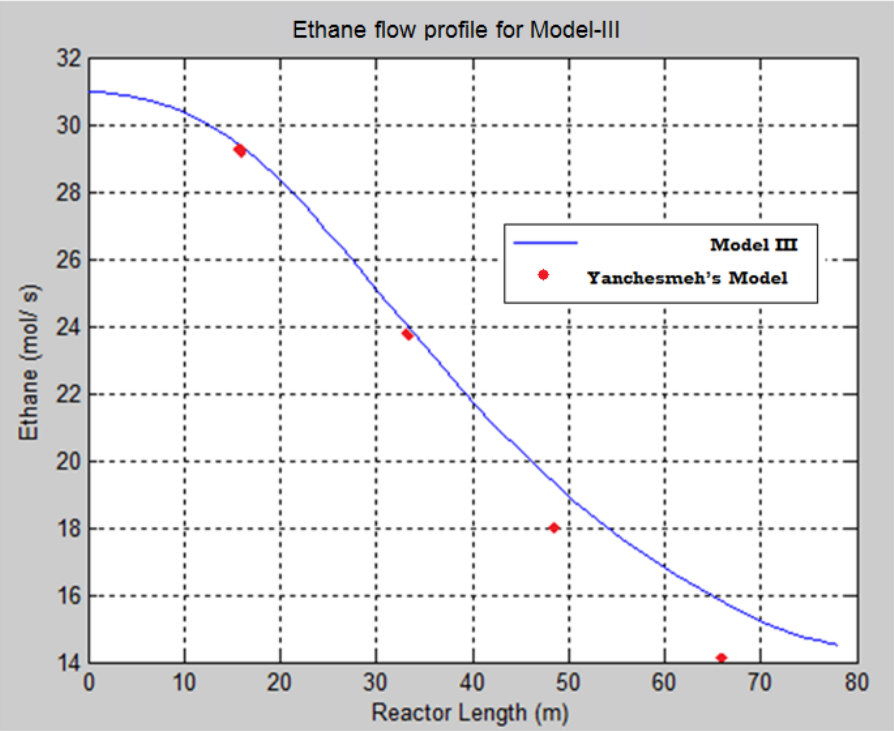

Figure 7.7 Ethane Consumption

Finally, the coke formation and the coke removal reactions are validated on the Figure 7.8. The coke formation increases through the outlet of the coil because of the temperature increment. The coke thickness is calculated by the model after 30 days of operation and the result is compared with the result in literature on Figure 7.8. As can be seen, the results are close at least at the outlet of the coil where the coke formation has the highest rate. Also, the coke formation started at the same location on the tube when compared with the Yancheshmeh's Model.

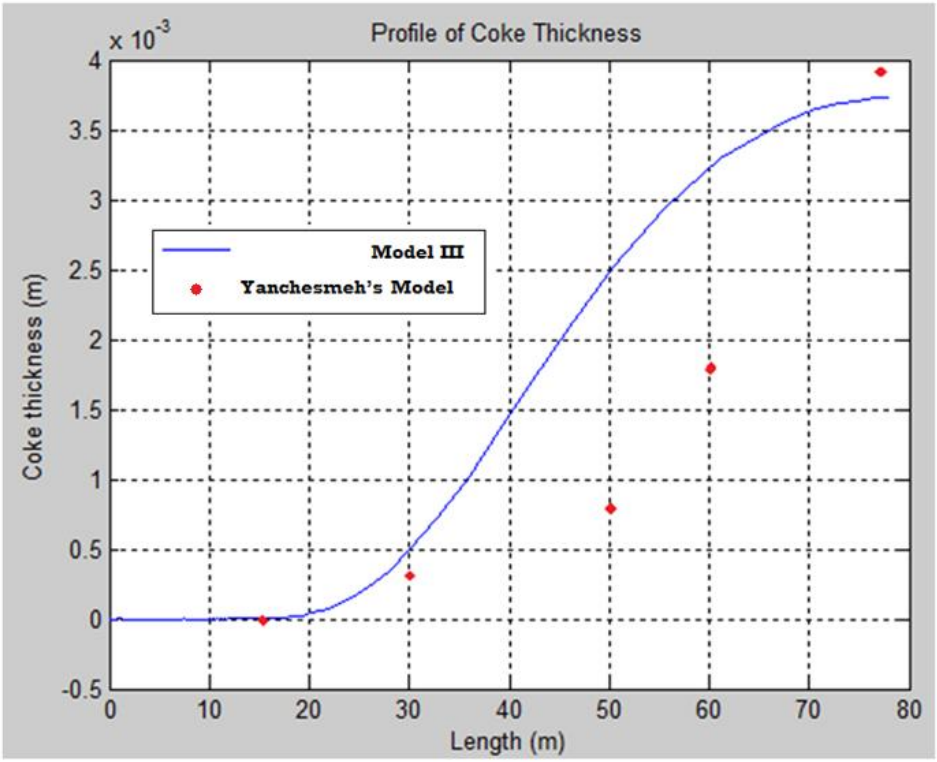

Figure 7.8 Coke Thickness Profile

To summarize, two selected model from the literature are used to validate the proposed model. Froment's Model uses five-reactions in network with coke formation. On the other hand, Yancheshmeh's Model uses eight-reactions in network with coke formation and coke removal reactions. The proposed models in this study have similar results with the models in the literature in terms of temperature, pressure, ethane conversion, ethylene production and coke formation. Therefore, the proposed model, especially Model III, is used to determine the effect of process conditions on product yields for the domestic plant, PETKIM.

7.2 Comparison of Model-II and Model-III

In model validation part, input values such as reactor length, tube diameter, inlet temperature and pressure, feed flow rate and composition values from the literature are used in the developed algorithm. The model outputs are compared with the results of two selected studies on steam ethane cracking from the literature. In this part, input variables of industrial steam ethane cracker of PETKİM Co. is used in two

models, Model-II and Model-III. The major input variables for ethane thermal cracking and outputs are shown in Figure 7.9.

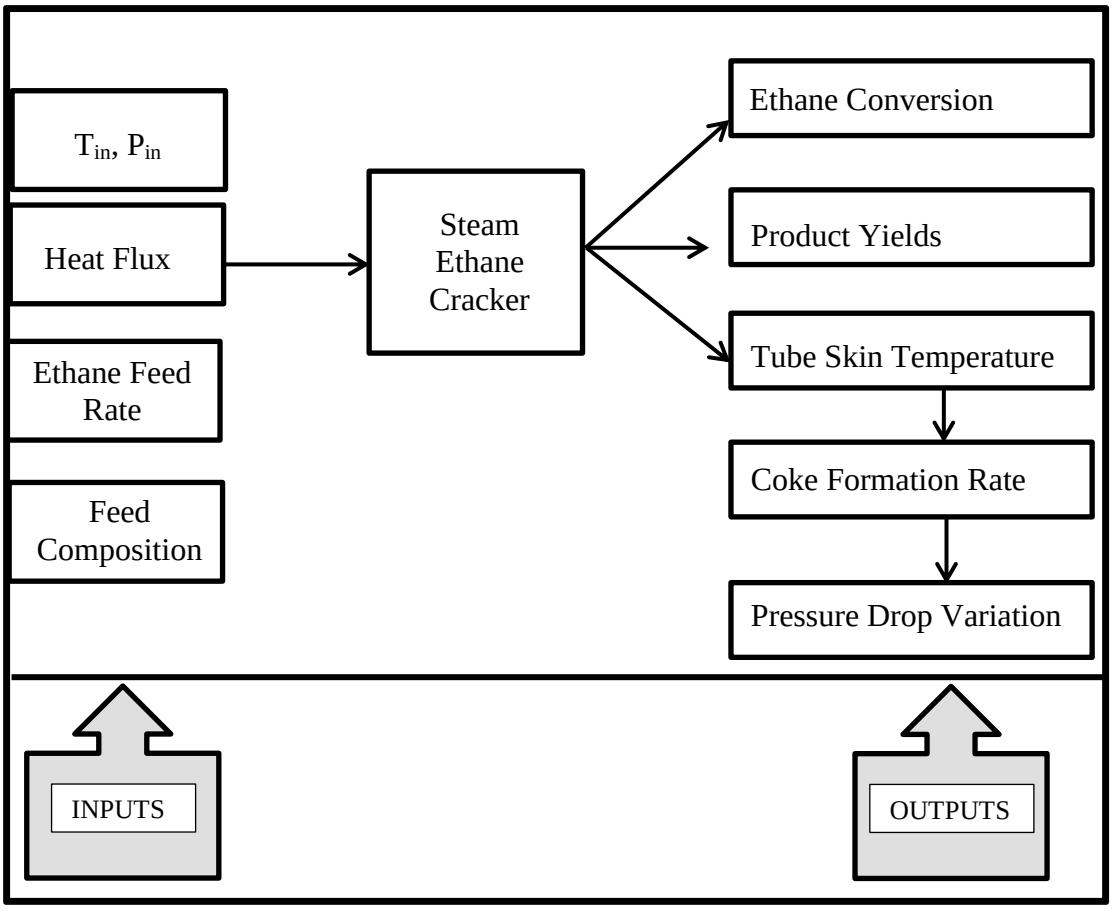

Figure 7.9 Ethane Cracker Process with Input and Output Variables

According to models coil outlet temperature is calculated as 1076^{o}C in which total coil length of PETKİM Steam ethane cracker is 160 m. When process gas temperature reaches approximately 1035^{o}C at 40 meters, cracking reactions take place. Since cracking reactions are highly endothermic, during cracking reactions increasing trend of process gas temperature has to be stopped. Another important operational parameter is coke formation. High temperatures favor this phenomenon. In an industrial steam cracker, operators as well as process engineers monitor the process gas temperature as well as tube skin temperature in order to decide when to shut down the unit for decoking operation. When temperature reaches to maximum allowable tube temperature that means excess amount of coke is deposited and accumulated within the tubes, urgent decoking is required in order to prevent hot

spot formation/tube rupture within the cracker. In Figure 7.10 temperature profile of Model II and Model III are compared.

In Figure 7.10, temperature profile of Model-II and Model-III are compared. Since Model-III includes coke removal reactions, coke thickness is calculated less for Model-III. Thus, the process gas temperature of Model-III is found to be 5^{o}C higher than Model-II due to the difference in the coke thickness with equal amount of heat flux for Model-II and Model-III. As the coke thickness decreases with coke removal reactions, the absorbed heat amount increases with the constant heat flux for Model-III. Therefore, the temperature is found to be higher for Model-III and it is much closer to the predicted temperature of SPYRO than Model-II.

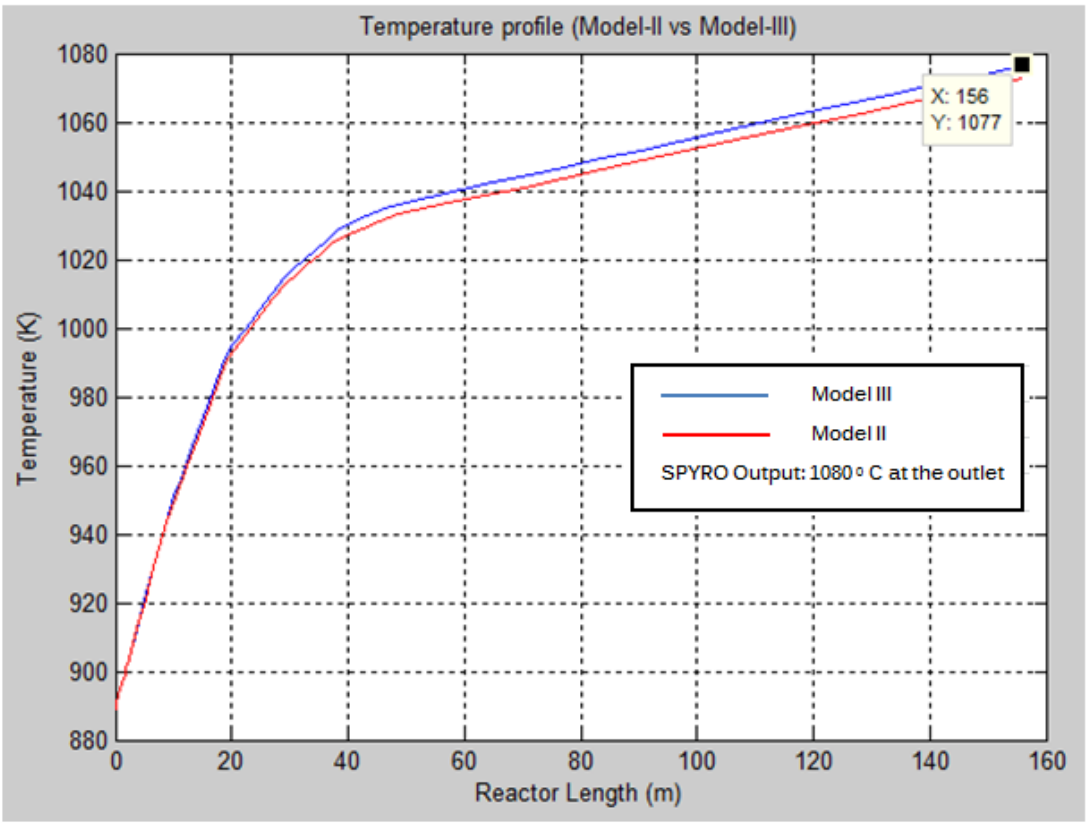

Figure 7.10 Temperature Profiles of Model-II and Model-III

Pressure drop evaluated along the reactor length is given in Figure 7.11 and that value is increased due to coke formation and their deposition on tube wall internals. Many furnace vendors provide several types of coil configurations in order to minimize pressure drop along the tubes. Common configuration is U-shaped coils for ethane cracker but also there exist S-shaped ones which are placed from top to

bottom of radiant section of the cracker. Figure 7.11 shows the pressure drop profiles for both Model-II and Model-III using the operational data of PETKİM Co. Figure 7.11 shows the pressure drop profiles for both Model-II and Model-III using the operational data of PETKİM Co. As can be seen on Figure 7.11, the pressure drop is calculated less for Model-III due to coke removal reactions. Indeed, the pressure drop is found to be much closer to the SPYRO output for Model-III due to involved coke removal reactions.

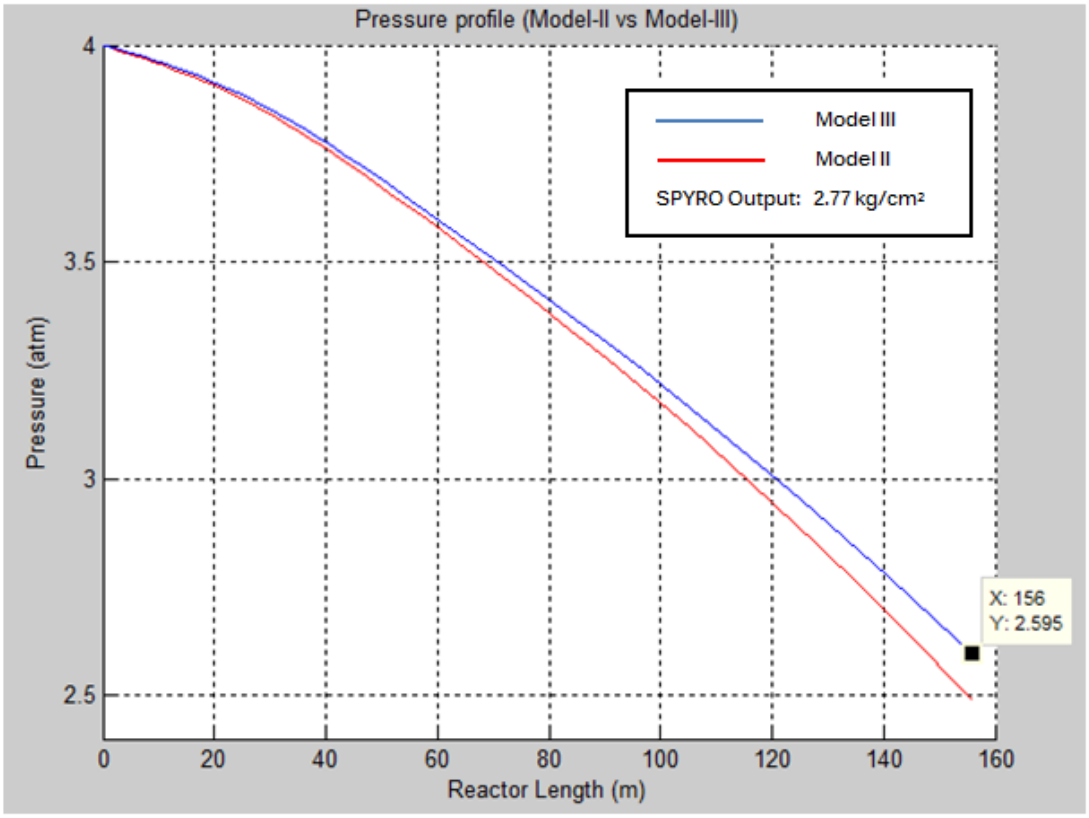

Figure 7.11 Pressure drop profile along the reactor length

In addition, PETKİM SYPRO outputs for product yields are shown in the Table 7.4 below. These results are compared with the Model-III outputs. Model-III inputs are the exact operational data of PETKİM Steam Ethane Cracker. When considering ethylene composition at the coil outlet, model results fit well into SPYRO outputs. On the other hand, ethane composition in Model-III is lower than that of SPYRO because total absorbed heat duty of PETKİM cracker is greater than assumed total heat duty. Detailed furnace model will provide exact heat distribution per tube and more accurate ethane and hydrogen composition at the coil outlet. In addition,

selectivity of ethane to ethylene is lower and more side products are observed at the coil outlet due to selected reaction network in Model III. Hydrogen composition is found to be quite high at the coil outlet. Since hydrogen is one of the main products and at the same time utility for hydrotreater, efficient operation of the cracker can provide more hydrogen and more side benefits. Since SPYRO uses thousands of cracking and dehydrogenation reactions Model III might be improved by regular laboratory analysis on sites.

Table 7.4 Product Composition of Model-III and PETKİM Steam Cracker Output

	Model III	PETKİM Cracker (SPYRO)
Ethane	23.87 %	28.32 %
Ethylene	29.77 %	30.42 %
Propylene	0.179 %	0.599 %
Methane	8.51 %	5.68 %
Hydrogen	37.78 %	33.25 %

In both models there are three main coke precursors in the steam cracking of ethane. These are ethylene, which is the major product of steam cracking, propylene and 1-3 butadiene. Model II and Model III use same input variables which belong to industrial steam ethane cracker of PETKİM Co. Therefore, Model II and Model III nearly have same profile for conversion as it is expected. Cracking reactions are equilibrium reactions therefore coke formation or partial removals of coke reactions do not directly affect the ethane conversion. Thus, steam ethane cracker of PETKİM Co. operation data for conversion is about 0.71, that value is validated as it seen from the Figure 7.12 and it is 0.6648. As can be seen on Figure 7.12, the ethane conversion along the reactor length is shown and the calculated ethane conversion is much closer for Model-III. Model II and Model III ethane conversion values (% 66.48) are slightly lower than that of PETKİM steam ethane cracker value (% 71). This is due to supplied heat flux to the cracker which is increased gradually per tube according to the developed model. However, at total heat duty values greater than $1.93*10^5 j/m^2.s$, due to maximum allowable tube wall temperature increase of heat flux is limited. Another reason for low total absorbed heat duty is because of the fact that the tubes at the radiant section inlet require greater heat duty in order to favor

cracking reactions. Several attempts for increasing of this duty were done but program do not converge with these values. As a result, more accurate modeling of heat flux distribution may be applied for further detailed studies.

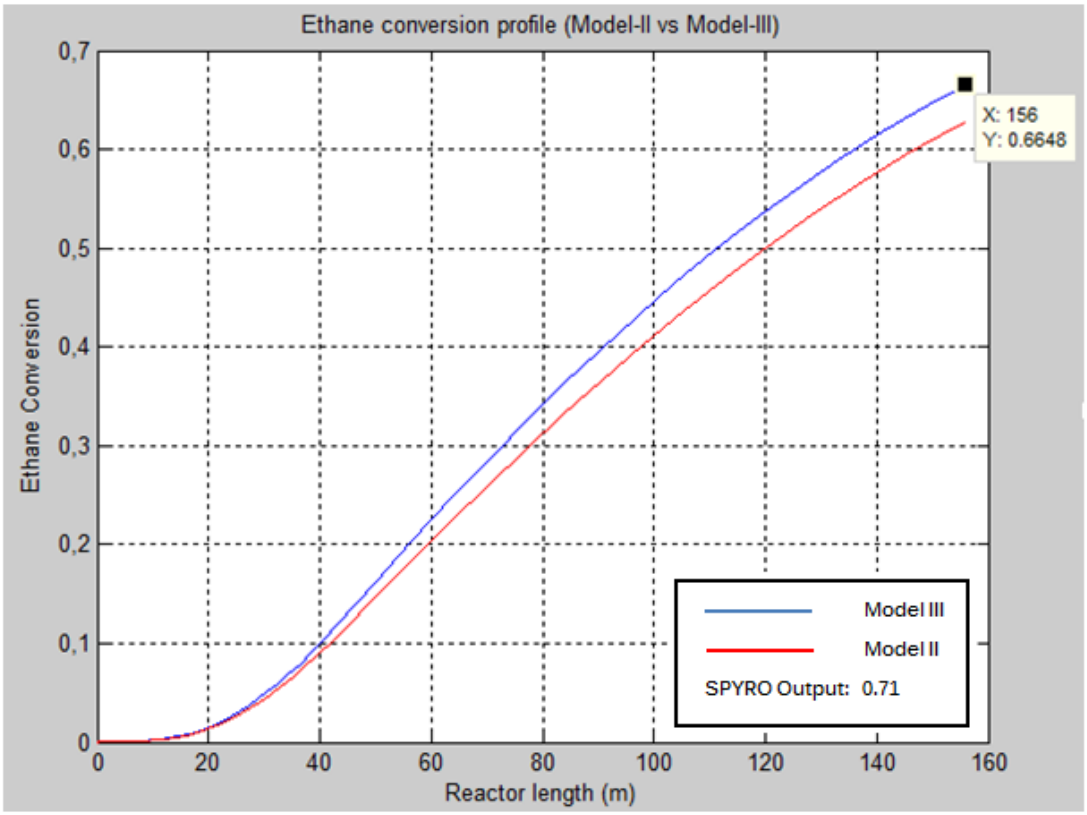

Figure 7.12 Ethane conversion profile for the Model-II and Model-III

Since Model-III involves coke removal reactions, lower coke formation rate is expected than that of Model II that can be seen in Figure 7.13. As it is stated before, in order to check process variables in steam ethane cracker with the model outputs, SPYRO (Steam Pyrolysis) software is used. At the coil outlet, Model-III output coke formation rate is 0.1232mol/s whereas SPYRO value is 0.109mol/s for the same input variables. Although model and actual process data values do not differ so much, like in ethane conversion comparison, inaccurate coke formation rate is probably due to maldistribution of heat flux within the furnace. Coke thickness profile is also derived from the coke formation rate profile according to model by doing some reasonable assumptions such as run length of ethane cracker is ninety days. At the end of run length, volume of coke formed and then coke thickness can be calculated.

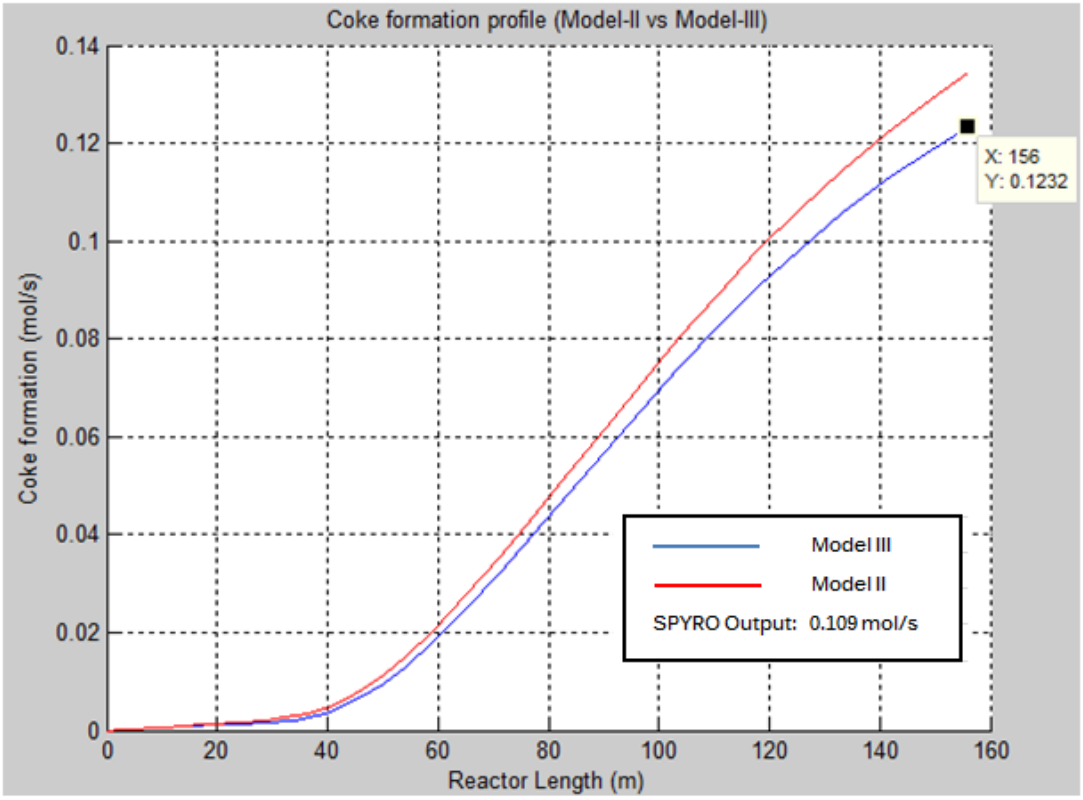

Figure 7.13 Coke formation profile along the reactor

In Figure 7.14 coke thickness is 3.7 mm for Model II whereas it is 3.4 mm for Model-III since coke removal reactions are taken into account. The thickness of coke is low for Model III. As stated before, shut down of the cracker is related to whether maximum allowable tube skin temperature is achieved or not. Dilution steam amount or cracker heat duty may be increased or decreased according to process heuristics of operators or process engineers. The point of such a kinetic modeling study is to predict process variables behaviors in the presence of any disturbances such as deviations in the feed, inlet temperature at the radiant section. Especially for heater operation such a model might reduce the utility cost of unit, considering fuel and steam consumptions.

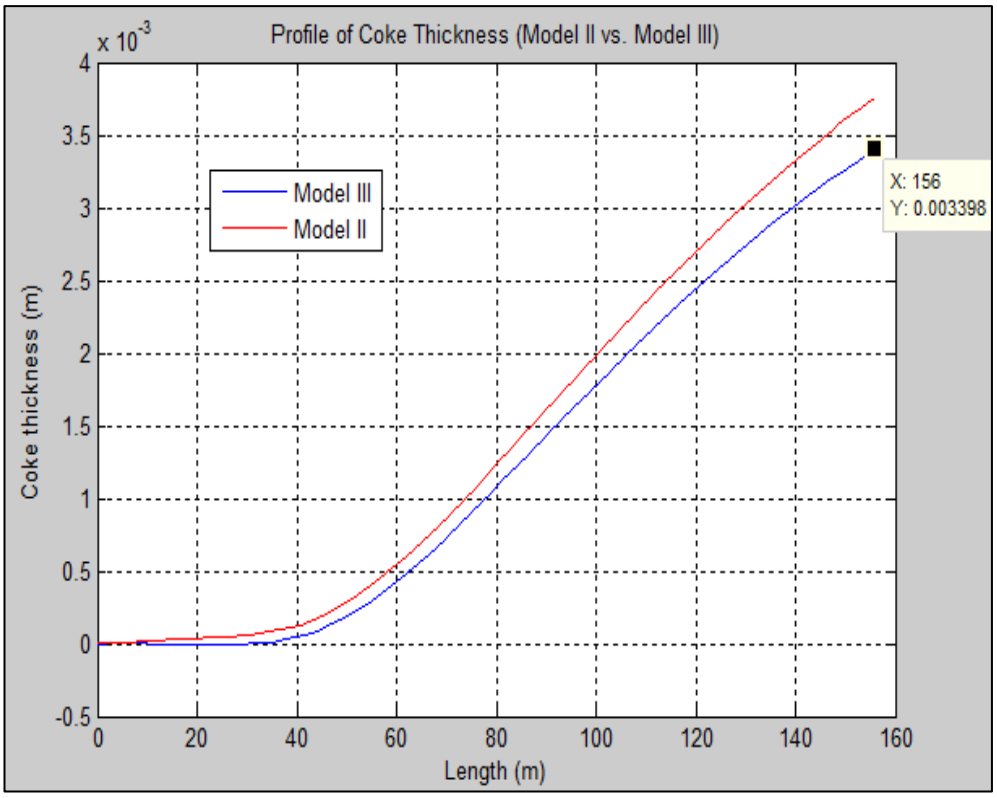

Figure 7.14 Coke thickness profile along the reactor length

Model-II and Model-III use the same reaction network with addition of two more reactions for the partial removal of coke in Model-III. In previous chapters, dilution steam is considered only for the partial reduction of hydrocarbon pressures and not taken as a reactant. However, in Model-III, steam also reacts with formed coke to produce H_2 and CO during the normal operation of cracking reactions. So, as it is seen from the Figure 7.15 dilution steam amount is decreasing. In fact this phenomenon is expected to occur at the decoking period of the cracking operation in which deposited coke is burned off using steam/ air mixture. As a result of these additional coke removal reactions, low rate of coke formation is expected which also extends tube length.

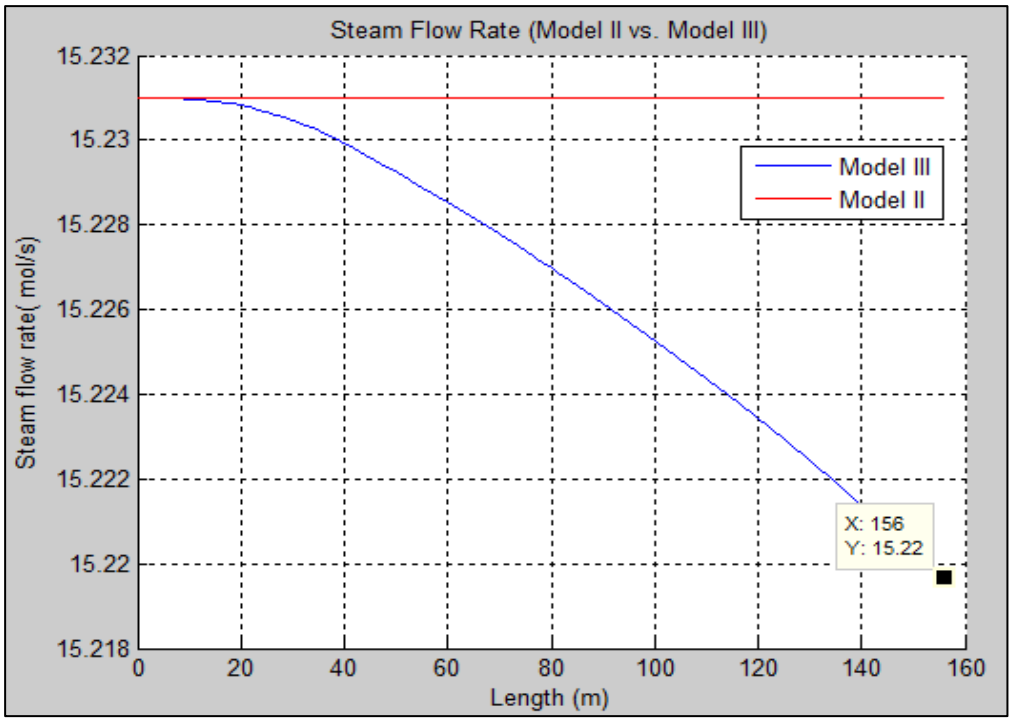

Figure 7.15 Dilution steam profile along the reactor

7.3 Effect of Tube Wall Temperature on Process Variables

As it is previously stated, both the ethane cracking and coke formation reactions are endothermic reactions. Thus, high temperature favors the reaction network toward the products and more ethane cracks to form more ethylene. On the other hand, as the ethylene production increases, the coke formation reactions also increase since ethylene is one of the major coke precursors. The increment on the coke formation rate reduces the run length. As a result, more frequent decoking operation has to be carried out which reduces the yearly ethylene production namely unit profitability. Therefore, it is necessary to set the process conditions in such a way that both ethylene yield and run length have to be high enough. In Figures 7.16 - 7.21, effect of supplied heat to the cracker on process variables is studied. The series named as "mod. (Moderate) conversion" represents the PETKIM operating data. On the other hand, series named as "low conversion" and "high conversion" represents the model outputs which run with lower heat input and greater heat input, respectively. As can be seen on Figure 7.16; the outlet process gas temperature increases as the heat input to the furnace increase as it is expected. Even, the outlet temperature is approximately 20^{o}C greater than the tube design limit of 1100 K for high conversion mode.

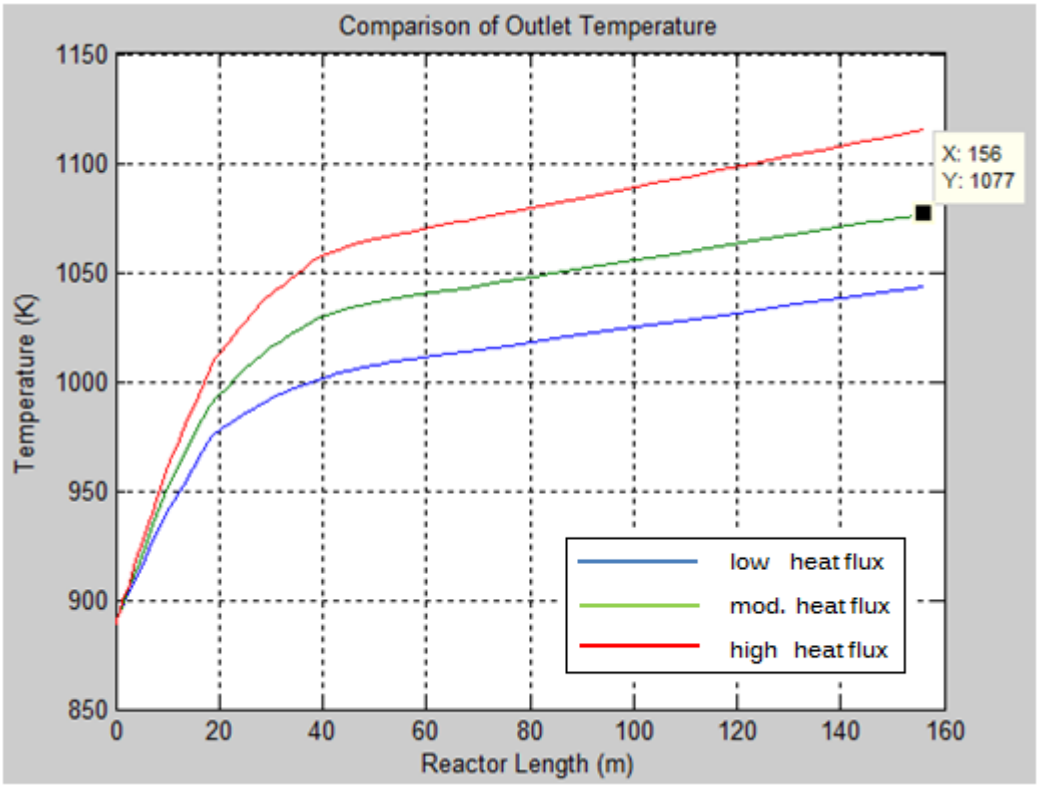

Figure 7.16 Effect of heat on process gas temperature along the reactor

In accordance with the temperature increase, the conversion of ethane increases too, as a result of increase in heat input. This is because of the fact that the net reactions in ethylene production by ethane cracking are endothermic. The effect of heat input on ethane conversion can be seen on Figure 7.17. Conversions are approximately 0.43 and 0.78 for the “low conversion” and “high conversion” operation modes. On the other hand, moderate conversion represents the PETKİM operation as it is close to the conversion of 0.64. Furthermore, Figure 7.18 represents the ethylene production change with respect to the heat input to the furnace. The ethylene production increases as the ethane conversion increases. However, the high conversion mode series show that the ethylene flow rate stays stable even starts to decrease through the outlet of the tube. This is because of the fact that the coke formation reactions become faster than ethylene formation reactions after a certain temperature limit. Even, the ethylene which is the main coke precursor decomposes to the coke as the temperature increases more towards the outlet of the tubes.

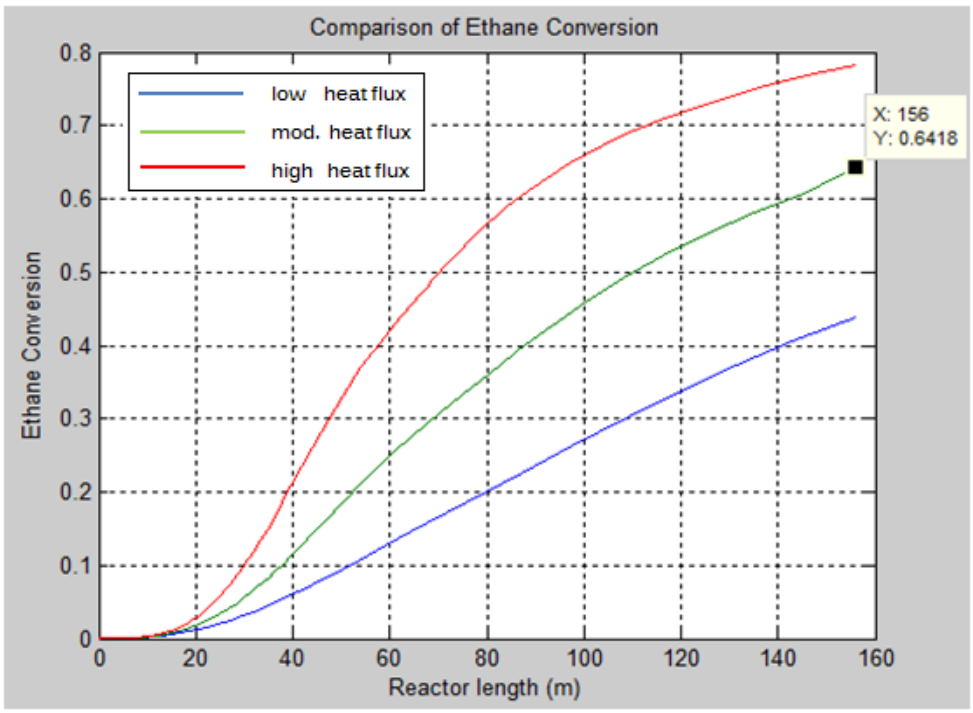

Figure 7.17 Effect of heat on ethane conversion along the reactor

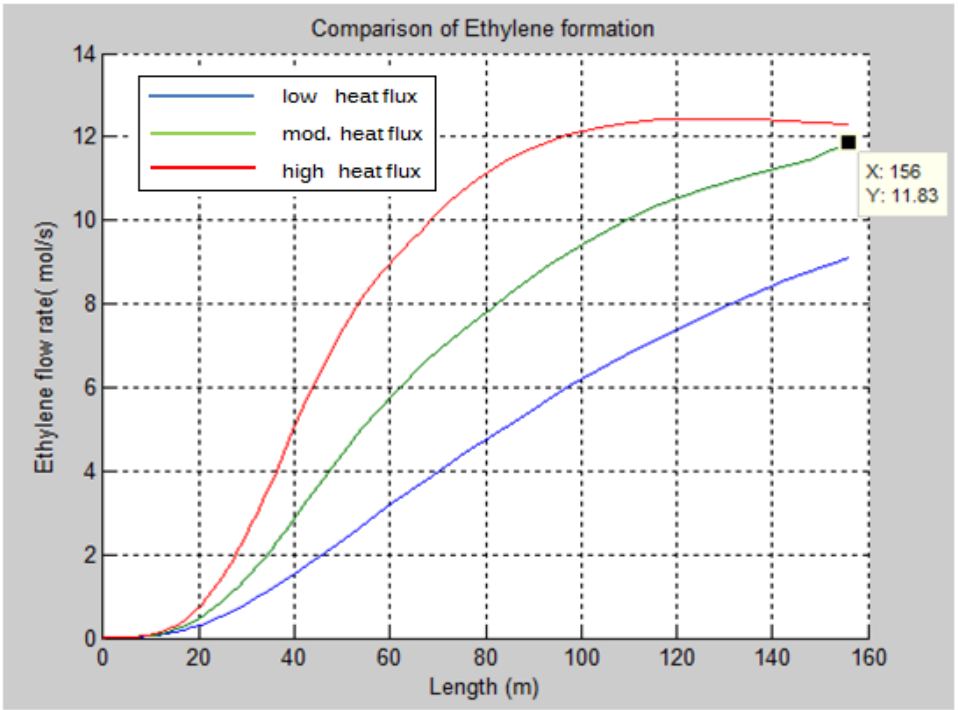

Figure 7.18 Effect of heat on ethylene flow rate along the reactor

As it was mentioned before, the high temperature favors not only the ethylene production but also the coke formation rate since both of them are endothermic.

Figure 7.19 represents the coke formation rate change with respect to heat input to the furnace.

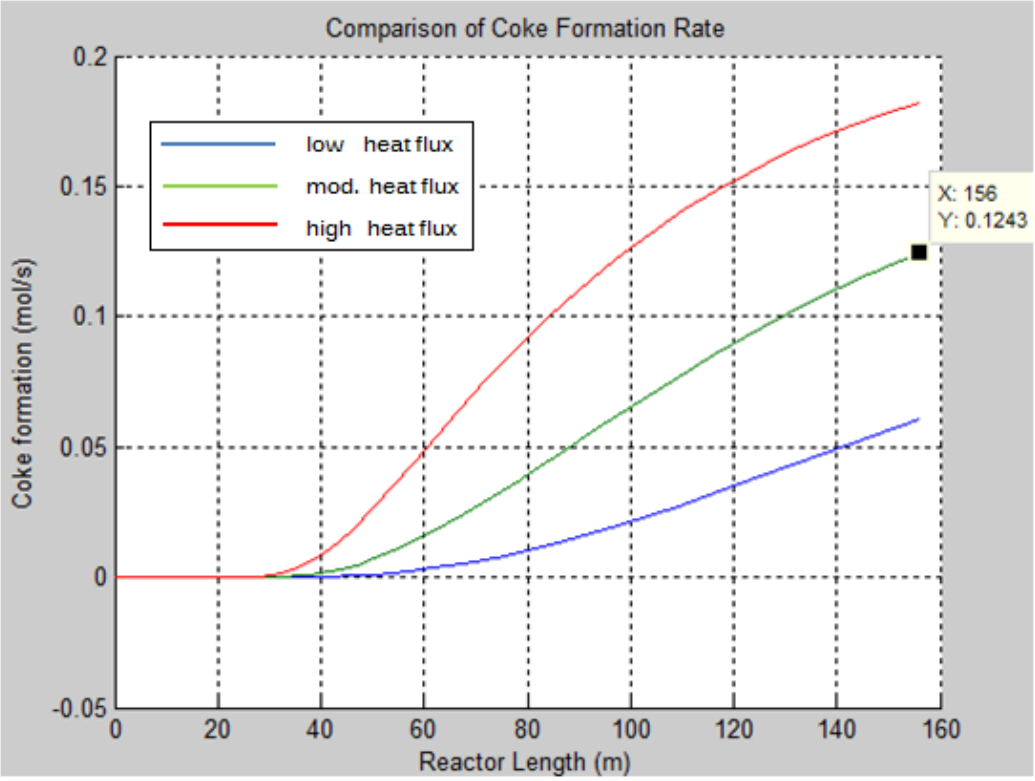

Figure 7.19 Effect of heat on coke formation rate along the reactor

Finally, the expected coke thicknesses for each conversion operation modes after 30 days of operation can be seen in Figure 7.20. As it was explained before, the endothermic ethane cracking reactions and coke formation reactions increase with the heat supply. As can be seen from the Figure 7.20, the expected coke thickness at the tube outlet is 5 mm for high conversion operation mode. On the other hand, it is 3 mm for moderate conversion operation mode. As the coke thickness increases through the outlet of the tube, the pressure drop increases which limits the process. At the end, the plant has to be shut-down for de-coking process which is a production loss, in turn.

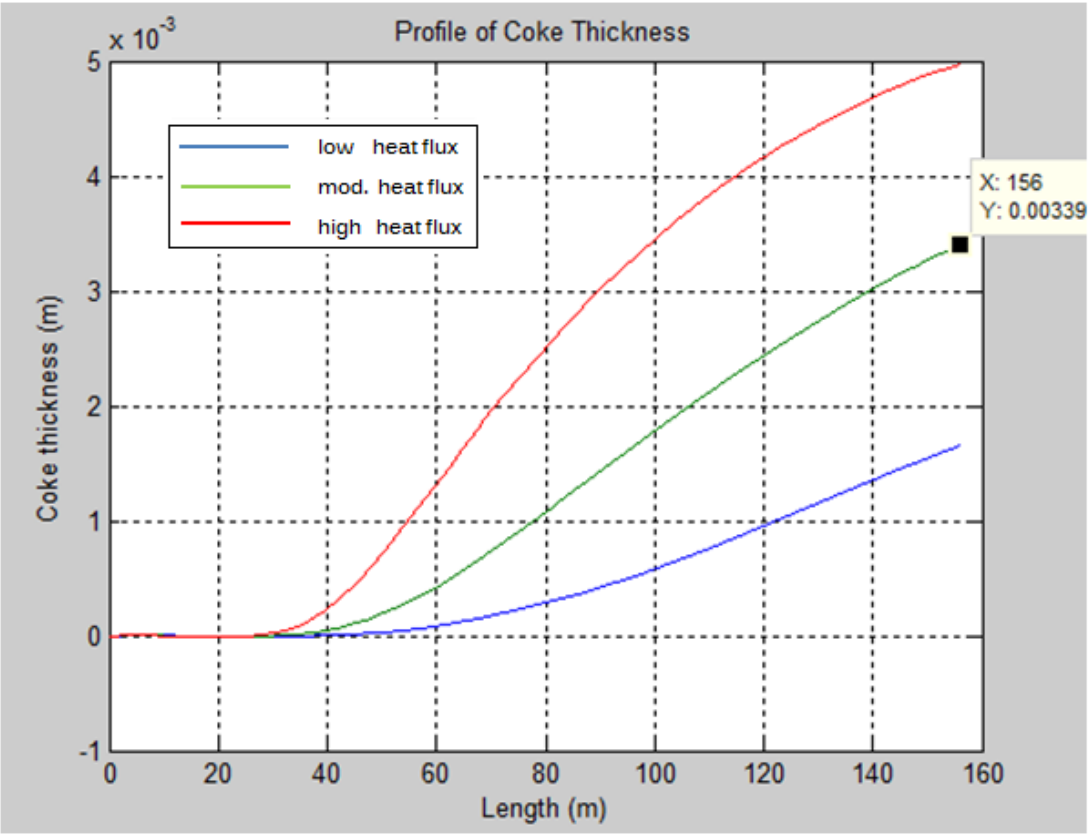

Figure 7.20 Effect of heat on coke thickness along the reactor

In summary, there is a tradeoff between the coke formation and ethylene formation with respect to the process gas temperature. Although the ethylene flow rate increases, the cycle length decreases inversely proportional with the coke formation rate. Thus, there is a need for optimization for ethylene conversion and cycle length.

CHAPTER 8

CONCLUSIONS

Ethylene is one of the major petrochemical products and has wide variety of daily life applications. Its production via thermal cracking of naphtha/ethane is the main building block of petrochemical industry. In this study steam ethane cracking operation is modeled by considering three different models according to their reaction network. Throughout the calculations, industrial plant data is considered as initial values for simulation studies (26.27mol/s ethane, 0.025mol/s propylene flow rates, steam-to-ethane ratio as 0.35, 889 K and 4atm as radiant zone inlet temperature and pressure, respectively). Mass, energy and momentum balances are coupled and simultaneously solved by the ode solver which is built-in function in MATLAB.

- Model-I in which coke formation and coke removal reactions are omitted, conversion is attained at a length of 100m. However, PETKİM steam ethane cracker has two coils running parallel and each coil has a 160m length. That situation shows the need for revised model for the reaction network.
- Model II is validated by using Froment's data whereas Model-III is validated by Yanchesmesh data given in the literature.
- Model-II and Model-III are further used in simulation with the initial value of PETKİM Data and the results of simulation are compared with PETKİM outputs.
- Using Model-II and Model-III with the operation initial conditions, overall ethane conversion of PETKIM is found approximately % 66.48. This conversion is attained while industrial conversion is % 71.

- Model-II and Model-III have a relatively similar temperature profiles that means coke formation takes significant amount of heat and also at a certain level the number of moles of ethane that goes into reaction increases but process gas temperature will maintain its value and does not change much.
- Coke formation rate differs for Model-II and Model-III; their values are 0.1375mol/s and 0.1232mol/s, respectively. Model-III has lower formation rate since coke removal reactions are taken into account.
- Run length for the steam ethane cracker is about 90 days and after this operating period decoking with air or steam/ air mixture should be done.
- Model-III results are much closer to the results of PETKİM. Using Model-III, temperature profile of the reactor tubes can be predicted by an input data and control of the operation can be done in a better way.

REFERENCES

Alper, E. “Petroleum Refinery Engineering”, Lecture Notes, METU, 2012.

Angeria, C. S. M.,“Hydrocarbons Thermal Cracking Selectivity Depending on Their Structure and Cracking Parameters”, Universidade do Porto: Institute of Chemical Technology, 2008.

Berman, H.L.,“Fired Heaters-I, Finding the basic design for your application”, Chemical Engineering June 19, 1978.

Cai, H., Krzywicki A., Oballa M. C., “Coke Formation in Steam Crackers for Ethylene Production”, Chemical Engineering and Processing, Vol. 41, Pages 199-214, 2002.

Dehandschutter, H., “Modeling Steam Cracking of Complex Hydrocarbons”, Universiteit Gent, Faculteit Ingenieurswetenschappen, Vakgroep Chemische Proceskunde en Technische Chemie, 2006.

Froment, G.F. and K. B. Bischoff, K.B., “Chemical Reactor Analysis and Design”, John Wiley & Sons, 1979.

Froment, G. F., Sundaram K. M., Van Damme, “Coke Deposition in the Thermal Cracking of Ethane” AlChe Journal, Vol. 27, pp. 946-951, 1981.

Froment G. C., Reyniers G. C., Zimmermann G., Kopinke F. D. “Coke Formation in the Thermal Cracking of Hydrocarbons” Ind. Eng. Chem. Res. 1994, 33, pp. 2584, 1994.

Geem, K.V., “Single Event Microkinetic Model for Steam Cracking of Hydrocarbons”. Universiteit Gent, Faculteit Ingenieurswetenschappen, Vakgroep Chemische Proceskunde en Technische Chemie, 2006.

Hernandez, A. Y. R., “A Model for the Prediction of Olefin Production and Coke Deposition during Thermal Cracking of Light Hydrocarbons”, Universidad Nacional de Colombia, Facultad de Minas, Escuella de Procesos Energia, 2012.

Matar, S., Hatch L.F., “Chemistry of Petrochemical Processes”, Texas: Gulf Publishing Company, (2nd edition), 1981.

Perry, H.R.,“Perry’s Chemical Engineers’ Handbook”, McGraw-Hill, 7th Edition, 1997.

Poling, B.E., Thomson, G.H., Friend, D.G., Rowley, R.L “Perry’s Chemical Engineers”, Chapter 2, 8th Edition, pp. 179, 2008.

Ranjan, P. et. al.,“Modeling of Ethane Thermal Cracking Kinetics in a Pyrocracker”, Chem. Eng. Tech., Vol. 35, No.6, pp. 1093-1097, 2012.

Rase, H. F. (2n.d), “Cracking of Ethane to Produce Ethylene”. Chemical Reactor Design for Process Plants, Volume Two: Case Studies and Design Data, 1977.

Speybroeck V. V., Reyniers M. F., Marin G.B., Waroquier M. “Modeling Elementary Reactions in Coke Formation from First Principles” Prepr. Pap. - Am. Chem. Soc., Div. Fuel Chem. 49(2), pp. 781-784, 2004.

Tham, C.M.,”Pyrolysis Furnace”, http://www.docstoc/docs/108128654/PYROLYSIS-FURNACE, 2014.

Yancheshmesh, M.S.S. and Haghighi, S.S., “Modeling ethane pyrolysis process: A study on effects of steam and carbon dioxide on ethylene and hydrogen productions”, Chemical Engineering Journal, 215-216, pp. 550-560, 2013.

Wauters, S., Marin, G. B., “Kinetic Modeling of Coke Formation during Steam Cracking”, Ind. Eng. Chem. Res., Vol. 41, pp. 2379-2391, 2002.

Wiseman, P. “Petrochemicals”, Umist Series in Science and Technology, 1986

Zhang, G. and Evans, B., “Progress of Modern Pyrolysis Furnace Technology”, Advances in Materials Physics and Chemistry, Vol. 2, pp. 169-172, 2012.

APPENDICES

A. Component Related Information

Table A.1 Heat Capacity Correlation Coefficients for Model-III (Perry, 1997)

Name	**Chemical Formula**	**C1x10^{-5}**	**C2x10^{-5}**	**C3x10^{-3}**	**C4x10^{-5}**	**C5**
Carbon Monoxide	CO	0.29108	0.08773	3.0851	0.084553	1538.2
Carbon Dioxide	CO_2	0.2937	0.3454	1.428	0.264	588

Table A.2 Heat capacity coefficients of components (Perry, 1997)

Name	**Chemical Formula**	**C1x10^{-5}**	**C2x10^{-5}**	**C3x10^{-3}**	**C4x10^{-5}**	**C5**
Ethane	C_2H_6	0.40326	1.3422	1.6555	0.73223	752.87
Ethylene	C_2H_4	0.33380	0.9479	1.5960	0.5510	740.80
Propane	C_3H_8	0.51920	1.9245	1.6265	1.1680	723.60
Propylene	C_3H_6	0.43852	1.5060	1.3988	0.74754	616.46
Acethylene	C_2H_2	0.31990	0.5424	1.5940	0.4325	607.10
Methane	CH_4	0.33298	0.79933	2.0869	0.41602	991.96
1-3 Butadiene	C_4H_6	0.50950	1.7050	1.5324	1.3370	685.60
Hydrogen	H_2	0.27617	0.0956	2.4660	0.0376	567.60
Steam	H_2O	0.33363	0.2679	2.6105	0.08896	1169.00

Table A.3 Critical parameters of components in the reaction network (Perry, 1997)

Name	**T_c (K)**	**P_c (bar)**	**V_c (m^3/kmol)**	**Z_c**
CH_4	190.4	46.0	0.09947	0.288
C_2H_2	308.3	61.4	0.11160	0.270
C_2H_4	282.4	50.4	0.13101	0.280
C_2H_6	305.4	48.8	0.14133	0.285
C_3H_6	364.9	46.0	0.18431	0.274
C_3H_8	369.8	42.5	0.19842	0.281
C_4H_6	425.0	43.3	0.23259	0.270
H_2	33.0	12.9	0.06653	0.303
H_2O	647.3	221.2	0.05700	0.235

B. MATLAB MAIN DRIVER CODE

B.1 Model I

```
% **********************************
% **********

clc
clear all

% Program responds and calculates the values until reactor length of
100m

lspan=[0,100];
yspan=[0,5];

y0=[0 0 0 3.47 0.025 0 0 0 2.0367 953 4];
[l,y]=ode23(@ethane,lspan,y0);

figure(1)
% subplot(321)
plot(l,y)
hold on
%loglog(l,y)
title('Steam Cracking  of Ethane')
xlabel('Reactor Length (m)')
ylabel('Profile of all, only T is visible')
grid


figure(2)
conv=(3.47-y(:,4))/3.47;
% subplot(322)
plot(l,conv)
title('Ethane conversion profile')
xlabel('Reactor length (m)')
ylabel('Ethane Conversion')
grid


figure(3)
yaxisT=y(:,10);
% subplot(323)
plot(l,yaxisT)
hold on
title('Temperature profile')
xlabel('Length (m)')
ylabel('Temperature (K)')
grid
```

```
figure(4)
yaxisP=y(:,11);
% subplot(324)
hold on
plot(l,yaxisP)
title('Pressure profile')
xlabel('Length (m)')
ylabel('Pressure (atm)')
grid


figure(5)
yaxis_ethylene=y(:,3);
% subplot(324)
hold on
plot(l,yaxis_ethylene)
title('Ethylene flow')
xlabel('Length (m)')
ylabel('Ethylene flow( mol/s)')
grid


figure(6)
yaxis_ethane=y(:,4);
% subplot(324)
hold on
plot(l,yaxis_ethane)
title('Ethane flow profile ')
xlabel('Length (m)')
ylabel('Ethane flow( mol/s)')
grid


% if F unit is mol/s then ethane molar flow rate
figure(7)
yaxisFethane=y(:,4).*(30*(10^-6)*3600);
% subplot(325)
plot(l,yaxisFethane)
hold on
title('Ethane Mass flow Proile')
xlabel('Length,m')
ylabel('Ethane Mass flow rate, ton/h ')
grid


% Dilution steam flow rate   mol/ s
figure(8)
yaxisFH2O=y(:,9);
% subplot(326)
plot(l,yaxisFH2O)
hold on
title('Dilution Steam Cons. Profile')
xlabel('Length,m ')
ylabel('DS Flow rate, ton/h ')
grid
```

B.2 Model-II

```
clc
clear all

lspan=[0,88];
yspan=[0,5];

% run with petkim molar flow rates
y0=[0 0 0 18.46 0.0025 0 0 0 15.69 0.000001 925 2.9];

[l,y]=ode23(@Model_II_validation,lspan,y0);

% global yaxis_ethylene_perry
% global conv_perry
% global yaxis_ethane_perry

figure(1)
% subplot(321)
plot(l,y,'LineWidth',10)
hold on
%loglog(l,y)
title('Steam Cracking  of Ethane')
xlabel('Reactor Length (m)')
ylabel('Profile of all, only T is visible')
grid

figure(2)
conv=(18.46-y(:,4))/18.46;
% subplot(212)
plot(l,conv)
hold on
title('Ethane conversion profile for Model-II Froment Validation')
xlabel('Reactor length (m)')
ylabel('Ethane Conversion')
grid

figure(3)
yaxisT=y(:,11);
% subplot(211)
hold on
plot(l,yaxisT)
title('Temperature profile for Model-II Froment Validation')
xlabel('Reactor Length (m)')
ylabel('Temperature (K)')
grid

figure(4)
yaxisP=y(:,12);
% subplot(212)
plot(l,yaxisP)
hold on
title('Pressure profile for Model-II Froment Validation')
xlabel('Reactor Length (m)')
ylabel('Pressure (bar)')
grid

% figure(5)
% yaxis_coke=y(:,10).*7.77.*12;
```

```
% % subplot(324)
% plot(l,yaxis_coke)
% hold on
% title('Profile of Coke Amount')
% xlabel('Length (m)')
% ylabel('Amount of Coke Formation (ton)')
% grid

% figure(5)
% yaxis_coke=y(:,10);
% % subplot(212)
% plot(l,yaxis_coke)
% hold on
% title('Coke formation profile for Model-II')
% xlabel('Reactor Length (m)')
% ylabel('Coke formation rate (mol/s)')
% grid

% figure(7)
% yaxis_ethane=y(:,4);
% subplot(211)
% % axis tight
% plot(l,yaxis_ethane)
% hold on
% title('Ethane flow profile for Case-II')
% xlabel('Reactor Length (m)')
% ylabel('Ethane (mol/ s)')
% grid

figure(6)
yaxis_ethylene=y(:,3);
plot(l,yaxis_ethylene)
hold on
title('Ethylene flow profile Model-II Froment Validation')
xlabel('Length, (m)')
ylabel('Ethylene flow, (mol/s)')
grid

% figure(9)
% yaxisyield_noCO=(y(:,3)./3.47)*100;
% % subplot(326)
% plot(l,yaxisyield_noCO)
% hold on
% title('Ethylene Yield Profile for Case-II')
% xlabel('Length,m ')
% ylabel('Ethylene yield (mol%)')
% grid

% figure(6)
% yaxis_H2=y(:,8);
% % subplot(212)
% plot(l,yaxis_H2)
% hold on
% title('H2 flow for Model-II')
% xlabel('Reactor Length (m)')
% ylabel('H2 flow rate (mol/s)')
% grid

% figure(7)
% yaxis_methane=y(:,1);
```

```
% % subplot(212)
% plot(l,yaxis_methane)
% hold on
% title('Methane flow for Model-II')
% xlabel('Reactor Length (m)')
% ylabel('Methaneflow rate (mol/s)')
% grid

% figure(7)
% yaxis_ethane=y(:,4);
% % subplot(212)
% plot(l,yaxis_ethane)
% hold on
% title('Ethane flow for Model-II Froment Validation')
% xlabel('Reactor Length (m)')
% ylabel('Ethane flow rate (mol/s)')
% grid

% figure(8)
yaxis_coke=y(:,10).*3600.*24.*30.*1.*1/(1000.*3.14.*156.*1600.*0.121
);
% % subplot(324)
% plot(l,yaxis_coke)
% hold on
% title('Profile of Coke Thickness')
% xlabel('Length (m)')
% ylabel('Coke thickness (m)')
% grid

% figure(8)
% yaxis_propylene=y(:,5);
% % subplot(211)
% plot(l,yaxis_propylene)
% hold on
% title('Propylene flow profile for Model-II ')
% xlabel('Reactor Length (m)')
% ylabel('Propylene (mol/ s)')
% grid
```

B.3 Model-III

```
clc
clear all

lspan=[0,156];
yspan=[0,5];

% Algorithm is run with petkim molar flow rates

y0=[0 0 0 26.27 0.025 0 0 0 15.231 0.000001 0.1 0 889 4.00];

[l,y]=ode23(@Petkim_I,lspan,y0);

% figure(1)
% % subplot(321)
% plot(l,y)
% hold on
% %loglog(l,y)
% title('Steam Cracking  of Ethane')
% xlabel('Reactor Length (m)')
% ylabel('Profile of all, only T is visible')
% grid

figure(3)
conv=(26.27-y(:,4))/26.27;
% subplot(212)
plot(l,conv)
hold on
title('Ethane conversion profile for Model-III')
xlabel('Reactor length (m)')
ylabel('Ethane Conversion')
grid

figure(1)
yaxisT=y(:,13);
% subplot(211)
plot(l,yaxisT)
hold on
title('Temperature profile for Model-III')
xlabel('Reactor Length (m)')
ylabel('Temperature (K)')
grid

figure(2)
yaxisP=y(:,14);
% subplot(212)
hold on
plot(l,yaxisP)
title('Pressure profile for Model-III')
xlabel('Reactor Length (m)')
ylabel('Pressure (atm)')
grid

% figure(5)
% yaxis_coke=y(:,12).*7.77.*12;
% % subplot(324)
% plot(l,yaxis_coke)
% hold on
```

```
% title('Profile of Coke Amount')
% xlabel('Length (m)')
% ylabel('Coke form. rate (ton)')
% grid

figure(10)
yaxis_coke=y(:,12).*3600.*24.*30.*1.*1/(1000.*3.14.*156.*1600.*0.121
);
% subplot(324)
plot(l,yaxis_coke)
hold on
title('Profile of Coke Thickness')
xlabel('Length (m)')
ylabel('Coke thickness (m)')
grid
figure(9)
yaxis_coke=y(:,12);
% subplot(212)
hold on
plot(l,yaxis_coke)
title('Coke formation rate profile for Model-III')
xlabel('Reactor Length (m)')
ylabel('Coke formation (mol/s)')
grid

figure(4)
yaxis_ethane=y(:,4);
% subplot(211)
plot(l,yaxis_ethane)
hold on
title('Ethane flow profile for Model-III ')
xlabel('Reactor Length (m)')
ylabel('Ethane (mol/ s)')
grid

figure(6)
yaxis_ethane=y(:,8);
% subplot(211)
plot(l,yaxis_ethane)
hold on
title('Hydrogen flow profile for Model-III ')
xlabel('Reactor Length (m)')
ylabel('Hydrogen (mol/ s)')
grid

figure(5)
yaxis_ethane=y(:,1);
% subplot(211)
plot(l,yaxis_ethane)
hold on
title('Methane flow profile for Model-III ')
xlabel('Reactor Length (m)')
ylabel('Methane (mol/ s)')
grid


figure(8)
yaxis_ethane=y(:,5);
% subplot(211)
plot(l,yaxis_ethane)
```

```
hold on
title('Propylene flow profile for Model-III ')
xlabel('Reactor Length (m)')
ylabel('Propylene (mol/ s)')
grid

figure(7)
yaxis_ethylene_perry=y(:,3);
% subplot(211)
hold on
plot(l,yaxis_ethylene_perry)
title('Ethylene formation')
xlabel('Length (m)')
ylabel('Ethylene flow rate( mol/s)')
grid

% figure(9)
% yaxisyield=(y(:,3)./31.00)*100;
% % subplot(211)
% plot(l,yaxisyield)
% hold on
% title('Ethylene Yield Profile for Model-III')
% xlabel('Reactor Length,m ')
% ylabel('Ethylene yield (mol%)')
% grid

figure(11)
yaxis_ethylene_perry=y(:,9);
% subplot(211)
hold on
plot(l,yaxis_ethylene_perry)
title('Steam Flow Rate')
xlabel('Length (m)')
ylabel('Steam flow rate( mol/s)')
grid

% figure(15)
% yaxis_ethylene_perry=y(:,3)./SUMYDOT;
% % subplot(211)
% hold on
% plot(l,yaxis_ethylene_perry)
% title('Ethylene Yield Profile')
% xlabel('Length (m)')
% ylabel('Ethylene Yield( mol/s)')
% grid

% figure(16)
% yaxis_ethylene_perry=y(:,1)/SUMYDOT;
% % subplot(211)
% hold on
% plot(l,yaxis_ethylene_perry)
% title('Methane')
% xlabel('Length (m)')
% ylabel('Methane( mol/s)')
% grid
% figure(17)
% yaxis_ethylene_perry=y(:,8)./SUMYDOT;
% % subplot(211)
% hold on
% plot(l,yaxis_ethylene_perry)
% title('H2 Yield Profile')
```

```
% xlabel('Length (m)')
% ylabel('H2( mol/s)')
% grid

% figure(18)
% yaxis_ethylene_perry=y(:,4)./SUMYDOT;
% % subplot(211)
% hold on
% plot(l,yaxis_ethylene_perry)
% title('Ethane ')
% xlabel('Length (m)')
% ylabel('Ethane comp( mol/s)')
% grid

% figure(15)
% yaxis_ethylene_perry=y(:,3)./SUMYDOT;
% % subplot(211)
% hold on
% plot(l,yaxis_ethylene_perry)
% title('Ethylene Yield Profile')
% xlabel('Length (m)')
% ylabel('Ethylene Yield( mol/s)')
% grid
```

C. MATLAB CALCULATION CODE

C.1 Model-I

```
function ydot=ethane(l,y)

 FT=0;
 CPT=0;
 SUMDHR=0;
 TCM=0;
 SUMZC=0;
 SUMVC=0;
 FOQM=0;
 FOPM=0;
 SUMYDOT=0;
 BMM=0;

 RR=8.314;
 RX=.08206;
 RZ=82.06;
 DT=0.108;
 PI=3.141592654;

 V=180;
 A=1;
 ALFAR=2.05E-3;
 RB=.356./2;
 TO=835+273;
 TREF=298.2;
 PO=1.2;

 a1=1.245E-3;
 b1=1.6553;
 c1=.4489;
 d1=1.7368;
 f1=.9425;

 a2=5.1726;
 b2=1.2723;
 c2=3.0578;
 d2=2.2310;
 f2=-.1853;
 GAMA=-.3286;
 SIGMA=-37.7332;
 EITA=-7.6351;
 AIN=.4489;
```

```
%  Critical temperatures of components
    TC(1)=190.4;
    TC(2)=308.3;
    TC(3)=282.4;
    TC(4)=305.4;
    TC(5)=364.9;
    TC(6)=369.8;
    TC(7)=425;
    TC(8)=33;
    TC(9)=647.3;

%  Molecular weights of components
    BM(1)=16.043;
    BM(2)=26.038;
    BM(3)=28.054;
    BM(4)=30.07;
    BM(5)=42.081;
    BM(6)=44.094;
    BM(7)=54.092;
    BM(8)=2.016;
    BM(9)=18.015;
%
%  Critical pressures of components PC(1)=46;
    PC(2)=61.4;
    PC(3)=50.4;
    PC(4)=48.8;
    PC(5)=46;
    PC(6)=42.5;
    PC(7)=43.3;
    PC(8)=12.9;
    PC(9)=221.2;
%
%  Critical volumes of components
    VC(1)=99.2;
    VC(2)=112.7;
    VC(3)=130.4;
    VC(4)=148.3;
    VC(5)=181;
    VC(6)=203;
    VC(7)=221;
    VC(8)=64.3;
    VC(9)=57.1;
%
%   Compressibilty factors
    ZC(1)=.288;
    ZC(2)=.27;
    ZC(3)=.28;
    ZC(4)=.285;
    ZC(5)=.274;
    ZC(6)=.281;
    ZC(7)=.27;
    ZC(8)=.303;
    ZC(9)=.235;
%
%   Dipole moments of components
    DPM(1)=0;
    DPM(2)=0;
    DPM(3)=0;
    DPM(4)=0;
    DPM(5)=.4;
    DPM(6)=0;
```

```
    DPM(7)=0;
    DPM(8)=0;
    DPM(9)=1.8;


    AC=PI.*DT.^2./4;
    for i = 1:9
    F(i)=y(i);
    FT=FT+F(i)
    end
    for i=1:9 ,
    C(i)=F(i).*y(11)./(FT.*RX.*y(10));
    end
%
%  Reaction rate expressions
    R(1)=4.56E13.*exp(-273020./(RR.*y(10))).*C(4)
    R(2)=8.75E8.*exp(-136870./(RR.*y(10))).*C(3).*C(8)
    R(3)=3.85E11.*exp(-273190./(RR.*y(10))).*C(4).^2
    R(4)=9.81E8.*exp(-154580./(RR.*y(10))).*C(5)
    R(5)=5.87E4.*exp(-29480./(RR.*y(10))).*C(2).*C(1)
    R(6)=1.03E12.*exp(-172750./(RR.*y(10))).*C(2).*C(3)
    R(7)=7.08E13.*exp(-253010./(RR.*y(10))).*C(3).*C(4)
%
%  Heat capacity of components
    CP(1)=19.250+5.213E-2.*y(10)+1.197E-5.*y(10).^2-1.132E-
8.*y(10).^3
    CP(2)=26.820+7.578E-2.*y(10)-5.007E-5.*y(10).^2+1.412E-
8.*y(10).^3
    CP(3)=3.8060+1.566E-1.*y(10)-8.348E-5.*y(10).^2+1.755E-
8.*y(10).^3          %ETHYLENE
    CP(4)=5.4090+1.781E-1.*y(10)-6.938E-5.*y(10).^2+8.713E-
9.*y(10).^3          %ETHANE
    CP(5)=3.7100+2.345E-1.*y(10)-1.160E-4.*y(10).^2+2.205E-
8.*y(10).^3          %PROPYLENE
    CP(6)=-4.224+3.063E-1.*y(10)-1.586E-4.*y(10).^2+3.215E-
8.*y(10).^3
    CP(7)=-1.687+3.419E-1.*y(10)-2.340E-4.*y(10).^2+6.335E-
8.*y(10).^3
    CP(8)=27.140+9.274E-3.*y(10)-1.381E-5.*y(10).^2+7.645E-
9.*y(10).^3
    CP(9)=32.240+1.924E-3.*y(10)+1.055E-5.*y(10).^2-3.596E-
9.*y(10).^3

%  Calculation of total -average- heat capacity of mixture
    for i=1:9
    yy(i)=F(i)./FT
    CPT=CPT+yy(i).*CP(i)
    end
%
%   Prediction of viscosity according to corresponding state
    DHFO1=-7.49E4
    DHFO2=2.269E5
    DHFO3=5.234E4
    DHFO4=-8.474E4
    DHFO5=2.043E4
    DHFO6=-1.039E5
    DHFO7=1.102E5
    DHFO8=0
    DHFO9=-2.42E5

    T1=(y(10)-TREF);
```

```
T2=(y(10).^2-TREF.^2)./2;
T3=(y(10).^3-TREF.^3)./3;
T4=(y(10).^4-TREF.^4)./4;

DHF1=DHFO1+19.25.*T1+5.213E-2.*T2+1.197E-5.*T3-1.132E-8.*T4
DHF2=DHFO2+26.82.*T1+7.578E-2.*T2-5.007E-5.*T3+1.412E-8.*T4
DHF3=DHFO3+3.806.*T1+1.566E-1.*T2-8.348E-5.*T3+1.755E-8.*T4
DHF4=DHFO4+5.409.*T1+1.781E-1.*T2-6.938E-5.*T3+8.713E-9.*T4
DHF5=DHFO5+3.710.*T1+2.345E-1.*T2-1.160E-4.*T3+2.205E-8.*T4
DHF6=DHFO6-4.224.*T1+3.063E-1.*T2-1.586E-4.*T3+3.215E-8.*T4
DHF7=DHFO7-1.687.*T1+3.419E-1.*T2-2.340E-4.*T3+6.335E-8.*T4
DHF8=DHFO8+27.14.*T1+9.274E-3.*T2-1.381E-5.*T3+7.645E-9.*T4
DHF9=DHFO9+32.24.*T1+1.924E-3.*T2+1.055E-5.*T3-3.596E-9.*T4

DH(1)=DHF3-DHF4+DHF8
DH(2)=-DHF3+DHF4-DHF8
DH(3)=DHF1-2.*DHF4+DHF6
DH(4)=DHF1+DHF2-DHF5
DH(5)=-DHF1-DHF2+DHF5
DH(6)=-DHF2-DHF3+DHF7
DH(7)=DHF1-DHF3-DHF4+DHF5

for i=1:7
    SUMDHR=SUMDHR+DH(i).*R(i)
end

for i=1:9
TCM=TCM+yy(i).*TC(i)
SUMZC=SUMZC+yy(i).*ZC(i)
SUMVC=SUMVC+yy(i).*VC(i)
BMM=BMM+yy(i).*BM(i)
FOQ(i)=1;
FOP(i)=1;
end
PCM=RZ.*TCM.*SUMZC./SUMVC;

FOQ(8)=1.1708.*(1+.00385.*(y(10)./TC(8)-12).^(.9920635));
FOP(9)=1+.221369.*abs(.96+.1.*(y(10)./TC(9)-.7));

MS1=0;
for i=1:9
    if yy(i)>0.0
    MS1=MS1+1;
    Xyy(MS1)=yy(i);
    XBM(MS1)=BM(i);
    end
end

BMH=XBM(MS1);
for i=1:MS1
    if XBM(i)>BMH
    BMH=XBM(i);
    yyH=Xyy(i);
    end
end
```

```
    BML=XBM(MS1);
    for i=1:MS1
        if XBM(i)<BML
        BML=XBM(i);
        end
    end


    if BMH./BML<9.0
    A=1;
    else
    A=1-.01.*(BMH./BML).^(0.87);
    end

    if yyH<0.05
        A=1;
    end
    if yyH>0.7
        A=1;
    end

    for i=1:9
    FOQM=FOQM+yy(i).*FOQ(i).*A;
    FOPM=FOPM+yy(i).*FOP(i);
    end

    PRM=y(11)./PCM;
    TRM=y(10)./TCM;

    Z1M=(.807.*TRM.^.618-.357.*exp(-.449.*TRM)+.34.*exp(-
4.058.*TRM)+.018).*FOPM.*FOQM;

    a=a1.*exp(a2.*TRM.^GAMA)./TRM;
    b=a.*(b1.*TRM-b2);
    cc=c1.*exp(c2.*TRM.^SIGMA)./TRM;
    d=d1.*exp(d2.*TRM.^EITA)./TRM;
    e=1.3088;
    ff=f1.*exp(f2.*TRM.^AIN);

    Z2M=Z1M.*(1+a.*PRM.^e./(b.*PRM.^ff+1./(1+cc.*PRM.^d)));

    YR=Z2M./Z1M;

    FPM=(1+(FOPM-1).*YR.^(-3))./FOPM;
    FQM=(1+(FOQM-1).*(1./YR-.007.*(log(YR)).^4))./FOQM;

    ETE=.176.*(TCM./((BMM.^3).*(PCM.^4))).^(1.0./6.0)

    VISC=Z2M.*FPM.*FQM.*1.0E-7./ETE

    EE=(.7+V.*.35./90).*(.051+.19.*DT./RB)

    G=FT.*BMM
    RE=DT.*G./VISC
    FF=.046.*RE.^(-.2)


    BMW=9.5;
```

```
    if l>BMW.*5
        QZ=59;
    elseif l>BMW.*4
        QZ=63;
    elseif l>BMW.*3
        QZ=71;
    elseif l>BMW.*2
        QZ=80;
    elseif l>BMW.*1
        QZ=84;
    else
        QZ=96;
    end

% Governing differential mass balance equations
    ydot(1)=(R(3)+R(4)-R(5))
    ydot(2)=(R(4)-R(5)-R(6))
    ydot(3)=(R(1)-R(2)-R(6)-R(7))
    ydot(4)=(-R(1)+R(2)-2.*R(3)-R(7))
    ydot(5)=(-R(4)+R(5)+R(7))
    ydot(6)=(R(3))
    ydot(7)=(R(6))
    ydot(8)=(R(1)-R(2))
    ydot(9)=0.0

    for i=1:9, SUMYDOT=SUMYDOT+ydot(i)
    end

ydot(10)=(QZ.*PI.*DT./AC-SUMDHR)./(CPT.*FT)

ydot(11)=(SUMYDOT./G+(ydot(10)./y(10)+(2.*FF./DT+EE./(PI.*RB))))./BMM
)./(1./(BMM.*y(11))-y(11)./(ALFAR.*(G.*AC).^2.*y(10)))

ydot=ydot';
```

C.2 Model-II

```
% clc
% clear all
% Model-II Ethane Pyrolysis Process
% M.S. Shokrollahi Yancheshmeh et al. / Chemical Engineering Journal
% 215-216 (2013) 550- 560

%  Unit conversions
% 1 atm=1.013 bar
% 1 bar= 10^5 Pa
% 1 cal=4.1869 joules

function ydot=Model_II_validation(l,y)

global SUMDHR_ethane
global QZ_rxn_from_eqn
global T
global F_ethane
global K

FT=0;                   % total molar flow rate,              kmol/s
CPT=0;                  % total/ mixture heat capacity,      j/mol.K
SUMDHR_ethane=0;        % summation of heat of rxns,          j/mol
TCM=0;                  % Critical temperature of the mixture, K
SUMZC=0;                % Sum of compressibility factors
SUMVC=0;                % Sum of critical volumes of components,
SUMYDOT=0;              % Sum of dFj/dz
BMM=0;                  % Molecular weight of mixture

RR=8.314;               % Ideal Gas constant,                j/mol.K
RX=0.08206;             % Ideal Gas constant,           m3.atm/kmol.K
RZ=82.06;               % Ideal Gas constant,       L.atm/kmol.K  or
cm3.atm/mol.K
DT=0.108;               % "Petkim" internal tube diameter,   meters
PI=3.141592654;

V=180;                  % Angle described by the bend here 180o
ALFAR=2.05E-3;          % alpha*R   parameter value within the
momentum balance

RB=0.306./2;            % Radius of the bend,                meters
% TO=651+273.15;        % Temperature at the inlet of the radiant
section,      K
TREF=298.15;            % Reference temperature,                 K
% PO=1.2;               % Inlet Pressure

%  Critical temperatures of components,                          K
    TC(1)=190.4;
    TC(2)=308.3;
    TC(3)=282.4;
    TC(4)=305.4;
    TC(5)=364.9;
    TC(6)=369.8;
    TC(7)=425;
    TC(8)=33;
    TC(9)=647.3;
    TC(10)=0;                                        % Carbon
```

```
%  Molecular weights of components,                    kg/ kmol
    BM(1)=16.043;
    BM(2)=26.038;
    BM(3)=28.054;
    BM(4)=30.07;
    BM(5)=42.081;
    BM(6)=44.094;
    BM(7)=54.092;
    BM(8)=2.016;
    BM(9)=18.015;
    BM(10)=12;                                          % Carbon

%  Critical pressures of components,                    bar
    PC(1)=46;
    PC(2)=61.4;
    PC(3)=50.4;
    PC(4)=48.8;
    PC(5)=46;
    PC(6)=42.5;
    PC(7)=43.3;
    PC(8)=12.9;
    PC(9)=221.2;
    PC(10)=0;                                           % Carbon

%  Critical volumes of components     m3/ kmol
    VC(1)=0.09947;
    VC(2)=0.1116;
    VC(3)=0.13101;
    VC(4)=0.14133;
    VC(5)=0.18431;
    VC(6)=0.19842;
    VC(7)=0.23259;
    VC(8)=0.06653;
    VC(9)=0.057;
    VC(10)=0;

%   Compressibilty factors
    ZC(1)=.288;
    ZC(2)=.27;
    ZC(3)=.28;
    ZC(4)=.285;
    ZC(5)=.274;
    ZC(6)=.281;
    ZC(7)=.27;
    ZC(8)=.303;
    ZC(9)=.235;
    ZC(10)=0;

    AC=PI.*(DT.^2)./4

    for i = 1:10
        F(i)=y(i);
        FT=FT+F(i);          % mol /s       from initial value array
    end

    for i=1:10
        C(i)=F(i).*y(12)./(FT.*RX.*y(11))               % kmol/ m3 s
    End

% Reaction rate expressions
```

```
% Equilibrium Constants as a function of Temperature that are used
within
% rate expressions

if y(11)<775+273.15
    Kc1=8.90E3;
    Kc5=9.85E3;
elseif(y(11)>=775+273.15) && (y(11)<=800+273.15)
    Kc1=1.28E2;
    Kc5=1.38E2;
else y(11)>800+273.15;
    Kc1=1.80E2;
    Kc5=1.89E2;
end


    R(1)=4.65E13.*exp(-273020./(RR.*y(11))).*((C(4)-
(1./Kc1).*C(3).*C(8)))
    R(2)=3.85E11.*exp(-2.73E5./(RR.*y(11))).*C(4)
    R(3)=5.89E10.*exp(-2.15E5./(RR.*y(11))).*C(6)
    R(4)=4.69E10.*exp(-2.12E5./(RR.*y(11))).*C(6)
    R(5)=9.81E8.*exp(-1.54E5./(RR.*y(11))).*((C(5)-
(1./Kc5).*C(2).*C(1)))
    R(6)=1.03E12.*exp(-1.73E5./(RR.*y(11))).*C(2).*C(3)
    R(7)=6.37E13.*exp(-5.3E5./(RR.*y(11))).*C(4)
% changed from E23 to E13
    R(8)=7.08E13.*exp(-2.53E5./(RR.*y(11))).*C(4).*C(3)

if y(11)<=900
    R(9)=0;
    R(10)=0;
    R(11)=0;
elseif y(11)>900
    R(9)=5.00E9.*exp(-
2.24E5./(RR.*y(11))).*((C(3)*1000).^1.34)./1000
% Coke formation rxn1 C2H4 --> C
       R(10)=2.77E6.*exp(-
1.16E5./(RR.*y(11))).*((C(5).*1000)^1.34)./1000
% Coke formation rxn2 C3H6 --> C
       R(11)=5.61E5.*exp(-
2.74E5./(RR.*y(11))).*((C(7).*1000)^1.37)./1000
% Coke formation rxn3
end


% Heat capacity of components, cp, [j/ mol.K]
% Perry's Handbook Chapter 2  [179 /521]


CP(1)=(0.33298E5+0.79939E5.*((2086.9./y(11))./(sinh(2.0869E3./y(11))
)).^2+0.41602E5.*((991.96./y(11))./(cosh(991.96./y(11)))).^2)./1000
% Methane
CP(2)=(0.3199E5+0.5424E5.*((1.594E3./y(11))./(sinh(1.594E3./y(11))))
.^2+0.4325E5.*((607.1./y(11))./(cosh(607.1./y(11)))).^2)./1000
% Acethylene

CP(3)=(0.3338E5+0.9479E5.*((1.596E3./y(11))./(sinh(1.596E3./y(11))))
.^2+0.551E5.*((740.8./y(11))./(cosh(740.8./y(11)))).^2)./1000
% ETHYLENE
```

```
CP(4)=(0.40326E5+1.3422E5.*((1.6555E3./y(11))./(sinh(1.6555E3./y(11)
))).^2+0.73223E5.*((752.87./y(11))./(cosh(752.87./y(11)))).^2)./1000
% Ethane


CP(5)=(0.43852E5+1.506E5.*((1.3988E3./y(11))./(sinh(1.3988E3./y(11))
)).^2+0.74754E5.*((616.46./y(11))./(cosh(616.46./y(11)))).^2)./1000
% Propylene


CP(6)=(0.5192E5+1.9245E5.*((1.6265E3./y(11))./(sinh(1.6265E3./y(11))
)).^2+1.168E5.*((723.6./y(11))./(cosh(723.6./y(11)))).^2)./1000
% Propane


CP(7)=(0.5095E5+1.705E5.*((1.5324E3./y(11))./(sinh(1.5324E3./y(11)))
).^2+1.337E5.*((685.6./y(11))./(cosh(685.6./y(11)))).^2)./1000


CP(8)=(0.27617E5+0.0956E5.*((2.466E3./y(11))./(sinh(2.466E3./y(11)))
).^2+0.0376E5.*((567.6./y(11))./(cosh(567.6./y(11)))).^2)./1000
% Hydrogen


CP(9)=(0.33363E5+0.2679E5.*((2.6105E3./y(11))./(sinh(2.6105E3./y(11)
))).^2+0.08896E5.*((1169./y(11))./(cosh(1169./y(11)))).^2)./1000
% Steam


CP(10)=(2.673+(0.002617.*y(11)-116900./(y(11).^2))).*4.1868
% graphite form
% Carbon cal/mol.K then convert it to joules

% CP(10) initial unit was [cal/ mol.K ] so energy unit is converted
to joules final form is [joules/ mol.K ]


% Calculation of total average heat capacity of mixture,
    for i=1:10
        yy(i)=F(i)./FT;
        CPT=CPT+yy(i).*CP(i)                %  j/ mol K
    end


% Prediction of viscosity according to corresponding state
    DHFO1=-7.49E4;          % Heat of formation of methane,     j/ mol
    DHFO2=2.269E5;
    DHFO3=5.234E4;
    DHFO4=-8.474E4;         % Heat of Formation of Ethane
    DHFO5=2.043E4;
    DHFO6=-1.039E5;         % Heat of Formation of Propane
    DHFO7=1.102E5;
    DHFO8=0;                % Heat of Formation of Hydrogen
    DHFO9=-2.42E5;
    DHFO10=0;               % Heat of Formation of Carbon
    P=(y(11)-TREF)
```

```
% units of the components' enthalpies at evaluated temperatures j/
mol

DHF1=DHFO1+(0.33298E5.*P+(0.79933E5.*2.0869E3).*(coth(2.0869E3./y(11
))-coth(2.0869E3./TREF))-(0.41602E5.*991.96).*(tanh(991.96./y(11))-
tanh(991.96./TREF))./1000                              % Methane

DHF2=DHFO2+(0.3199E5.*P+(0.5424E5.*1.594E3).*(coth(1.594E3./y(11))-
coth(1.594E3./TREF))-(0.41602E5.*991.96).*(tanh(991.96./y(11))-
tanh(991.96./TREF))./1000                              % Acethylene

DHF3=DHFO3+(0.3338E5.*P+(0.9479E5.*1.596E3).*(coth(1.596E3./y(11))-
coth(1.596E3./TREF))-(0.551E5.*740.8).*(tanh(740.8./y(11))-
tanh(740.8./TREF))./1000                               % Ethylene

DHF4=DHFO4+(0.40326E5.*P+(1.3422E5.*1.6555E3).*(coth(1.6555E3./y(11)
)-coth(1.6555E3./TREF))-(0.73223E5.*752.87).*(tanh(752.87./y(11))-
tanh(752.87./TREF))./1000                              % Ethane

DHF5=DHFO5+(0.43852E5.*P+(1.506E5.*1.3988E3).*(coth(1.3988E3./y(11))
-coth(1.3988E3./TREF))-(0.74754E5.*616.46).*(tanh(616.46./y(11))-
tanh(616.46./TREF))./1000                              % Propylene

DHF6=DHFO6+(0.5192E5.*P+(1.9245E5.*1.6265E3).*(coth(1.6265E3./y(11))
-coth(1.6265E3./TREF))-(1.168E5.*723.6).*(tanh(723.6./y(11))-
tanh(723.6./TREF))./1000                               % Propane

DHF7=DHFO7+(0.5095E5.*P+(1.705E5.*1.5324E3).*(coth(1.5324E3./y(11))-
coth(1.5324E3./TREF))-(1.337E5.*685.6).*(tanh(685.6./y(11))-
tanh(685.6./TREF))./1000

DHF8=DHFO8+(0.27617E5.*P+(0.0956E5.*2.466E3).*(coth(2.466E3./y(11))-
coth(2.466E3./TREF))-(0.0376E5.*567.6).*(tanh(567.6./y(11))-
tanh(567.6./TREF))./1000                               % Hydrogen

DHF9=DHFO9+(0.33363E5.*P+(0.2679E5.*2.6105E3).*(coth(2.6105E3./y(11)
)-coth(2.6105E3./TREF))-(0.08896E5.*1169).*(tanh(1169./y(11))-
tanh(1169./TREF))./1000                                % Steam

DHF10=DHFO10+(2.673.*P+(0.002617./2).*(y(11).^2-
TREF^2)+116900.*(1./y(11)-1./TREF)).*4.1868          % Carbon



    DH(1)=DHF3+DHF8-DHF4
    DH(2)=DHF6+DHF1-2.*DHF4
    DH(3)=DHF5+DHF8-DHF6
    DH(4)=DHF3+DHF1-DHF6
    DH(5)=DHF2+DHF1-DHF5
    DH(6)=DHF7-DHF3-DHF2
    DH(7)=2.*DHF1+DHF3-2.*DHF4
    DH(8)=DHF5+DHF1-DHF3-DHF4
    DH(9)=-1.*(DHF10-DHF3)
    DH(10)=-1.*(DHF10-DHF5)
    DH(11)=-1.*(DHF10-DHF7)
```

```
for i=1:11
    SUMDHR_ethane=SUMDHR_ethane+DH(i).*R(i)           %% j/mol
end

for i=1:10
    TCM=TCM+yy(i).*TC(i);
    SUMZC=SUMZC+yy(i).*ZC(i);
    SUMVC=SUMVC+yy(i).*VC(i);
    BMM=BMM+yy(i).*BM(i);     % mixture Molecular Weight   calc by
multiplying with mole fractions
end

PCM=RZ.*TCM.*SUMZC./(SUMVC*1000);
    TRM=y(11)./TCM;           % Tr of the mixture for calculation of
mixture viscosity
    PRM=y(12)./(PCM);

 MS1=0;
for i=1:10
    if yy(i)>0.0
       MS1=MS1+1
       Xyy(MS1)=yy(i);
       XBM(MS1)=BM(i);
       end
end

BMH=XBM(MS1)                        % Highest molecular weight value
for i=1:MS1
    if XBM(i)>BMH
       BMH=XBM(i);
       yyH=Xyy(i);                  % mole fraction of component that
has higher molecular weight among other components
       end
end

BML=XBM(MS1);

for i=1:MS1
    if XBM(i)<BML
       BML=XBM(i);
       end
end



% Viscosity calculation expression
% From Perry's Handbook Chapter 2 [507/521]   Yoon-Thodos Method
% Input Data: TCM,PCM,BMM( MW of mix)

    VISC=(46.1.*(TRM.^0.618)-20.4.*exp(-0.449.*TRM)+19.4.*exp(-
4.058.*TRM)+1)./(2.173424.*10^11*(TCM^(1/6))*(BMM^(1/2))*((PCM.*10^5
)^(-2/3)))
    EE=(0.7+V.*0.35./90).*(0.051+0.19.*DT./RB);
    G=(FT.*BMM./1000)./AC
% FT [mol/s]   and BMM [kg/ kmol]   then G [kg/m2.s] mass flow rate
    RE=DT.*G./VISC
    FF=0.046.*RE.^(-0.2);
```

```
 BMW=9.5;
    if l>BMW.*5
        QZ=0.45E4;
    elseif l>BMW.*4
        QZ=0.55E4;
    elseif l>BMW.*3
        QZ=0.80E4;
    elseif l>BMW.*2
        QZ=1.40E4;
    elseif l>BMW.*1
        QZ=4.60E4;
    else
        QZ=6.10E4;
    end


%  Governing differential mass balance equations
    ydot(1)=(R(2)./2+R(4)+R(5)+R(7)+R(8)).*1000.*AC
    ydot(2)=(R(5)-R(6)).*1000.*AC
    ydot(3)=(R(1)+R(4)-R(6)+R(7)./2-R(8)-R(9)).*1000.*AC
    ydot(4)=(-R(1)-R(2)-R(7)-R(8)).*1000.*AC
    ydot(5)=(R(3)-R(5)+R(8)-R(10)).*1000.*AC
    ydot(6)=(R(2)./2-R(3)-R(4)).*1000.*AC
    ydot(7)=(R(6)-R(11)).*1000.*AC
    ydot(8)=(R(1)+R(3)).*1000.*AC
    ydot(9)=(0).*1000.*AC
    ydot(10)=(R(9)+R(10)+R(11)).*1000.*AC          % kmol/ m3.s

    for i=1:10
        SUMYDOT=SUMYDOT+ydot(i);
    end

    cp_f=0;
    for i=1:10
        cp_f=cp_f+CP(i).*F(i)
    end

    display(cp_f)
ydot(11)=(QZ.*PI.*DT-AC.*SUMDHR_ethane)./(cp_f)
ydot(12)=((SUMYDOT./1)./(G.*AC)+((ydot(11)./y(11)+(2.*FF./DT+12.*EE.
/(PI.*RB))./BMM))./((1./(BMM.*y(12)))-(y(12)./(1E-
5.*RX.*(G.^1).*y(11))));

ydot=ydot';
```

C.3 Model-III

```
% Model-III that is accepted and run with Petkim Steam Ethane
Cracker Inputs
% M.S. Shokrollahi Yancheshmeh et al. / Chemical Engineering Journal
% 215-216 (2013) 550- 560

%  Unit conversions
% 1 atm=1.013 bar
% 1 bar= 10^5 Pa
% 1 cal=4.1869 joules

function ydot=ethane_cracker(l,y)

global SUMYDOT

FT=0;             % total molar flow rate,                    kmol/s
CPT=0;            % total/ mixture heat capacity,            j/mol.K
SUMDHR_ethane=0; % summation of heat of rxns,                 j/mol
TCM=0;            % Critical temperature of the mixture,      K
SUMZC=0;          % Sum of compressibility factors
SUMVC=0;          % Sum of critical volumes of components,
SUMYDOT=0;        % Sum of dFj/dz
BMM=0;            % Molecular weight of mixtures


RR=8.314;         % Ideal Gas constant,                       j/mol.K
RX=0.08206;       % Ideal Gas constant,                  m3.atm/kmol.K
RZ=82.06;         % Ideal Gas constant, L.atm/kmol.K or cm3.atm/mol.K
DT=0.1;           % "Petkim" internal tube diameter,          meters
PI=3.141592654;

V=180;            % Angle described by the bend here 180o
RB=0.356./2;      % Radius of the bend,                        meters
TREF=298.15;      % Reference temperature,                          K


%  Critical temperatures of components, K
    TC(1)=190.4;
    TC(2)=308.3;
    TC(3)=282.4;
    TC(4)=305.4;
    TC(5)=364.9;
    TC(6)=369.8;
    TC(7)=425;
    TC(8)=33;
    TC(9)=647.3;

    TC(10)=134.5;              % Carbon Monoxide
    TC(11)=304.2;              % Carbon Dioxide
    TC(12)=0;                  % Carbon

%  Molecular weights of components, kg/ kmol
    BM(1)=16.043;
    BM(2)=26.038;
    BM(3)=28.054;
    BM(4)=30.07;
    BM(5)=42.081;
    BM(6)=44.094;
```

```
    BM(7)=54.092;
    BM(8)=2.016;
    BM(9)=18.015;
    BM(10)=28.01;                % Carbon Monoxide
    BM(11)=44.10;                % Carbon Dioxide
    BM(12)=12;                   % Carbon

%  Critical pressures of components, bar
    PC(1)=46;
    PC(2)=61.4;
    PC(3)=50.4;
    PC(4)=48.8;
    PC(5)=46;
    PC(6)=42.5;
    PC(7)=43.3;
    PC(8)=12.9;
    PC(9)=221.2;
    PC(10)=35;                   % Carbon Monoxide
    PC(11)=73.8;                 % Carbon Dioxide
    PC(12)=0;                    % Carbon


%  Critical volumes of components, m3/kmol
    VC(1)=0.09947;
    VC(2)=0.11196;
    VC(3)=0.13101;
    VC(4)=0.14133;
    VC(5)=0.18431;
    VC(6)=0.19842;
    VC(7)=0.23259;
    VC(8)=0.06653;
    VC(9)=0.057;
    VC(10)=0.09243;
    VC(11)=0.09173;
    VC(12)=0;


%   Compressibilty factors
    ZC(1)=.288;
    ZC(2)=.27;
    ZC(3)=.28;
    ZC(4)=.285;
    ZC(5)=.274;
    ZC(6)=.281;
    ZC(7)=.27;
    ZC(8)=.303;
    ZC(9)=.235;
    ZC(10)=((PC(10)./1.013).*VC(10)./(RX.*TC(10)));
    ZC(11)=((PC(11)./1.013).*VC(11)./(RX.*TC(11)));
    ZC(12)=0;

    AC=PI.*(DT.^2)./4;



    for i = 1:12
        F(i)=y(i);
        FT=FT+F(i);
    end
```

```
    for i=1:12
        C(i)=F(i).*y(14)./(FT.*RX.*y(13));          % kmol/ m3. s
    end


%  Reaction rate expressions
% Equilibrium Constants as a function of Temperature that are used
within rate expressions


if y(13)<775+273.15
    Kc1=8.90E3;
    Kc5=9.85E3;
elseif(y(13)>=775+273.15) && (y(13)<=800+273.15)
    Kc1=1.28E2;
    Kc5=1.38E2;
else y(13)>800+273.15;
    Kc1=1.80E2;
    Kc5=1.89E2;
end

    R(1)=4.65E13.*exp(-273020./(RR.*y(13))).*(C(4)
(1./Kc1).*C(3).*C(8));
    R(2)=3.85E11.*exp(-2.73E5./(RR.*y(13))).*C(4);
    R(3)=5.89E10.*exp(-2.15E5./(RR.*y(13))).*C(6);
    R(4)=4.69E10.*exp(-2.12E5./(RR.*y(13))).*C(6);
    R(5)=9.81E8.*exp(-1.54E5./(RR.*y(13))).*(C(5)-
(1./Kc5).*C(2).*C(1));
    R(6)=1.03E12.*exp(-1.73E5./(RR.*y(13))).*C(2).*C(3);
    R(7)=6.37E13.*exp(-5.3E5./(RR.*y(13))).*C(4);
    R(8)=7.08E13.*exp(-2.53E5./(RR.*y(13))).*C(4).*C(3);

if y(13)<=900
    R(9)=0;
    R(10)=0;
    R(11)=0;

elseif y(13)>900

    R(9)=5.0E9.*exp(-
2.24E5./(RR.*y(13))).*((C(3).*1000).^1.34)./1000;
% Coke formation rxn1 C2H4 --> C
    R(10)=2.77E6.*exp(-
1.16E5./(RR.*y(13))).*((C(5).*1000).^1.34)./1000;
% Coke formation rxn2 C3H6 --> C
    R(11)=5.61E5.*exp(-
2.74E5./(RR.*y(13))).*((C(7).*1000).^1.37)./1000;
% Coke formation rxn3

End
```

```
if F(12)<=0
   R(12)=0;
   R(13)=0;

elseif F(12)>0

  R(12)=5.09E1.*exp(-
2.38E5./(RR.*y(13))).*(F(9).*y(14).*10^5./FT)./1;
% Partial removal of coke formation   C+H2O --> CO+ H2
  R(13)=1.12E5.*exp(-
2.45E5./(RR.*y(13))).*(0.*(F(11).*y(14).*10^5./FT).^0.31);
% Partial removal of coke formation   C+CO2 --> 2CO

end


% Heat capacity of components, cp, [j/ mol.K]
% Perry's Handbook Chapter 2  [179 /521]


CP(1)=(0.33298E5+0.79939E5.*((2.0869E3./y(13))./(sinh(2.0869E3./y(13
))))^2+0.41602E5.*((991.96/y(13))./(cosh(991.96/y(13))))^2)./1000;
% Methane


CP(2)=(0.3199E5+0.5424E5.*((1.594E3./y(13))./(sinh(1.594E3./y(13))))
^2+0.4325E5.*((607.1/y(13))./(cosh(607.1/y(13))))^2)./1000;
% Acethylene


CP(3)=(0.3338E5+0.9479E5.*((1.596E3./y(13))./(sinh(1.596E3./y(13))))
^2+0.551E5.*((740.8/y(13))./(cosh(740.8/y(13))))^2)./1000;
% Ethylene


CP(4)=(0.40326E5+1.3422E5.*((1.6555E3./y(13))./(sinh(1.6555E3./y(13)
)))^2+0.73223E5.*((752.87/y(13))./(cosh(752.87/y(13))))^2)./1000;
% Ethane


CP(5)=(0.43852E5+1.506E5.*((1.3988E3./y(13))./(sinh(1.3988E3./y(13))
))^2+0.74754E5.*((616.46/y(13))./(cosh(616.46/y(13))))^2)./1000;
% Propylene


CP(6)=(0.5192E5+1.9245E5.*((1.6265E3./y(13))./(sinh(1.6265E3./y(13))
))^2+1.168E5.*((723.6/y(13))./(cosh(723.6/y(13))))^2)./1000;
% Propane


CP(7)=(0.5095E5+1.7056E5.*((1.5324E3./y(13))./(sinh(1.5324E3./y(13))
))^2+1.337E5.*((685.6/y(13))./(cosh(685.6/y(13))))^2)./1000;
% Butadiene


CP(8)=(0.27617E5+0.0956E5.*((2.466E3./y(13))./(sinh(2.466E3./y(13)))
)^2+0.0376E5.*((567.6/y(13))./(cosh(567.6/y(13))))^2)./1000;
% Hydrogen
```

```
CP(9)=(0.33363E5+0.2679E5.*((2.6105E3./y(13))./(sinh(2.6105E3./y(13)
)))^2+0.08896E5.*((1169/y(13))./(cosh(1169/y(13))))^2)./1000;
% Steam


CP(10)=(0.29108E5+0.08773E5.*((3.0851E3./y(13))./(sinh(3.0851E3./y(1
3))))^2+0.084553E5.*((1538.2/y(13))./(cosh(1538.2/y(13))))^2)./1000;
% Carbon Monoxide

CP(11)=(0.2937E5+0.3454E5.*((1.428E3./y(13))./(sinh(1.428E3./y(13)))
)^2+0.264E5.*((588/y(13))./(cosh(588/y(13))))^2)./1000;
% Carbon Dioxide

CP(12)=(2.673+(0.002617.*y(13)-116900./(y(13).^2))).*4.1868;
% Carbon cal/mol.K then convert it to joules

% Calculation of total average heat capacity of mixture

for i=1:12
    yy(i)=F(i)./FT;
    CPT=CPT+yy(i).*CP(i);
end

% Prediction of viscosity according to corresponding state
    DHFO1=-7.49E4;            % Heat of formation of methane,j/ mol
    DHFO2=2.269E5;
    DHFO3=5.234E4;
    DHFO4=-8.474E4;           % Heat of Formation of Ethane
    DHFO5=2.043E4;
    DHFO6=-1.039E5;           % Heat of Formation of Propane
    DHFO7=1.102E5;
    DHFO8=0;                  % Heat of Formation of Hydrogen
    DHFO9=-2.42E5;
    DHFO10=-11.06E4;          % Heat of Formation of CO
    DHFO11=-3.938E5;          % Heat of Formation of CO2
    DHFO12=0;                 % Heat of Formation of Carbon

    P=(y(13)-TREF);

% units of the components' enthalpies at evaluated temperatures; j/
mol

DHF1=DHFO1+(0.33298E5.*P+(0.79933E5.*2.0869E3).*(coth(2.0869E3./y(13
))-coth(2.0869E3./TREF))-(0.41602E5.*991.96).*(tanh(991.96./y(13))-
tanh(991.96./TREF))./1000;                              % Methane


DHF2=DHFO2+(0.3199E5.*P+(0.5424E5.*1.594E3).*(coth(1.594E3./y(13))-
coth(1.594E3./TREF))-(0.41602E5.*991.96).*(tanh(991.96./y(13))-
tanh(991.96./TREF))./1000;                              % Acethylene


DHF3=DHFO3+(0.3338E5.*P+(0.9479E5.*1.596E3).*(coth(1.596E3./y(13))-
coth(1.596E3./TREF))-(0.551E5.*740.8).*(tanh(740.8./y(13))-
tanh(740.8./TREF))./1000;                               % Ethylene


DHF4=DHFO4+(0.40326E5.*P+(1.3422E5.*1.6555E3).*(coth(1.6555E3./y(13)
```

```
)-coth(1.6555E3./TREF))-(0.73223E5.*752.87).*(tanh(752.87./y(13))-
tanh(752.87./TREF)))./1000;                              % Ethane

DHF5=DHFO5+(0.43852E5.*P+(1.506E5.*1.3988E3).*(coth(1.3988E3./y(13))
-coth(1.3988E3./TREF))-(0.74754E5.*616.46).*(tanh(616.46./y(13))-
tanh(616.46./TREF)))./1000;                              % Propylene

DHF6=DHFO6+(0.5192E5.*P+(1.9245E5.*1.6265E3).*(coth(1.6265E3./y(13))
-coth(1.6265E3./TREF))-(1.168E5.*723.6).*(tanh(723.6./y(13))-
tanh(723.6./TREF)))./1000;                               % Propane


DHF7=DHFO7+(0.5095E5.*P+(1.705E5.*1.5324E3).*(coth(1.5324E3./y(13))-
coth(1.5324E3./TREF))-(1.337E5.*685.6).*(tanh(685.6./y(13))-
tanh(685.6./TREF)))./1000;                               % Butadiene


DHF8=DHFO8+(0.27617E5.*P+(0.0956E5.*2.466E3).*(coth(2.466E3./y(13))-
coth(2.466E3./TREF))-(0.0376E5.*567.6).*(tanh(567.6./y(13))-
tanh(567.6./TREF)))./1000;                               % Hydrogen


DHF9=DHFO9+(0.33363E5.*P+(0.2679E5.*2.6105E3).*(coth(2.6105E3./y(13)
)-coth(2.6105E3./TREF))-(0.08896E5.*1169).*(tanh(1169./y(13))-
tanh(1169./TREF)))./1000;                                % Steam


DHF10=DHFO10+(0.29108E5.*P+(0.08773E5.*3.0851E3).*(coth(3.0851E3./y(
13))-coth(3.0851E3./TREF))-
(0.084553E5.*1538.2).*(tanh(1538.2./y(13))-
tanh(1538.2./TREF)))./1000;                              % Carbon
Monoxide


DHF11=DHFO11+(0.2937E5.*P+(0.3454E5.*1.428E3).*(coth(1.428E3./y(13))
-coth(1.428E3./TREF))-(0.264E5.*588).*(tanh(588./y(13))-
tanh(588./TREF)))./1000;                                 % Carbon
Dioxide


DHF12=DHFO12+(2.673.*P+(0.002617./2).*(y(13).^2-
TREF^2)+116900.*(1./y(13)-1./TREF)).*4.1868;             % Carbon



DH(1)=DHF3+DHF8-DHF4;
DH(2)=DHF6+DHF1-2.*DHF4;
DH(3)=DHF5+DHF8-DHF6;
DH(4)=DHF3+DHF1-DHF6;
DH(5)=DHF2+DHF1-DHF5;
DH(6)=DHF7-DHF3-DHF2;
DH(7)=2.*DHF1+DHF3-2.*DHF4;
DH(8)=DHF5+DHF1-DHF3-DHF4;
DH(9)=-1.*(DHF12-DHF3);
DH(10)=-1.*(DHF12-DHF5);
DH(11)=-1.*(DHF12-DHF7);
DH(12)=DHF10+DHF8-DHF9-DHF12;
DH(13)=2.*DHF10-DHF11-DHF12;
```

```
    for i=1:13
        SUMDHR_ethane=SUMDHR_ethane+DH(i).*R(i);    % R(i) mol/ m3.s
    end



      for i=1:12

        TCM=TCM+yy(i).*TC(i);
        SUMZC=SUMZC+yy(i).*ZC(i);
        SUMVC=SUMVC+yy(i).*VC(i);
        BMM=BMM+yy(i).*BM(i); % mixture Molecular Weight calc by
multiplying with mole fractions

      end


    PCM=RZ.*TCM.*SUMZC./(SUMVC.*1000);      % atm
    TRM=y(13)./TCM;                         % Tr of the mixture for
calculation of mixture viscosity
    PRM=y(14)./PCM;




 MS1=0;
    for i=1:12
        if yy(i)>0.0
        MS1=MS1+1
        Xyy(MS1)=yy(i);
        XBM(MS1)=BM(i)
        end
    end

BMH=XBM(MS1);                       % Highest molecular weight value
    for i=1:MS1
        if XBM(i)>BMH
        BMH=XBM(i);
        yyH=Xyy(i);                 % mole fraction of component that
has higher molecular weight among other components
        end
    end

BML=XBM(MS1);

    for i=1:MS1
        if XBM(i)<BML
        BML=XBM(i);
        end
    end

% Viscosity calculation expression
% From Perry's Handbook Chapter 2 [507/521]   Yoon-Thodos Method
% Input Data: TCM,PCM(Pa)       ,BMM( MW of mix)

VISC=(46.1.*(TRM.^0.618)-20.4.*exp(-0.449.*TRM)+19.4.*exp(-
4.058.*TRM)+1)./(2.173424.*10^11*(TCM^(1/6))*(BMM^(1/2))*((PCM.*10^5
)^(-2/3)));                          % kg/ ms
```

```
EE=(0.7+V.*0.35./90).*(0.051+0.19.*DT./RB);
G=(FT.*BMM./1000)./AC;
RE=DT.*G./VISC;
FF=0.046.*RE.^(-0.2);


BMW=9.5;
    if l>BMW.*5
        QZ=0.80E4;
    elseif l>BMW.*4
        QZ=1.00E4;
    elseif l>BMW.*3
        QZ=1.75E4;
    elseif l>BMW.*2
        QZ=3.00E4;
    elseif l>BMW.*1
        QZ=5.60E4;
    else
        QZ=6.90E4;
    end



%  Governing differential mass balance equations
    ydot(1)=(R(2)./2+R(4)+R(5)+R(7)+R(8)).*1000.*AC;
    ydot(2)=(R(5)-R(6)).*1000.*AC;
    ydot(3)=(R(1)+R(4)-R(6)+R(7)./2-R(8)-R(9)).*1000.*AC;
    ydot(4)=(-R(1)-R(2)-R(7)-R(8)).*1000.*AC;
    ydot(5)=(R(3)-R(5)+R(8)-R(10)).*1000.*AC;
    ydot(6)=(R(2)./2-R(3)-R(4)).*1000.*AC;
    ydot(7)=(R(6)-R(11)).*1000.*AC;
    ydot(8)=(R(1)+R(3)+R(12)).*1000.*AC;
    ydot(9)=(-R(12)).*1000.*AC;
    ydot(10)=(R(12)+2.*R(13)).*1000.*AC;
    ydot(11)=(-R(13)).*1000.*AC;
    ydot(12)=(R(9)+R(10)+R(11)-R(12)-R(13)).*1000.*AC;
for i=1:12
        SUMYDOT=SUMYDOT+ydot(i);
    end

    cp_f=0;
    for i=1:12
        cp_f=cp_f+CP(i).*F(i);
    end

ydot(13)=(QZ.*PI.*DT-SUMDHR_ethane.*AC)./(cp_f);

ydot(14)=((SUMYDOT./1)./(G.*AC)+((ydot(13)./y(13)+(2.*FF./DT+12.*EE.
/(PI.*RB)))./BMM))./((1./(BMM.*y(14)))-(y(14)./(1E-
5.*RX.*(G.^1).*y(13))));

ydot=ydot';
```

,

D. PETKIM Ethane Cracker DCS Diagram

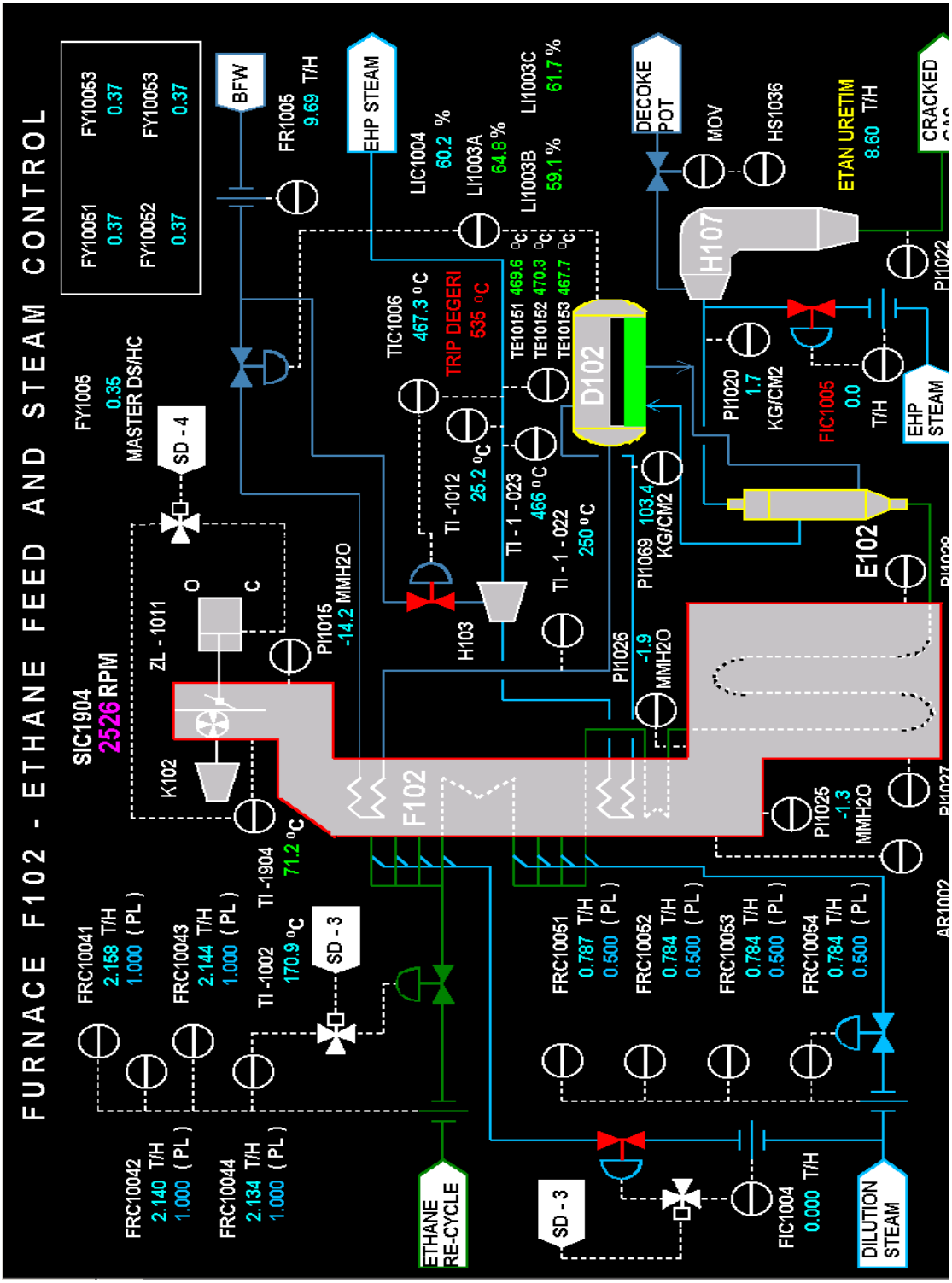

Figure D.1 Ethane cracker plant snapshot

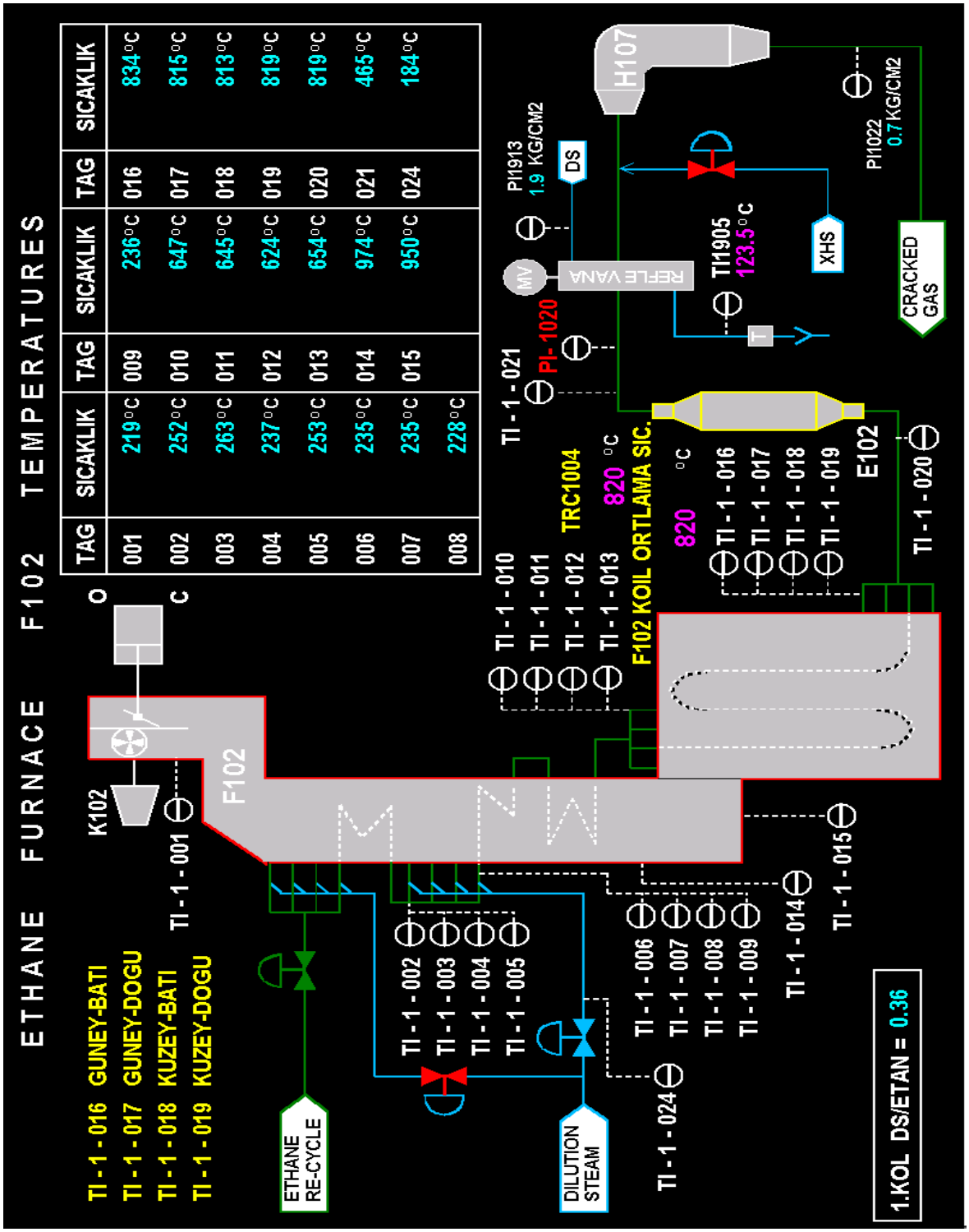

Figure D.2 Ethane cracker PFD showing all unit TIs